Methods and Examples in Flavor Model Building

By

Bradley Lewis Rachlin

Dissertation

Submitted to the Faculty of the

Graduate School of Vanderbilt University

in partial fulfillment of the requirements

for the degree of

DOCTOR OF PHILOSOPHY

in

Physics

August 9th, 2019

Nashville, Tennessee

Approved:

Tom Kephart, Ph.D.

Tom Weiler, Ph.D.

Paul Sheldon, Ph.D.

Will Johns, Ph.D.

Marcelo Disconzi, Ph.D.

ACKNOWLEDGMENTS

First, I would like to thank my mother for always encouraging me to follow my curiosity wherever it took me. I wouldn't be where I am today if you hadn't read me all those Curious George books and taken me to see that Albert Einstein exhibit back in seventh grade. I'd like to thank my father for always being there and believing in me. Thank you to my sister Niki for inspiring me to help others and to be a better person. I am also grateful to Eileen and David and the rest of the group for helping me cope with the stresses of early adulthood and for facilitating so much personal growth.

Thank you to my advisor Tom Kephart for countless thoughtful and entertaining discussions and for your invaluable expertise in guiding my research. Many thanks to Paul Sheldon for helping me make the transition to graduate school and for supporting me early on in my research career. Thank you to Tom Weiler, Will Johns, and Marcelo Disconzi for serving on my committee and taking interest in my work. Thanks to my friend and office mate Daniel Kidd, graduate school would not have been nearly as fun and enjoyable without you. I would also like to express my gratitude to the Vanderbilt Physics Department for granting me the opportunity to spend six years doing what I love and for providing much needed academic and professional support.

Finally, thank you to Jessica for your unwavering love and commitment. Thank you for being there to listen to my problems and to cheer me up when I am feeling down. Thank you for your constant companionship and for continually pushing me to be a better version of my self. I will always appreciate having you in my life.

FUNDING ACKNOWLEDGMENTS

This work was supported in part by DoE grant No. DE-SC-0019235 and by DoE grant No. DE-SC-001198.

TABLE OF CONTENTS

LIST OF TABLES

LIST OF FIGURES

Chapter 1

Introduction: The Flavor Puzzle

Fifty years into its existence, the Standard Model remains largely untarnished. All known particles are accounted for and sorted neatly into irreducible representations (irreps) of Lie groups. Three out of the four fundamental forces have been explained elegantly as a consequence of the gauge invariance of the Standard Model Lagrangian. Particle masses arise from spontaneous symmetry breaking via the Higgs mechanism. With all this in mind, what is there left to do in particle physics? Perhaps most obviously there is still no complete quantum theory of gravity; this problem falls outside the scope of this dissertation and will be left for other works. Just as ambitious a goal is grand unification, i.e. can we formulate a complete theory in which the three fundamental forces of the Standard Model are the low energy residues of one unified force? The quest for a grand unified theory dates back one hundred years but became more tangible with the advent of quantum gauge symmetries. The task at hand is to find a master gauge group which can spontaneously break to the standard model gauge groups, the canonical example of this being Georgi and Glashow's SU(5) theory [1]. But this task is not as simple as it may seem, the precise structure of the grand unified theory, i.e. its particle representations, symmetry breaking patterns, scalar sector, etc. all have far reaching consequences for measurables like decay processes, conservation laws, particle masses and mixing angles. For example, the continued absence of proton decay has ruled out Georgi and Glashow's SU(5) theory.

There are innumerable options for grand unified theories, spanning different choices of gauge groups and representation structures and proposing new mechanisms such as supersymmetry and string theory. It is a monumental task to even begin building a unified model. One often fruitful approach is to work from the "bottom up", i.e., to search for hints of nature's high energy structure in the physics that is currently accessible via experiment. The

goal of this approach is not necessarily to formulate a complete grand unified theory but to describe physics at the next higher energy scale. If a given formulation is proven correct, models can be built iteratively at higher and higher energy scales until a theory of physics at the GUT scale is reached. An advantage of this approach is that the model's low energy structure is built in; the model is built on top of existing physics which avoids having to reconcile with known results after the fact. Another advantage is that via this approach the theory is much more likely to have predictions that are experimentally testable presently or in the near future. This will ensure that incorrect theories can be ruled out relatively quickly and that not too much time is spent going down the wrong path.

It is in this context that we examine what is known as the flavor puzzle. The phenomenon of flavor is one of the strongest hints of physics beyond the Standard Model. Electrons, up quarks, and down quarks form the basis of ordinary matter, the four vector bosons mediate the fundamental forces, and the Higgs boson interacts with all particles to give them mass. Other particles arise from gauge invariance: The electron neutrino is the result of an SU(2) gauge rotation of the electron, positron and anti-quarks are U(1) (Electromagnetic) gauge rotations, and blue, green and red quarks are the result of SU(3) gauge rotations. All of these particles are required to exist by the rules of the Standard Model. Absent from this discussion is flavor. Under the standard model there are three distinct families of fermions: the electron, electron neutrino, up and down quark being the lightest, with the others successively heavier (see Figure 1.1 below).

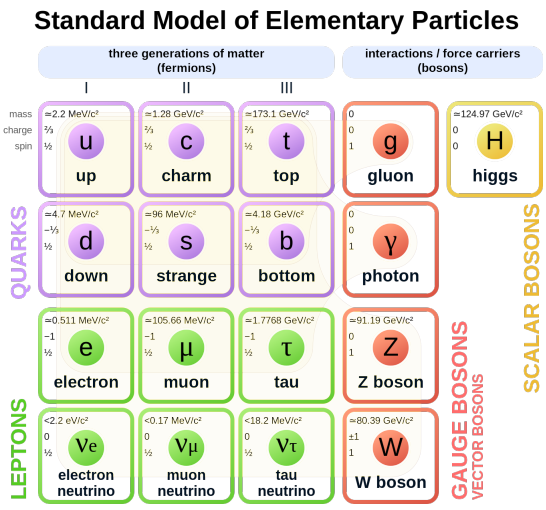

Figure 1.1: The Standard Model of Particle Physics

This structure is suggestive of a flavor symmetry, a gauge symmetry in addition to that of the Standard Model that rotates between different flavored particles. This would give a reason for the different flavors to exist, they would be particles with different charges under a flavor force. Unfortunately, at observable energy scales there is no such force; different flavors of particles are identical save for their increased masses.

This however does not preclude the existence of a flavor force at a higher energy scale. The mass difference between particles of different flavors can be seen as a residue of the theory's high energy structure. This is analogous to electroweak (EW) symmetry breaking, which gives fermions mass values proportional to the EW breaking scale and renders the weak force nearly undetectable at low energies. A review of spontaneous symmetry breaking in the Standard model can be found in Section 2 below. A key ingredient in flavor models are the scalar particles that facilitate the spontaneous breaking of the flavor gauge symmetries. The existence of new scalars is an important prediction of flavor models and can be used as an experimental signature to test the veracity of a given model. Section 3 will outline a systematic approach to breaking gauge symmetries via the Higgs mechanism, and carry out this approach for many different example breaking patterns. Predictions and

mass bounds are given for the scalar multiplets involved in each breaking.

In addition to mass differences, particles of different flavors are allowed to mix under the weak interaction. For example, an up quark usually couples to the down quark in decay interactions, but flavor changing decays can also occur where the up is coupled to the strange or bottom quark instead. A brief overview of flavor mixing in the quark and lepton sectors will be given in Section 4. It is by examining these mixing patterns that the use of discrete symmetries for model building became popularized. In contrast to the Standard Model, where $SU_L(2) \times U_Y(1)$ breaks to the continuous group $U_{EM}(1)$, flavor models often will take a continuous flavor force at high energies and have it spontaneously break to a discrete group such as A_4 or T'. One can then derive mixing matrices compatible with experimental results by considering a Lagrangian that has the specified discrete symmetry. Lastly, Section 5 will describe a specific model in which an SU(2) flavor symmetry breaks to T', quark and lepton mixing matrices are derived, and predictions for new particles required to complete the SU(2) theory and cancel anomalies are given.

Chapter 2

Standard Model Symmetry Breaking

2.1 Spontaneous Symmetry Breaking in the Standard Model

This section will provide a brief overview of Spontaneous Symmetry Breaking (SSB) in the Standard Model. We will first construct the Lagrangian above the electroweak scale, then we carry out SSB for the breaking pattern $SU(2)_L \times U_Y(1) \rightarrow U_{EM}(1)$ and review the resulting scalar and vector mass states.[1] From these steps we will develop a prescription for symmetry breaking that we will follow for more complex breaking patterns later in this work.

2.1.1 Gauge Invariant Lagrangian

We begin with the lepton sector [2–4] . For each generation of lepton (e,μ,τ) we have a left handed doublet $\Psi^L(x) = (\nu(x), l(x))$ and a right handed singlet for the neutrino $\nu_R(x)$ and charged lepton $l_R(x)$ fields. We can write down the lepton Lagrangian $\mathcal{L}_l$:

$$\mathcal{L}_l = i[\overline{\Psi}^L(x) \not{D} \Psi^L(x) + \bar{l}_R(x) \not{D} l_R(x) + \overline{\nu}_R(x) \not{D} \nu_R(x)] \tag{2.1}$$

We define the covariant derivative D to ensure invariance under $SU(2)_L \times U_Y(1)$ gauge transformations:

$$\begin{aligned} D^\mu \Psi^L(x) &= [\partial^\mu + \frac{1}{2} i g \tau_j W_j^\mu(x) - \frac{1}{2} i g' Y B^\mu(x)] \Psi^L(x) \\ D^\mu l_R(x) &= [\partial^\mu - i g' Y B^\mu(x)] l_R(x) \\ D^\mu \nu_R(x) &= \partial^\mu \nu_R(x) \end{aligned} \tag{2.2}$$

Where g and g' are coupling constants, τ_j are the Pauli spin matrices, and Y is the hyper-

[1] The derivations in this chapter are adapted from chapters 17-19 of [78]

charge of the appropriate fermion. We have four vector bosons: $B^\mu(x)$ is the generator and force carrier associated with the $U_Y(1)$ (hypercharge) symmetry and $W_i^\mu(x)$ (where $i = 1, 2, 3$) are the generators and force carriers of the $SU(2)_L$ (weak) symmetry.

Next we detail the quark sector. For each quark generation we have a left-handed doublet $Q^L(x) = (u(x), d(x))$ where $u(x)$ and $d(x)$ represent the up type and down type quark fields respectively. In addition we have right-handed singlets for the up type and down type fields, u_R and d_R. Our quark Lagrangian is:

$$\mathcal{L}_q = i[\overline{Q}_L(x)\not{D}Q^L(x) + \overline{u}_R(x)\not{D}u_R(x) + \overline{d}_R(x)\not{D}d_R(x)] \tag{2.3}$$

With covariant derivatives:

$$\begin{aligned} D^\mu Q_L(x) &= [\partial^\mu + \frac{1}{2}ig\tau_j W_j^\mu(x) - \frac{1}{2}ig'YB^\mu(x)]Q_L(x) \\ D^\mu u_R(x) &= [\partial^\mu - ig'YB^\mu(x)]u_R(x) \\ D^\mu d_R(x) &= [\partial^\mu - ig'YB^\mu(x)]d_R(x) \end{aligned} \tag{2.4}$$

Next we examine the vector boson sector. Their gauge invariant Lagrangian is:

$$\mathcal{L}_B = -\frac{1}{4}B_{\mu\nu}(x)B^{\mu\nu}(x) - \frac{1}{4}G_{i\mu\nu}(x)G_i^{\mu\nu}(x) \tag{2.5}$$

Where $B^{\mu\nu} = \partial^\nu B^\mu(x) - \partial^\mu B^\nu(x)$ and $G^{i\mu\nu} = \partial^\nu W_i^\mu(x) - \partial^\mu W_i^\nu(x) + g\epsilon_{ijk}W_j^\mu(x)W_k^\nu(x)$

At this scale, all non-scalars must be massless because typical mass terms of the form:

$$\begin{aligned} &m_l\overline{\psi}(x)\psi(x) \\ &m_b W_{i\mu}^\dagger(x)W_i^\mu(x) \end{aligned} \tag{2.6}$$

are not gauge invariant[2]. Masses will be introduced below the EW breaking scale via the Higgs Mechanism.

[2]This is actually not true for right-handed neutrino field, but since these fields are not included in the Standard Model we delay discussion until Chapter 4

2.1.2 Higgs Mechanism

We now introduce the Higgs into the model in order to spontaneously break $SU(2)_L \times U_Y(1) \rightarrow U_{EM}(1)$. The Standard Model Higgs is a complex scalar $SU(2)_L$ doublet:

$$\Phi(x) = \begin{pmatrix} \phi_a(x) + i\phi_b(x) \\ \phi_c(x) + i\phi_d(x) \end{pmatrix} \tag{2.7}$$

Physically, this means that above the electroweak scale there are four spin-0, particles with degenerate mass. We construct the scalar Lagrangian $\mathcal{L}_H$:

$$\begin{aligned} &\mathcal{L}_H = [D^\mu \Phi(x)]^\dagger [D^\mu \Phi(x)] - V(\Phi) \\ &V(\Phi) = \mu^2 \Phi^\dagger(x)\Phi(x) + \lambda[\Phi^\dagger(x)\Phi(x)]^2 \\ &\mu^2 < 0 \end{aligned} \tag{2.8}$$

Where V is the potential energy part of the Lagrangian. In order to preserve gauge invariance, we define the covariant derivative D^μ by:

$$D^\mu \Phi(x) = [\partial^\mu + \frac{1}{2} i g \tau_j W_j^\mu + i g' Y B^\mu(x)]\Phi(x) \tag{2.9}$$

The potential has a set of minima defined by:

$$\Phi_0^\dagger \Phi_0 = \frac{-\mu^2}{2\lambda} \tag{2.10}$$

We then spontaneously break the $SU(2)_L \times U_Y(1)$ symmetry by choosing the particular ground state, also known as a Vacuum Expectation Value (VEV):

$$\Phi_0 = \begin{pmatrix} 0 \\ \frac{v}{\sqrt{2}} \end{pmatrix} \tag{2.11}$$

Where

$$v = \sqrt{\frac{-\mu^2}{\lambda}} \tag{2.12}$$

We show below that this choice of vacuum is still invariant under a general $U_{EM}(1)$ gauge transformation if we define the hypercharge of the Higgs doublet to be $Y = \frac{1}{2}$:

$$e^{-i(Q)ef(x)}\Phi_0 = e^{-i(Y+I_3^W)ef(x)}\Phi_0 = \Phi_0 \tag{2.13}$$

Where Q is the electromagnetic charge, I_3^W is the third component of weak isospin, and $f(x)$ is an arbitrary function of x. Thus for this vacuum alignment we have preserved $U_{EM}(1)$ gauge symmetry below the breaking scale. We can now express $\Phi(x)$ in terms of deviations from its minimum, Φ_0:

$$\Phi(x) = \frac{1}{\sqrt{2}} \begin{pmatrix} \eta_1(x) + i\eta_2(x) \\ v + \sigma(x) + i\eta_3(x) \end{pmatrix} \tag{2.14}$$

We can then simplify this expression by gauging away the fields $\eta(x)$:

$$\Phi(x) = \frac{1}{\sqrt{2}} \begin{pmatrix} 0 \\ v + \sigma(x) \end{pmatrix} \tag{2.15}$$

Which is allowed due to the gauge invariance of $\Phi(x)$. Transforming $\Phi(x)$ in this way is known as going to the "unitary gauge". Inserting this form into the scalar Lagrangian (2.8) will produce a term

$$\frac{1}{2}m_H^2\sigma^2 \quad \text{where} \quad m_H^2 = \sqrt{-2\mu^2} \tag{2.16}$$

Thus giving a mass m_H to the scalar boson σ, which can now be identified as the Higgs particle. Additionally we will have terms like $m_W^2 W_\mu^\dagger W^\mu$, with m_W proportional to the breaking scale v, which are identified as mass terms for the gauge bosons. We will see that three of the four gauge bosons gain a mass while one remains massless, as is to be expected

from the breaking pattern.

One recognizes that the three massive gauge bosons will be the $W^+,\ W^-$ and Z while the massless particle is the photon. There is an additional wrinkle in that these are not just the low energy equivalents of the B and W_i but are actually linear combinations defined by:

$$\begin{aligned} W^+_\mu(x) &= \frac{1}{\sqrt{2}}[W_{1\mu}(x) - iW_{2\mu}(x)] \\ W^-_\mu(x) &= \frac{1}{\sqrt{2}}[W_{1\mu}(x) + iW_{2\mu}(x)] \\ Z_\mu(x) &= \cos(\Theta_W)W_{3\mu}(x) - \sin(\Theta_W)B_\mu(x) \\ A_\mu(x) &= \cos(\Theta_W)B_\mu(x) + \sin(\Theta_W)W_{3\mu}(x) \end{aligned} \tag{2.17}$$

Where Θ_W is a free parameter known as the weak mixing angle. Making these substitutions into Equations (2.8) and (2.5) we obtain the full boson Lagrangian:

$$\begin{aligned} \mathcal{L}_B + \mathcal{L}_H = &-\frac{1}{4}F_{\mu\nu}F^{\mu\nu} - \frac{1}{2}F^\dagger_{W\mu\nu}F^{\mu\nu}_W - \frac{1}{2}Z_{\mu\nu}Z^{\mu\nu} + m^2_W W^\dagger_\mu W^\mu + \frac{1}{2}m^2_Z Z_\mu Z^\mu \\ &+ \frac{1}{2}\partial^\mu\sigma\partial_\mu\sigma - \frac{1}{2}m^2_H\sigma^2 + \text{interaction terms} \end{aligned} \tag{2.18}$$

with:

$$m_W = \frac{1}{2}vg, \qquad m_Z = \frac{m_W}{\cos\Theta_W}, \qquad m_H = \sqrt{-2\mu^2} \tag{2.19}$$

Where the first three terms are the field strength tensors of the newly defined photon, W^{+-}, and Z bosons, respectively.

In addition to boson mass terms, we have interaction terms between fermions and $\Phi(x)$. E.g. for the charged leptons we have:

$$Y_l\overline{\Psi}^L(x)l_R(x)\Phi(x) + \text{hermitian conjugate} \tag{2.20}$$

Terms of this form are known as Yukawa terms, with constants (e.g. Y_l) known as Yukawa couplings. The existence of these terms dictate that when $\Phi(x)$ obtains a VEV below the

breaking scale $\frac{v}{\sqrt{2}}$, all fermions in the theory obtain a mass proportional to this scale via their interactions with Φ.

With that we have carried out the full process for spontaneous breaking of the electroweak symmetry. To summarize, above the breaking scale we have a theory that is symmetric under $SU(2)_L$, which gives rise to the weak force mediated by its 3 associated massless bosons W_j. It is also symmetric under $U_Y(1)$, which gives rise to an additional force mediated by the massless B boson. We also have four scalar particles that form a complex doublet $\Phi(x)$. We break this symmetry by giving a vacuum expectation value to $\Phi(x)$, so that below the scale of the VEV we have a $U_{EM}(1)$ symmetric theory with one associated massless gauge boson, the photon. We are left with one heavy scalar σ which is identified as the Standard Model Higgs, the remaining three scalars become extra degrees of freedom of the now massive $W^{\pm}$, and Z gauge bosons. These bosons are now heavy, so at energies below the breaking scale they must be produced off shell by interacting fermions. This leads to the weak force being exponentially weaker below the breaking scale and explains why it so much weaker than the electromagnetic force at low energies.

In the following chapter we will build on this relatively simple example by constructing a general framework for the spontaneous breaking of gauge groups.

Chapter 3

Spontaneous Breaking of Gauge Symmetries to Discrete Groups

3.1 Introduction

In the following chapter, we treat cases where a flavor gauge group breaks to a discrete group at an energy far above the electroweak scale, and examine the phenomenology of the scalar sector needed to carry out these breakings. Before we dive into the specifics of these breaking patterns, it is worth explaining why discrete symmetries are used in flavor model building. The Standard Model does not explain quark and lepton masses, nor does it explain how quarks and leptons mix. All of these values are treated as free parameters of the theory, i.e. the model provides no predictions as to their magnitude. These parameters can be constrained by imposing a discrete symmetry Γ on the Lagrangian. Particles are then assigned into irreducible representations (irreps) of Γ and predictions for masses and mixings can be derived from symmetry constraints. Many choices of this discrete flavor symmetry have been tried. As expected, larger groups can typically provide a fuller description of flavor physics, but there are examples of relatively small nonabelian discrete groups like A_4 and T' that are somewhat more economical. Here we take an agnostic approach as to the choice of discrete group and study a representative set of examples that have been used in model building.

Notable early extensions of the standard model with discrete symmetries include the work of Pakvasa and Sugawara [5] who used $\Gamma = S_3$ and focused on the quark sector, as well as Ma and collaborators [6, 7] who used $\Gamma = A_4$ to describe the lepton sector. Many other choices for Γ have been used in model building, several of which will be discussed below. For an early brief review of possible discrete groups that can be used for SM extensions see [8]. Recent extensive reviews with more complete and up to date bibliographies are also available. See for instance [9–12].

We have thus far framed discrete extensions of the Standard Model as residues of a high energy flavor gauge theory. Although this provides an elegant explanation for the origins of the discrete symmetry, there are also more practical reasons for having it arise in this way. Global discrete symmetries are violated by gravity [13], the discrete group can be anomalous [14], unwanted cosmic defects can be produced [15], etc. To avoid as many of these problems as possible the most expedient approach is to gauge the discrete symmetry, i. e., extend the SM by a continuous group G in such a way that no chiral anomalies are produced. Then one breaks this gauge group to the desired discrete group, $G \to \Gamma$, where now Γ is effectively anomaly free and avoids problems with gravity.

Various examples of gauge groups breaking to discrete groups have been discussed in the literature, but only in a few cases have the details of the minimization of the scalar potential and the extraction of the scalar spectrum been investigated. Here we plan to include these important details for many of the discrete groups of interest via the following procedure:

(i) First we provide irreps of G that contain trivial Γ singlets. These results are summarized in Appendix A.

(ii) Next we set up scalar potentials V with scalars in one of these irreps.

(iii) Then we find a vacuum expectation value (VEV) via the Reynolds operator [16] (similar to the perhaps more familiar Molien series [17]) that can break G to Γ.

(iv) Next we minimize V to show that the VEV indeed does properly break the symmetry.

(v) Finally, we provide the spectrum of scalar masses at the Γ level after the breaking. Our calculations are carried out with Mathematica and checked by hand where practical.

Many of the methods we employ were developed in work by Luhn [18] and by Merle and Zwicky [19], where some of the results summarized here can be found. We believe our results will be of interest to many model builders, since it will allow them to include the minimal set of scalars necessary to break a gauge symmetry to a discrete symmetry of interest. A few examples that go beyond the minimal set of scalars are also included, where

the symmetry breaking is carried out from a nonminimal G irrep or a non-minimal G.

3.2 Lie Group Invariant Potentials

Our task in this section is to construct Higgs potentials invariant under Lie groups G for specific irreps. But first we must see which irreps are suitable for spontaneous symmetry breaking (SSB), i.e., irreps whose decompositions include a trivial singlet of the desired subgroup $\Gamma \subset G$ to which we hope to break. Using the Mathematica package *decomposeLGreps* [20] along with GAP to generate the groups [21], one can easily produce tables of branching rules from Lie group irreps to subgroup irreps and find such singlets. We have done this for a number of cases and have included them in a short appendix for convenience.

3.2.1 Gauge Group Representations Containing Discrete Gauge Singlets

The discrete groups Γ we will discuss and the gauge groups where they can be minimally embedded are $A_4, S_4, A_5 \subset SO(3)$; $Q_6, T', O', I' \subset SU(2)$; and $T_7, \Delta(27), PSL(2,7) \subset SU(3)$.

These discrete groups can also be embedded non-minimally. For example, we include the case $A_4 \subset SU(3)$. Minimal and non-minimal embedding of other discrete groups can be handled in a way similar to what is discussed here, and we hope that the examples we discuss are sufficiently informative to aid in other cases.

To spontaneously break G to Γ with some irrep R of G, it is necessary that R contains a trivial Γ singlet. It is straightforward to look at the decomposition of R from G to Γ to make this determination. The decomposition can be carried out by standard techniques starting from character tables. Since it is the character tables that are usually provided in the literature, we here provide an appendix with the tables of decompositions of the first few irreps of $SO(3)$, $SU(2)$, and $SU(3)$ to discrete groups of interest. For example, as one can see in Table A.1 of the Appendix, the 7 and 9 dimensional irreps of $SO(3)$ have

trivial A_4 singlets, therefore these irreps are candidates for the scalar potential that allows the spontaneous symmetry breaking $SO(3) \to A_4$.

3.2.2 $SO(3)$ Potentials

We will begin our study of SSB by starting with relatively simple examples and then proceed to more sophisticated cases. But first, a note on cubic terms in the potential; a general renormalizable potential has quadratic, cubic, and quartic terms, but the cubic terms tend to significantly complicate the analysis. We exclude these terms for simplicity by imposing a Z_2 symmetry (or, like in some cases, they vanish upon summation), so the following potentials are actually $SO(3) \times Z_2$ invariant. (The Z_2 symmetry can be avoided by including the cubic terms or by gauging it too.) The effect of including the cubic terms is studied for some cases where the analysis is tractable in Section 3.4. We now proceed to our first example, the breaking pattern $SO(3) \to A_4$.

3.2.2.1 A_4

We begin by constructing an $SO(3)$ invariant potential [1]. As stated above, which irrep we use depends on the discrete subgroup of interest. For example, if we want to break to the tetrahedral group A_4, which has been used to describe the tri-bimaximal neutrino mixing pattern [10] [23] and co-bimaximal mixing [24], we look at Table A.1 and see that the lowest dimensional irrep we can use is the **7**. For references to other recent work with A_4 models see [25–27]. In terms of the fundamental **3** of $SO(3)$, we obtain a **7** as a direct product of three **3**s.

$$\mathbf{3} \times \mathbf{3} \times \mathbf{3} = \mathbf{1} + 3 \cdot \mathbf{3} + 2 \cdot \mathbf{5} + \mathbf{7} \tag{3.1}$$

[1] Group Theory Comments: The tetrahedral group $A_4 \subset SO(3)$ has double-valued representations that correspond to single-valued representations of the binary (double) tetrahedral group $T' \subset SU(2)$. As $SO(3)$ is not a subgroup of $SU(2)$, likewise A_4 is not a subgroup of T' [22]. Hence, besides the irreps of T' that are coincident with those of A_4, it has three additional spinor doublet-like irreps. The relationships between S_4 and O' and between A_5 and I' are similar.

This product gives a generic rank 3 tensor with 27 independent components. To isolate the **7**, we take only the totally symmetric part, which reduces the number of components from 27 to 10, giving the symmetric tensor S_{ijk}. Then, using the fact that the Kroenecker delta δ_{ij}, is an invariant of the fundamental irrep of SO groups (for a discussion of Lie group invariant tensors see [28]) we subtract off the three traces, $\sum_j^3 \delta_{jk} S_{ijk}$, i=1,2,3 , to obtain the traceless symmetric tensor T_{ijk}, which is our 7 dimensional $SO(3)$ irrep. As mentioned above, the most general renormalizable potential is constructed from the independent quadratic, cubic, and quartic contractions of this tensor. In this case there are two quartic terms, but notice that all the cubic terms, which necessarily include the anti-symmetric Levi-Civita Tensor, ϵ_{ijk} vanish upon summation. Hence the potential for the **7** is

$$V_7 = -m^2\, T_{ijk}T_{ijk} + \lambda\, (T_{ijk}T_{ijk})^2 + \kappa\; T_{ijm}T_{ijn}T_{kln}T_{klm} \tag{3.2}$$

In subsequent sections we find a vector (in a particular basis) pointing in the A_4 direction, then minimize the potential and find the mass eigenstates and show that they can all be positive which implies the minimum is stable. Minimization implies certain constraints on the coupling constants must be satisfied as will be discussed. We proceed in analogous fashion for other $G \to \Gamma$ cases, but first we will collect all the potentials we need for the purpose.

3.2.2.2 S_4

To break to the octahedral group, S_4, we see from Table A.2 that the lowest irrep we can use is the **9**. From examining Kroenecker products, we see that we must begin with the direct product of four **3**s. Similar to the results in the previous subsection, we take the symmetric part of this rank 4 tensor, S_{ijkl}, which reduces the number of components to 15. We then subtract off the six trace elements, $\sum \delta_{kl} S_{ijkl}$, to obtain the desired 9-component

tensor. The associated potential is

$$\begin{aligned} V_9 = &-m^2\, T_{ijkl}T_{ijkl} + \lambda\,(T_{ijkl}T_{ijkl})^2 + \kappa\, T_{ijkl}T_{ijkp}T_{mnop}T_{mnol} \\ &+\rho\, T_{ijkl}T_{ijop}T_{mnop}T_{mnkl} + \tau\, T_{ijkl}T_{ijmn}T_{kmop}T_{lnop} \end{aligned} \tag{3.3}$$

For examples where the octahedral group has been used to build models see [29, 30].

3.2.2.3 A_5

Another subgroup of interest, which has been used in a number of recent models [31–34], is A_5. From Table A.3 we see that the **13** is the lowest irrep that contains a trivial A_5 singlet. Again starting from the fundamental $SO(3)$ triplet one can show that the Kroenecker product of six **3**s is needed to get an irrep of this dimension. The symmetric part of this rank 6 tensor, S_{ijklmn} has 28 independent components, which is then reduced to 13 by subtracting off the 15 trace elements, $\sum \delta_{mn} S_{ijklmn}$. The potential is constructed in a fashion similar to the A_4 case.

$$\begin{aligned} V_{13} = &-m^2\, T_{ijklmn}T_{ijklmn} + \lambda\,(T_{ijklmn}T_{ijklmn})^2 + \kappa\, T_{ijklmn}T_{ijklmt}T_{opqrsn}T_{opqrst} \\ &+\rho\, T_{ijklmn}T_{ijklst}T_{opqrmn}T_{opqrst} + \tau\, T_{ijklmn}T_{ijkrst}T_{opqlmn}T_{opqrst} \end{aligned} \tag{3.4}$$

3.2.3 $SU(2)$ Potentials

We now proceed in a similar vein to construct $SU(2)$ invariant potentials. In fact, for the odd dimensional (real) representations, invariants must be constructed from triplets which furnish an unfaithful representation of $SU(2)$. As such the true symmetry of the theory is not given by the potential alone and must be determined from the specifics of the model, i.e., from the full Lagrangian. In the following cases, the omission of the cubic terms means the potentials have a $SU(2) \times U(1)$ symmetry, where the $U(1)$ is a phase. This phase can also be gauged and then broken if necessary to avoid problems with global symmetries, or in some cases cubic terms can be added that do not respect the $U(1)$.

3.2.3.1 Q_6

If we want to break to Q_6 we see from Table A.4 that the lowest dimensional irrep we can use is the **5**. However, as explained in [35, 36], this irrep will actually break to the continuous subgroup $Pin(2)$. So we must look at the next lowest irrep with a trivial $SU(2)$ singlet, the **7**. We cannot break with a real **7** as in Eq.(3.2) because there are no triplet representations of Q_6 that can be used to find a VEV in the unfaithful SO(3) representation. Thus we must use the complex **7**, which has the same potential as needed for the T' case which is given in Eq.(3.5) below.

3.2.3.2 T'

To break from $SU(2)$ to T', the binary tetrahedral group, we see from Table A.5 that the smallest $SU(2)$ irrep we can use is the **7**. Since we must construct it from triplets the potential is the same as in equation (3.2). The VEVs will also be the same.

Another possibility is to do the breaking to T' with a complex **7**, which can be thought of as a pair of real **7**s. We can now build our representation out of the fundamental doublets of $SU(2)$, where we get the **7** by taking the direct product of six **2**s and isolating the tensor symmetric on all indices. The potential is

$$\begin{aligned} V_{7_c} = & -m^2\, T_{ijklmn}T^{ijklmn} + \lambda\,(T_{ijklmn}T^{ijklmn})^2 + \kappa\, T_{ijklmn}T^{ijklmt}T_{opqrst}T^{opqrsn} \\ & +\rho\, T_{ijklmn}T^{ijklst}T_{opqrst}T^{opqrmn} + \tau\, T_{ijklmn}T^{ijkrst}T_{opqrst}T^{opqlmn} \end{aligned} \tag{3.5}$$

where the indices now run from 1 to 2. All cubic terms have vanished upon summation. T' models are economical and have been used to explain both quark and lepton sector parameters [8, 37–39, 39–43]. A more complete set of recent T' model references can be found in [43].

3.2.3.3 O'

To break from $SU(2)$ to O', the binary octahedral group, we see from Table A.6 that the smallest $SU(2)$ irrep we can use is the **9**. As in the S_4 example, we can construct our potential from triplets so the potential is the same as in equation (3.3) and the VEVs will again be the same.

We can also consider the case of a complex **9** and build the representation out of $SU(2)$ doublets. We obtain the **9** through the symmetric product of eight **2**s. The potential is

$$\begin{aligned} V_{9_c} = & -m^2\, T_{ijklmnop}T^{ijklmnop} + \lambda\,(T_{ijklmnop}T^{ijklmnop})^2 + \kappa\, T_{ijklmnop}T^{ijklmnox}T_{qrstuvwx}T^{qrstuvwp} \\ & +\rho\, T_{ijklmnop}T^{ijklmnwx}T_{qrstuvwx}T^{qrstuvop} + \tau\, T_{ijklmnop}T^{ijklmvwx}T_{qrstuvwx}T^{qrstunop} \\ & +\sigma\, T_{ijklmnop}T^{ijkluvwx}T_{qrstuvwx}T^{qrstmnop} \end{aligned} \tag{3.6}$$

O' is maximal in $SU(2)$, so the proper SSB is assured for a VEV that is O' invariant.

3.2.3.4 I'

The final $SU(2)$ breaking case we consider is I', the binary icosahedral group, which has been used in both three and four family extensions of the SM [44, 45]. Here the lowest $SU(2)$ irrep we can use is the real **13**, which yields the same potential as we used for A_5 (Eq. (3.4)).

Alternatively for the case of a complex **13** we see that it is given by the symmetric product of twelve **2**s. The potential has seven quartic invariants, and the first few terms are

$$\begin{aligned} V_{13_c} = & -m^2\, T_{abcdefghijkl}T^{abcdefghijkl} + \lambda\,(T_{abcdefghijkl}T^{abcdefghijkl})^2 \\ & +\kappa\, T_{abcdefghijkl}T^{abcdefghijkx}T_{mnopqrstuvwx}T^{mnopqrstuvwl} + \ldots \end{aligned} \tag{3.7}$$

Potentials for higher tensors can be cumbersome to write, so let us introduce a new notation to deal with them. For instance for the potential for the **13**, let us define

$$T_{12a} \cdot T^{12a} = T_{abcdefghijkl} T_{abcdefghijkl},$$

and

$$(T_{11a} \cdot T^{11a})^b_c (T_{11a} \cdot T^{11a})^c_b = T_{abcdefghijkl} T^{abcdefghijkx} T_{mnopqrstuvwx} T^{mnopqrstuvwl},$$

etc. Specifically we write na for the collection of indices $a_1 a_2 a_3 ... a_n$, etc. Then the full potential for the complex **13** takes the form

$$\begin{aligned} V_{13_c} = & - m^2 \, T_{12a} \cdot T^{12a} + \lambda \, (T_{12a} \cdot T^{12a})^2 + \kappa (T_{11a} \cdot T^{11a})^b_c (T_{11a} \cdot T^{11a})^c_b \\ & + \rho \, (T_{10a} \cdot T^{10a})^{2b}_{2c} (T_{10a} \cdot T^{10a})^{2c}_{2b} + \tau \, (T_{9a} \cdot T^{9a})^{3b}_{3c} (T_{9a} \cdot T^{9a})^{3c}_{3b} + \nu \, (T_{8a} \cdot T^{8a})^{4b}_{4c} (T_{8a} \cdot T^{8a})^{4c}_{4b} \\ & + \sigma \, (T_{7a} \cdot T^{7a})^{5b}_{5c} (T_{7a} \cdot T^{7a})^{5c}_{5b} + \chi \, (T_{6a} \cdot T^{6a})^{6b}_{6c} (T_{6a} \cdot T^{6a})^{6c}_{6b} \end{aligned} \tag{3.8}$$

This notation is consistent when the tensor T is totally symmetric on all of its indices [2].

Again, since I' is maximal in $SU(2)$, the proper SSB is assured for an I' invariant VEV.

3.2.4 $SU(3)$ potentials

Similar to the previous section, the omission of cubic terms means that the following potentials have an $SU(3) \times U(1)$ symmetry, where the $U(1)$ can be dealt with as described above.

[2] We could write an even more compact notation in generalized dyadic form, e.g., the ν term would be $\nu(T :^8 T) :^4 (T :^8 T)$ which again defines how the tensor contractions are to be made, but we find this form unnecessary here, but it could be useful for expressions involving more complicated group invariants. Cvitanovic's "Bird Track" notation[28] can also be useful for this purpose

3.2.4.1 A_4, T_7

In addition to SO(3), A_4 can originate from a broken $SU(3)$ symmetry. Looking at Table A.8 we see that the lowest dimensional irrep containing a trivial A_4 singlet is the **6**, but as explained in [18], neither the **6**, **10**, nor $\mathbf{15}'$ will break $SU(3)$ uniquely to A_4, i.e., giving these irreps an A_4 VEV will necessarily leave a group larger than A_4 unbroken. This leaves us with the **15** as the smallest irrep that will uniquely break to an A_4 subgroup, and the same logic applies to T_7. (A variety of T_7 models have been proposed, see [46–49].) To obtain a useful form of the $\mathbf{15}$ we first take the product $\mathbf{3} \times \mathbf{3} \times \bar{\mathbf{3}}$ in $SU(3)$; then by specifying the part that is symmetric on 2 indices, S^k_{ij}, we reduce the number of independent components from 27 to 18. Finally, subtracting off the three traces: $\sum_j^3 \delta_{jk} S^k_{ij},\ i = 1, 2, 3$, gives us the desired 15 component tensor. The associated potential [18] is

$$\begin{aligned} V_{15} = &- m^2\, T^k_{ij} T^{ij}_k + \lambda\, (T^k_{ij} T^{ij}_k)^2 + \kappa\, T^i_{jm} T^{jn}_i T^k_{ln} T^{lm}_k \\ &+ \rho\, T^i_{jm} T^{jn}_i T^m_{kl} T^{kl}_n + \tau\, T^m_{ij} T^{ij}_n T^n_{kl} T^{kl}_m + \nu\, T^i_{jm} T^j_{in} T^{km}_l T^{ln}_k \end{aligned} \tag{3.9}$$

3.2.4.2 $\Delta(27)$

From Table A.10 we see that we can use the **10** to spontaneously break from $SU(3)$ to $\Delta(27)$. We can get to this irrep by taking the product of three triplets and specifying the fully symmetric part of the resulting tensor, which reduces to the desired ten independent components. The potential is

$$V_{10} = -m^2\, T_{ijk} T^{ijk} + \lambda\, (T_{ijk} T^{ijk})^2 + \kappa\ T_{ijm} T^{ijn} T_{kln} T^{klm} \tag{3.10}$$

where the cubic terms have vanished upon summation. This result can also be found in [18]. Examples where $\Delta(27)$ has been used are [50, 51].

3.2.4.3 $PSL(2,7)$

Another group that has garnered considerable interest as a flavor symmetry is $PSL(2,7)$ [52]. Looking at Table A.11 we see that the lowest dimensional irrep of $SU(3)$ we can use to break to $PSL(2,7)$ is the **15′**, (Dynkin label [4 0]). To get to a **15′** we take the product of four fundamental triplets

$$\mathbf{3}\times\mathbf{3}\times\mathbf{3}\times\mathbf{3} = 3\cdot\mathbf{3} + 2\cdot\bar{\mathbf{6}} + 3\cdot\mathbf{15} + \mathbf{15'} \tag{3.11}$$

The generic rank 4 tensor has 81 independent components, requiring it be symmetric on all four indices reduces it to $\mathbf{15}'$ as required. The associated potential is

$$\begin{aligned} V_{15'} = &-m^2\, T_{ijkl}T^{ijkl} + \lambda\,(T_{ijkl}T^{ijkl})^2 \\ &+\kappa\, T_{ijkl}T^{ijkm}T_{mnop}T^{lnop} + \rho\, T_{ijkl}T^{ijmn}T_{mnop}T^{klop} \end{aligned} \tag{3.12}$$

Also of interest is the next lowest irrep suitable for breaking from $SU(3)$ to $PSL(2,7)$, the **28**. We build this irrep by taking the symmetric product of six triplets, giving a fully symmetric rank 6 tensor with 28 components. The associated potential is

$$\begin{aligned} V_{28} = &-m^2\, T_{ijklmn}T^{ijklmn} + \lambda\,(T_{ijklmn}T^{ijklmn})^2 \\ &+\kappa\, T_{ijklmn}T^{ijklmt}T_{opqrst}T^{opqrsn} + \rho\, T_{ijklmn}T^{ijklst}T_{opqrst}T^{opqrmn} \\ &+\tau\, T_{ijklmn}T^{ijkrst}T_{opqrst}T^{opqlmn} \end{aligned} \tag{3.13}$$

3.3 Vaccuum Alignments for Spontaneous Symmetry Breaking

3.3.1 Vacuua for $SO(3)$ Potentials

The invariant tensors from the previous section can be written in terms of a d-dimensional orthonormal bases, where d is the number of independent tensor components. To illustrate this consider the **5** of $SO(3)$ which is a second rank symmetric traceless tensor T_{ij}. It has

a basis

$$
\begin{aligned}
|1\rangle &= \frac{1}{\sqrt{2}}(|11\rangle - |22\rangle) \\
|2\rangle &= \frac{1}{\sqrt{6}}(|11\rangle + |22\rangle - 2\cdot|33\rangle) \\
|3\rangle &= \frac{1}{\sqrt{2}}(|12\rangle + |21\rangle) \\
|4\rangle &= \frac{1}{\sqrt{2}}(|13\rangle + |31\rangle) \\
|5\rangle &= \frac{1}{\sqrt{2}}(|23\rangle + |32\rangle)
\end{aligned}
\tag{3.14}
$$

Where $|ij\rangle$ is the ij^{th} component of the tensor. Using this basis the matrix form of T_{ij} is

$$
T_{ij} = \begin{pmatrix}
\frac{1}{\sqrt{2}}|1\rangle + \frac{1}{\sqrt{6}}|2\rangle & \frac{1}{\sqrt{2}}|3\rangle & \frac{1}{\sqrt{2}}|4\rangle \\
\frac{1}{\sqrt{2}}|3\rangle & -\frac{1}{\sqrt{2}}|1\rangle + \frac{1}{\sqrt{6}}|2\rangle & \frac{1}{\sqrt{2}}|5\rangle \\
\frac{1}{\sqrt{2}}|4\rangle & \frac{1}{\sqrt{2}}|5\rangle & -\sqrt{\frac{2}{3}}|2\rangle
\end{pmatrix}
\tag{3.15}
$$

With an explicit basis, it now makes sense to look for a d-component vacuum alignment that minimizes the potential and is invariant under the desired discrete subgroup. How do we find this specified direction? First, note that we can express our basis above in polynomial form, assigning component 1 to x, 2 to y, and 3 to z:

$$
\begin{aligned}
|1\rangle &= \frac{1}{\sqrt{2}}(x^2 - y^2) \\
|2\rangle &= \frac{1}{\sqrt{6}}(x^2 + y^2 - 2z^2) \\
|3\rangle &= \frac{1}{\sqrt{2}}(xy + yx) = \sqrt{2}xy \\
|4\rangle &= \sqrt{2}xz \\
|5\rangle &\sqrt{2}yz
\end{aligned}
$$

So if we find a polynomial that is invariant under the desired subgroup we can convert it into a vacuum alignment by expressing it as a vector in terms of these basis functions[19].

To find a polynomial, $\mathcal{I}(x,y,z)$, invariant under a group H, one employs the Reynolds Operator [16]

$$\mathcal{I}(x,y,z) = \frac{1}{|\mathcal{R}(H)|}\sum_{h\in\mathcal{R}(H)} f(h\circ\begin{pmatrix}x\\y\\z\end{pmatrix}) \tag{3.16}$$

Where $\mathcal{R}(H)$ is a representation of the group, $|\mathcal{R}(H)|$ is the number of elements in the group, and $f(h\circ\begin{pmatrix}x\\y\\z\end{pmatrix})$ signifies the result of a group element h acting on the vector (x,y,z) and then input into a trial function $f(x,y,z)$. Trial polynomials of the form $x^n y^m z^{d-n-m}$ will typically be most useful in finding invariants of degree d. Note we have specified polynomials in three variables here, but we can use the same procedure to find invariants in terms of any number of variables, real or complex. E.g., in two real dimensions we can find an invariant $\mathcal{I}(x,y)$ with a trial function $f(x,y)$.

3.3.1.1 A_4

As an initial practical example lets examine the symmetry breaking pattern $SO(3) \to A_4$. The irrep of interest is a $\mathbf{7}$ which is the symmetric, traceless part of $\mathbf{3}\times\mathbf{3}\times\mathbf{3}$. Expressed in terms of 7 independent components we have:

$$|1\rangle = \frac{1}{2}(|111\rangle - |122\rangle - |212\rangle - |221\rangle) \tag{3.17}$$

$$|2\rangle = \frac{1}{\sqrt{60}}(3\cdot|111\rangle + |122\rangle + |212\rangle + |221\rangle - 4\cdot|133\rangle - 4\cdot|313\rangle - 4\cdot|331\rangle) \tag{3.18}$$

$$|3\rangle = \frac{1}{2}(|222\rangle - |112\rangle - |121\rangle - |211\rangle) \tag{3.19}$$

$$|4\rangle = \frac{1}{\sqrt{60}}(3\cdot|222\rangle + |112\rangle + |121\rangle + |211\rangle - 4\cdot|233\rangle - 4\cdot|323\rangle - 4\cdot|332\rangle) \tag{3.20}$$

$$|5\rangle = \frac{1}{2}(|333\rangle - |113\rangle - |131\rangle - |311\rangle) \tag{3.21}$$

$$|6\rangle = \frac{1}{\sqrt{60}}(3\cdot|333\rangle + |113\rangle + |131\rangle + |311\rangle - 4\cdot|223\rangle - 4\cdot|232\rangle - 4\cdot|322\rangle) \tag{3.22}$$

$$|7\rangle = \frac{1}{\sqrt{6}}(|123\rangle + |132\rangle + |213\rangle + |231\rangle + |312\rangle + |321\rangle) \tag{3.23}$$

$$\tag{3.24}$$

Using xyz as a trial polynomial in equation (3.16), ($d = 3$, $n = m = 1$) gives us back xyz as our invariant polynomial. Expressed in terms of this basis our A_4 invariant vacuum alignment is remarkably simple:

$$v = [0, 0, 0, 0, 0, 0, 1] \tag{3.25}$$

The VEV for spontaneous breaking will be this unit vector multiplied by a constant which minimizes the potential. We must show that this VEV is unique to A_4. The gauge group will spontaneously break to the largest subgroup which leaves that VEV invariant. So G will only break to a desired subgroup, H, if there is no other group, H', which is invariant under the specified VEV and satisfies $H \subset H' \subset G$. It is difficult to systematically determine which subgroup will be left invariant for a given breaking, and in particular if there is a higher invariance than the desired discrete group, so each case must be considered individually. For the present case we start with the fact that the only groups that contain A_4 and are subgroups of $SO(3)$ are S_4 and A_5. Examining the branching rules for both these groups, one sees that a **7** of $SO(3)$ does not break to a trivial singlet of either S_4 or A_5, and thus the largest group left invariant by this VEV must be A_4. Hence we have obtained the desired result for the case at hand.

3.3.1.2 S_4

For the **9** of SO(3), it is more convenient to express our basis in terms of spherical harmonics:

$$|1\rangle = Y_4^0;\ \ |2\rangle = \frac{i}{\sqrt{2}}(Y_4^1 + Y_4^{-1});\ \ |3\rangle = \frac{1}{\sqrt{2}}(Y_4^1 - Y_4^{-1});\ \ |4\rangle = \frac{1}{\sqrt{2}}(Y_4^2 + Y_4^{-2});$$
$$|5\rangle = \frac{i}{\sqrt{2}}(Y_4^2 - Y_4^{-2});\ \ |6\rangle = \frac{i}{\sqrt{2}}(Y_4^3 + Y_4^{-3});\ \ |7\rangle = \frac{1}{\sqrt{2}}(Y_4^3 - Y_4^{-3});$$
$$|8\rangle = \frac{1}{\sqrt{2}}(Y_4^4 + Y_4^{-4});\ \ |9\rangle = \frac{i}{\sqrt{2}}(Y_4^4 - Y_4^{-4}). \tag{3.26}$$

We find that the polynomial, $x^4 + y^4 + z^4$ is S_4 invariant. Expressed in terms of our basis this is

$$v = [\sqrt{\frac{7}{5}}, 0, 0, 0, 0, 0, 0, 1, 0] \tag{3.27}$$

S_4 is also a maximal subgroup of SO(3), so we can be certain our alignment breaks SO(3) uniquely to S_4.

3.3.1.3 A_5

As mentioned previously, to break from $SO(3)$ to A_5 the irrep of interest is the totally symmetric traceless tensor with 13 independent components contained in $\mathbf{3} \times \mathbf{3} \times \mathbf{3} \times \mathbf{3} \times \mathbf{3} \times \mathbf{3}$. In this case it is again easier (and yields equivalent results) to express the components in terms of spherical harmonics[3] of degree l = 6, Y_6^m (where $m = -6, -5...0...5, 6$). In order to get real basis vectors, we define them as

$$|1\rangle = Y_6^0;\ \ |2\rangle = \frac{i}{\sqrt{2}}(Y_6^1 + Y_6^{-1});\ \ |3\rangle = \frac{1}{\sqrt{2}}(Y_6^1 - Y_6^{-1});\ \ |4\rangle = \frac{1}{\sqrt{2}}(Y_6^2 + Y_6^{-2});$$
$$|5\rangle = \frac{i}{\sqrt{2}}(Y_6^2 - Y_6^{-2});\ \ |6\rangle = \frac{i}{\sqrt{2}}(Y_6^3 + Y_6^{-3});\ \ |7\rangle = \frac{1}{\sqrt{2}}(Y_6^3 - Y_6^{-3});$$
$$|8\rangle = \frac{1}{\sqrt{2}}(Y_6^4 + Y_6^{-4});\ \ |9\rangle = \frac{i}{\sqrt{2}}(Y_6^4 - Y_6^{-4});\ \ |10\rangle = \frac{i}{\sqrt{2}}(Y_6^5 + Y_6^{-5});$$
$$|11\rangle = \frac{1}{\sqrt{2}}(Y_6^5 - Y_6^{-5}) \quad |12\rangle = \frac{1}{\sqrt{2}}(Y_6^6 + Y_6^{-6});\ \ |13\rangle = \frac{i}{\sqrt{2}}(Y_6^6 - Y_6^{-6}). \tag{3.28}$$

[3] One can also use this method for the A_4 case, see [53].

We find that a degree six invariant polynomial is $(\frac{(1+\sqrt{5})^2}{4}\,x^2-y^2)(\frac{(1+\sqrt{5})^2}{4}\,y^2-z^2)(\frac{(1+\sqrt{5})^2}{4}\,z^2-x^2)$ [19]. The associated VEV is proportional to

$$v = [1, 0, 0, -\sqrt{\frac{21}{2}}, 0, 0, 0, -\sqrt{7}, 0, 0, 0, \sqrt{\frac{105}{22}}, 0] \tag{3.29}$$

Because A_5 is a maximal subgroup of SO(3), i.e., there is no group H' that nontrivially satisfies $A_5 \subset H' \subset SO(3)$ for any VEV of the **13**, and again we can be sure the VEV in eq. (3.29) breaks $SO(3)$ uniquely to A_5.

3.3.2 Vacuua for SU(2) Potentials

3.3.2.1 Q_6

For the breaking $SU(2) \to Q_6$ we use the same basis as with T' above. We find the polynomial $\frac{1}{2}(x^6 + y^6)$ is left invariant by Q_6, and this leads to a VEV proportional to

$$v = [1, 1, 0, 0, 0, 0, 0, 0, 0, 0, 0, 0, 0, 0, 0] \tag{3.30}$$

To make sure we have broken to Q_6 and not any larger subgroups, we first note that the **7** does not break to any Q_n with $n > 6$ (see page 6 of [36]). The only other larger $SU(2)$ subgroup that can be spontaneously broken with a **7** is T', but we find that T' has only one degree six invariant which is given in the subsection above. Therefore, the VEV in Eq. (3.30) is the result we were seeking.

3.3.2.2 T'

Because $SU(2)$ breaks to T' from the same real seven dimensional irrep that breaks $SO(3)$ to A_4, the potentials are the same and the basis will be the same as in the A_4 section above. In addition, the Reynolds operator yields the same polynomial invariant xyz, so the VEV is identical. On the other hand the complex **7** has a different basis, specifically that of

the symmetric tensor with 6 indices[4].

$$
\begin{aligned}
|1\rangle =& |111111\rangle \\
|2\rangle =& \frac{1}{\sqrt{6}}(|111112\rangle + |111121\rangle + |111211\rangle + |112111\rangle + |121111\rangle + |211111\rangle) \\
|3\rangle =& \frac{1}{\sqrt{15}}(|111122\rangle + |111212\rangle + |111221\rangle + |112112\rangle + |112121\rangle + |112211\rangle + \\
& |121112\rangle + |121121\rangle + |121211\rangle + |122111\rangle + |211112\rangle + |211121\rangle + \\
& |211211\rangle + |212111\rangle + |221111\rangle) \\
|4\rangle =& \frac{1}{\sqrt{20}}(|111222\rangle + |112122\rangle + |112212\rangle + |112221\rangle + |121122\rangle + |121212\rangle + \\
& |121221\rangle + |122112\rangle + |122121\rangle + |122211\rangle + |211122\rangle + |211212\rangle + \\
& |211221\rangle + |212112\rangle + |212121\rangle + |212211\rangle + |221112\rangle + |221121\rangle + \\
& |221211\rangle + |222111\rangle) \\
|5\rangle =& \frac{1}{\sqrt{15}}(|112222\rangle + |121222\rangle + |122122\rangle + |122212\rangle + |122221\rangle + |211222\rangle +
\end{aligned}
$$

[4]Because this is a complex irrep there are actually 14 basis states; the basis states listed are the 7 real parts of the tensor components, while bases 8 through 14 are the imaginary parts. These conjugate components have been suppressed here since they will always be set to zero at vacuum in order to have a real VEV. This will be the case for most of the complex irreps we consider.

$$|212122\rangle + |212212\rangle + |212221\rangle + |221122\rangle + |221212\rangle + |221221\rangle +$$
$$|222112\rangle + |222121\rangle + |222211\rangle$$
$$|6\rangle = \frac{1}{\sqrt{6}}(|122222\rangle + |212222\rangle + |221222\rangle + |222122\rangle + |222212\rangle + |222221\rangle$$
$$|7\rangle = |222222\rangle$$

We find that the polynomial $\frac{1}{2}(xy^5 - yx^5)$ is left invariant for this representation and the associated VEV is proportional to

$$v = [0, -1, 0, 0, 0, 1, 0, 0, 0, 0, 0, 0, 0, 0] \tag{3.31}$$

To make sure we have broken to T′ we must show that this VEV does not break $SU(2)$ to any larger group. The only $SU(2)$ subgroups that contain T′ as a subgroup are I′, the binary icosahedral group, and O', the binary octahedral group. Looking at tables of branching rules we see that the **7** of $SU(2)$ does not contain a trivial singlet of either of these groups, so we can be sure the breaking is to T' as desired.

3.3.2.3 O'

Like the other double cover groups, the basis and vacuum direction for the breaking of O' with a real **9** of $SU(2)$ will be the same as its $SO(3) \to S_4$ counterpart above.

The complex **9** arises from the basis of the symmetric tensor with 8 doublet indices:

$$\begin{aligned}
&|1\rangle = |11111111\rangle\,; \;\; |2\rangle = |22222222\rangle\,; \;\; |3\rangle = \frac{1}{\sqrt{8}}(|11111112\rangle + perms);\\
&|4\rangle = \frac{1}{\sqrt{8}}(|22222221\rangle + perms); \;\; |5\rangle = \frac{1}{\sqrt{28}}(|11111122\rangle + perms);\\
&|6\rangle = \frac{1}{\sqrt{28}}(|22222211\rangle + perms);; \;\; |7\rangle = \frac{1}{\sqrt{56}}(|11111222\rangle + perms);\\
&|8\rangle = \frac{1}{\sqrt{56}}(|22222111\rangle + perms); \;\; |9\rangle = \frac{1}{\sqrt{70}}(|11112222\rangle + perms),
\end{aligned} \tag{3.32}$$

where here and in what follows '$+perms$' means we include all permutations of tensor indices.

Here the O' invariant polynomial is $x^8+y^8+14x^4y^4$, which leads to a VEV proportional to

$$v = [1, 1, 0, 0, 0, 0, 0, 0, \frac{14}{\sqrt{70}}, 0, 0, 0, 0, 0, 0, 0, 0, 0] \tag{3.33}$$

Where $|1\rangle = |2\rangle$ and $|9\rangle = \frac{14}{\sqrt{70}}|1\rangle$.

O' is a maximal subgroup of $SU(2)$, so we can be certain our alignment breaks SU(2) uniquely to O'.

3.3.2.4 I'

Similar to the spontaneous symmetry breaking behavior of the T' case relative to the A_4 case with a real **7**, the basis for the symmetry breaking to I' with the real **13** will be the same as for A_5 above. Additionally, both groups have the same invariant polynomial so the vacuum directions will be the same.

On the other hand, a complex **13** arises from the basis of the symmetric tensor with 12 doublet indices:

$$\begin{aligned}
&|1\rangle = \ |111111111111\rangle\,; \ \ |2\rangle = \ |222222222222\rangle\,; \ \ |3\rangle = \frac{1}{\sqrt{12}}(|111111111112\rangle + perms);\\
&|4\rangle = \frac{1}{\sqrt{12}}(|222222222221\rangle + perms); \ \ |5\rangle = \frac{1}{\sqrt{66}}(|111111111122\rangle + perms);\\
&|6\rangle = \frac{1}{\sqrt{66}}(|222222222211\rangle + perms);; \ \ |7\rangle = \frac{1}{\sqrt{220}}(|111111111222\rangle + perms);\\
&|8\rangle = \frac{1}{\sqrt{220}}(|222222222111\rangle + perms); \ \ |9\rangle = \frac{1}{\sqrt{495}}(|111111112222\rangle + perms);\\
&|10\rangle = \frac{1}{\sqrt{495}}(|222222221111\rangle + perms); \ \ |11\rangle = \frac{1}{\sqrt{792}}(|111111122222\rangle + perms);\\
&|12\rangle = \frac{1}{\sqrt{792}}(|222222211111\rangle + perms); \ \ |13\rangle = \frac{1}{\sqrt{924}}(|222222111111\rangle + perms).
\end{aligned} \tag{3.34}$$

Here the I' invariant polynomial is $x^{11}y + 11x^6y^6 - y^{11}x$, which leads to a VEV pro-

portional to

$$v = [0, 0, 1, -1, 0, 0, 0, 0, 0, 0, 0, 0, \sqrt{\frac{11}{12}}, 0, 0, 0, 0, 0, 0, 0, 0, 0, 0, 0, 0, 0] \tag{3.35}$$

Where clearly $|4\rangle = -|3\rangle$ and $|13\rangle = \sqrt{\frac{11}{12}} \cdot |3\rangle$.

I' is a known maximal subgroup of SU(2), so we can be certain our alignment breaks SU(2) uniquely to I'.

3.3.3 Vacuua for $SU(3)$ Potentials

First let us show that we can get discrete subgroups from continuous groups in a non-minimal way. For this purpose we use the example $SU(3) \to A_4$ where we break with a **15** of $SU(3)$. Then we find vacuua for the minimal cases discussed above. Then finally, for $PSL(2, 7)$ we give both a minimal case with a VEV for the $\mathbf{15'}$ of $SU(3)$ and a nonminimal breaking via a **28** of $SU(3)$ using the potential given in eq. (3.13).

3.3.3.1 A_4

The complex 15 dimensional basis needed to break SU(3) to A_4 is that of the traceless $3 \times 3 \times \bar{3}$ tensor that is symmetric on the first two indices [18].

$$
\begin{aligned}
|1\rangle &= \frac{1}{\sqrt{3}}(|111\rangle - |122\rangle - |212\rangle) \\
|2\rangle &= \frac{1}{2\sqrt{6}}(2\cdot|111\rangle + |122\rangle + |212\rangle - 3\cdot|133\rangle - 3\cdot|313\rangle) \\
|3\rangle &= \frac{1}{\sqrt{3}}(|222\rangle - |233\rangle - |323\rangle) \\
|4\rangle &= \frac{1}{2\sqrt{6}}(2\cdot|222\rangle + |233\rangle + |323\rangle - 3\cdot|211\rangle - 3\cdot|121\rangle) \\
|5\rangle &= \frac{1}{\sqrt{3}}(|333\rangle - |311\rangle - |131\rangle) \\
|6\rangle &= \frac{1}{2\sqrt{6}}(2\cdot|333\rangle + |311\rangle + |131\rangle - 3\cdot|322\rangle - 3\cdot|232\rangle) \\
|7\rangle &= |112\rangle\,;\ \ |8\rangle = |113\rangle\,;\ \ |9\rangle = |223\rangle \\
|10\rangle &= |221\rangle\,;\ \ |11\rangle = |331\rangle\,;\ \ |12\rangle = |332\rangle \\
|13\rangle &= \frac{1}{\sqrt{2}}(|123\rangle + |213\rangle);\ \ |14\rangle = \frac{1}{\sqrt{2}}(|231\rangle + |321\rangle);\ \ |15\rangle = \frac{1}{\sqrt{2}}(|312\rangle + |132\rangle)
\end{aligned}
\tag{3.36}
$$

Because this tensor is symmetric on only two indices we find that the invariant should be of degree 2 in the variables x, y, z and degree 1 in the conjugate variables, x^*, y^*, z^*. Inputting the trial polynomial xyz^* into the Reynolds operator produces the invariant: $xyz^* + yzx^* + xzy^*$. In this basis the VEV is proportional to

$$
v = [0,0,0,0,0,0,0,0,0,0,0,0,1,1,1,0,0,0,0,0,0,0,0,0,0,0,0,0,0,0,0] \tag{3.37}
$$

i.e., where $|13\rangle = |14\rangle = |15\rangle$ with all other components zero.

One can examine the generators of A_4 and SU(3) to see that this VEV breaks SU(3) uniquely to A_4, see [18].

3.3.3.2 T_7

The invariant tensor object and therefore our basis for T_7 is the same as for A_4 above. The invariant polynomial in this case is $x^2y^* + y^2z^* + z^2x^*$ and the corresponding VEV is proportional to

$$v = [0,0,0,0,0,0,1,0,1,0,1,0,0,0,0,0,0,0,0,0,0,0,0,0,0,0,0,0,0,0,0] \tag{3.38}$$

where $|7\rangle = |9\rangle = |11\rangle$.

Similarly to the A_4 case, one can verify this VEV uniquely breaks $SU(3)$ to T_7 by examining how the T_7 generators operate on v, see [18].

3.3.3.3 $\Delta(27)$

For $\Delta(27)$, the relevant invariant tensor is the fully symmetric part of $3 \times 3 \times 3$ with 10 independent components

$$\begin{aligned}
&|1\rangle = |111\rangle\,; \;\; |2\rangle = |222\rangle\,; \;\; |3\rangle = |333\rangle \\
&|4\rangle = \frac{1}{\sqrt{3}}(|112\rangle + |121\rangle + |211\rangle); \;\; |5\rangle = \frac{1}{\sqrt{3}}(|113\rangle + |131\rangle + |311\rangle) \\
&|6\rangle = \frac{1}{\sqrt{3}}(|221\rangle + |212\rangle + |122\rangle); \;\; |7\rangle = \frac{1}{\sqrt{3}}(|223\rangle + |232\rangle + |322\rangle) \\
&|8\rangle = \frac{1}{\sqrt{3}}(|331\rangle + |313\rangle + |133\rangle); \;\; |9\rangle = \frac{1}{\sqrt{3}}(|332\rangle + |323\rangle + |233\rangle) \\
&|10\rangle = \frac{1}{\sqrt{6}}(|123\rangle + |231\rangle + |312\rangle + |321\rangle + |213\rangle + |132\rangle)
\end{aligned} \tag{3.39}$$

The invariant polynomial is $x^3 + y^3 + z^3$, which gives us a VEV proportional to

$$v = [1,1,1,0,0,0,0,0,0,0,0,0,0,0,0,0,0,0,0,0,0,0,0,0,0] \tag{3.40}$$

Again explicit forms of the generators can be examined in order to verify the uniqueness of this VEV for breaking from $SU(3)$ to $\Delta(27)$ [18].

3.3.3.4 $PSL(2,7)$

Our basis for the $\mathbf{15'}$ is that of the fully symmetric $3 \times 3 \times 3 \times 3$ tensor

$$
\begin{aligned}
&|1\rangle = |1111\rangle\,; \;\; |2\rangle = |2222\rangle\,; \;\; |3\rangle = |3333\rangle \\
&|4\rangle = \frac{1}{2}(|1112\rangle + |1121\rangle + |1211\rangle + |2111\rangle); \;\; |5\rangle = \frac{1}{2}(|1113\rangle + |1131\rangle + |1311\rangle + |3111\rangle) \\
&|6\rangle = \frac{1}{2}(|2221\rangle + |2212\rangle + |2122\rangle + |1222\rangle); \;\; |7\rangle = \frac{1}{2}(|2223\rangle + |2232\rangle + |2322\rangle + |3222\rangle) \\
&|8\rangle = \frac{1}{2}(|3331\rangle + |3313\rangle + |3133\rangle + |1333\rangle); \;\; |9\rangle = \frac{1}{2}(|3332\rangle + |3323\rangle + |3233\rangle + |2333\rangle) \\
&|10\rangle = \frac{1}{\sqrt{6}}(|1122\rangle + perms); \;\; |11\rangle = \frac{1}{\sqrt{6}}(|1133\rangle + perms); \;\; |12\rangle = \frac{1}{\sqrt{6}}(|2233\rangle + perms) \\
&|13\rangle = \frac{1}{\sqrt{12}}(|1123\rangle + perms); \;\; |14\rangle = \frac{1}{\sqrt{12}}(|2213\rangle + perms); \;\; |15\rangle = \frac{1}{\sqrt{12}}(|3312\rangle + perms)
\end{aligned}
\tag{3.41}
$$

The relevant invariant polynomial is $x^3z + y^3x + z^3y$ [19], which gives a VEV proportional to

$$v = [0,0,0,0,1,1,0,0,1,0,0,0,0,0,0,0,0,0,0,0,0,0,0,0,0,0,0,0,0,0,0] \tag{3.42}$$

where the nonvanishing vacuum components are $|5\rangle = |6\rangle = |9\rangle$. We can be sure we have broken to the correct subgroup [5] because $PSL(2,7)$ is known to be a maximal in $SU(3)$.

Finally, for the **28** of $SU(3)$ we have the basis for the fully symmetric $\mathbf{3}^6$ tensor of the

[5] Luhn [54] has shown that the VEV in eq. (3.42) has a Z_{28} symmetry and the vacuum of the potential $V_{15'}$ in eq. (3.12) is also symmetric under this symmetry. However, other terms in the Lagrangian will violate this Z_{28}, e.g., the Yukawa terms. As it is a discrete symmetry, its breaking can not lead to a pseudo Goldstone boson, but there could be other phenomenological consequences of this Z_{28} that would be interesting to explore.

form

$$\begin{aligned}
&|1\rangle = |111111\rangle\,; \quad |2\rangle = |222222\rangle\,; \quad |3\rangle = |333333\rangle\,; \quad |4\rangle = \frac{1}{\sqrt{6}}(|111112\rangle + perms)\\
&|5\rangle = \frac{1}{\sqrt{6}}(|111113\rangle + perms); \quad |6\rangle = \frac{1}{\sqrt{6}}(|222221\rangle + perms)\\
&|7\rangle = \frac{1}{\sqrt{6}}(|222223\rangle + perms); \quad |8\rangle = \frac{1}{\sqrt{6}}(|333331\rangle + perms)\\
&|9\rangle = \frac{1}{\sqrt{6}}(|333332\rangle + perms); \quad |10\rangle = \frac{1}{\sqrt{15}}(|111122\rangle + perms)\\
&|11\rangle = \frac{1}{\sqrt{15}}(|111133\rangle + perms); \quad |12\rangle = \frac{1}{\sqrt{15}}(|222211\rangle + perms)\\
&|13\rangle = \frac{1}{\sqrt{15}}(|222233\rangle + perms); \quad |14\rangle = \frac{1}{\sqrt{15}}(|333311\rangle + perms)\\
&|15\rangle = \frac{1}{\sqrt{15}}(|333322\rangle + perms); \quad |16\rangle = \frac{1}{\sqrt{30}}(|111123\rangle + perms)\\
&|17\rangle = \frac{1}{\sqrt{30}}(|222231\rangle + perms); \quad |18\rangle = \frac{1}{\sqrt{30}}(|333312\rangle + perms)\\
&|19\rangle = \frac{1}{\sqrt{20}}(|111222\rangle + perms); \quad |20\rangle = \frac{1}{\sqrt{20}}(|111333\rangle + perms)\\
&|21\rangle = \frac{1}{\sqrt{20}}(|222333\rangle + perms); \quad |22\rangle = \frac{1}{\sqrt{60}}(|111223\rangle + perms)\\
&|23\rangle = \frac{1}{\sqrt{60}}(|111332\rangle + perms); \quad |24\rangle = \frac{1}{\sqrt{60}}(|222113\rangle + perms)\\
&|25\rangle = \frac{1}{\sqrt{60}}(|222331\rangle + perms); \quad |26\rangle = \frac{1}{\sqrt{60}}\,|333112\rangle + perms);\\
&|27\rangle = \frac{1}{\sqrt{60}}(|333221\rangle + perms) \quad |28\rangle = \frac{1}{\sqrt{90}}(|112233\rangle + perms)
\end{aligned} \tag{3.43}$$

The necessary invariant polynomial is $x^5y + y^5z + z^5x - 5x^2y^2z^2$[19], which gives real components with VEV proportional to

$$v = \left[0,0,0,1,0,0,1,1,0,0,0,0,0,0,0,0,0,0,0,0,0,0,0,0,0,0,0,-\sqrt{\frac{5}{3}}\right] \tag{3.44}$$

i.e., where $|4\rangle = |7\rangle = |8\rangle$, and $|28\rangle = -\sqrt{\frac{5}{3}} \cdot |4\rangle$ and where we recall that all conjugate components (29–56) are set to zero.

3.4 Vacuum Expectation Values and Mass Spectra

Thus far, we have discussed how to set up potentials corresponding to specific gauge group representations and then found vacuum alignments that can be used to break the gauge symmetry to desired subgroups. In this section we minimize the scalar potentials and show where symmetry breaking in the desired directions are allowed. We will find the scale of the symmetry breaking and resulting tree level scalar mass states in terms of the coupling constants of the potential. As usual, the minimization conditions of the potential will lead to constraints on the values of these constants.

3.4.1 $SO(3)$ Cases

3.4.1.1 A_4

We found earlier that a VEV in the direction (3.25) will break $SO(3)$ to A_4. The actual VEV is proportional to this direction vector, with the constant of proportionality being the scale of the breaking. To determine this scale one must minimize the potential (3.2). To achieve this we compute the first derivative with respect to each basis state, insert the alignment from (3.25), and set this equal to zero. This alignment (and all of our alignments below) will give an equation in terms of one basis state (or one linear combination of basis states). For the present case we solve for $|7\rangle$ and take the positive solution to obtain the VEV

$$\mathcal{V} = \sqrt{\frac{3m^2}{2(3\lambda+\kappa)}}\,[0,0,0,0,0,0,1] \tag{3.45}$$

As for any non-trivial stable vacuum, m^2 must be positive. To have a real value for our breaking scale $3\lambda+\kappa$ must also be positive. We find the scalar mass states by calculating the matrix of second derivatives (the Hessian), inserting the VEV from above, and computing the eigenvalues of the matrix. The resulting values and their multiplicities are given in Table 3.1.

Looking at Table A.1 in the Appendix, we see that the multiplicities of the eigenvalues

Value	Multiplicity
0	3
$4m^2$	1
$\frac{8m^2\kappa}{5(3\lambda+\kappa)}$	3

Table 3.1: Scalar mass eigenstates for the SSB pattern $SO(3) \to A_4$ using a real **7** of $SO(3)$.

match up with the branching of the **7** for $SO(3) \to A_4$, as expected. We see that there are three zero eigenvalues as expected corresponding to the three Goldstone bosons from the breaking of all the generators of $SO(3)$. Constraints on the coupling constants arise from the requirement that at a minimum of the potential, the eigenvalues must all be positive or zero. Since m^2 and $3\lambda + \kappa$ must be positive, requiring the third eigenvalue to be positive leads to the constraint $\kappa > 0$ in this case.

3.4.1.2 S_4

For S_4 we minimize the potential from (3.3) using the alignment (3.27). We obtain a VEV

$$\mathcal{V} = \sqrt{\frac{25m^2}{4(90\lambda + 10\kappa + 7\rho + 2\tau)}}\,[\sqrt{\frac{7}{5}}, 0, 0, 0, 0, 0, 0, 1, 0] \tag{3.46}$$

A real value for our breaking scale requires $90\lambda + 10\kappa + 7\rho + 2\tau > 0$.

The scalar mass states are found in Table 3.2 [6] and are all non-negative if

$$5\kappa + 8\rho - 2\tau > 0.$$

The three zeros correspond to the broken $SO(3)$ generators.

[6] In order to normalize the eigenvalues for S_4 to those in other cases when we use the spherical harmonic basis, we have multiplied all quadratic terms by a factor of $\frac{1}{8}$ and quartic terms by a factor of $\frac{1}{64}$.

Value	Multiplicity
0	3
$4m^2$	1
$\frac{5m^2(5\kappa+8\rho-2\tau)}{7(90\lambda+10\kappa+7\rho+2\tau)}$	3
$\frac{20m^2(5\kappa+8\rho-2\tau)}{7(90\lambda+10\kappa+7\rho+2\tau)}$	2

Table 3.2: Scalar mass eigenstates for the SSB pattern $SO(3) \to S_4$ using a real **9** of $SO(3)$.

3.4.1.3 A_5

For A_5, we minimize the potential from (3.4) using the alignment (3.29). We obtain a VEV

$$\mathcal{V} = \sqrt{\frac{1155m^2}{128(\lambda+140\kappa+84\rho+65\tau+14\nu+9\sigma-2\chi)}}\,[1,0,0,-\sqrt{\frac{21}{2}},0,0,0,,0,0,0,\sqrt{\frac{105}{22}},0] \tag{3.47}$$

A real value for our breaking scale requires $128\lambda+140\kappa+84\rho+65\tau+14\nu+9\sigma-2\chi > 0$. For the scalar mass states [7] are given in Table 3.3.

We see we have the three zeros corresponding to the broken $SO(3)$ generators and must satisfy the constraints

$$105\kappa+196\rho+240\tau-14\nu-19\sigma+12\chi > 0$$

$$14\rho+45\tau+14\nu-11\sigma+18\chi > 0.$$

[7] Again by expressing our states in terms of spherical harmonics, we obtain different normalizations for our basis states which lead to a different normalization scale for the VEV scale and scalar mass states. To correct this for A_5 we have multiplied the quadratic term by a factor of $\frac{5}{352}$ and the quartic terms by $(\frac{5}{352})^2$ so that our states are now normalized the same way as our other breakings.

Value	Multiplicity
0	3
$4m^2$	1
$\frac{28m^2(105\kappa+196\rho+240\tau-14\nu-19\sigma+12\chi)}{33(420\lambda+140\kappa+84\rho+65\tau+14\nu+9\sigma-2\chi}$	5
$\frac{28m^2(14\rho+45\tau+14\nu-11\sigma+18\chi)}{33(420\lambda+140\kappa+84\rho+65\tau+14\nu+9\sigma-2\chi}$	4

Table 3.3: Scalar mass eigenstates for the SSB pattern $SO(3) \to A_5$ using a real **13** of $SO(3)$.

3.4.2 $SU(2)$ Cases

3.4.2.1 Q_6

We break the symmetry of the potential given in Eq.(3.5) with the alignment in Eq.(3.30) to obtain a VEV

$$\mathcal{V} = \sqrt{\frac{m^2}{2(2\lambda+\kappa+\rho+\tau)}}\,[1,1,0,0,0,0,0,0,0,0,0,0,0,0,0] \tag{3.48}$$

Thus we require $\kappa + 2\lambda + \rho + \tau > 0$. The eigenvalues of the Hessian are given in Table 3.4.

The constraints from these mass eigenvalues are

$$\kappa > 0$$

$$\kappa > -(\rho+\tau)$$

$$2\rho+3\tau,\ 6\rho+7\tau,\ 8\rho+9\tau < 0$$

There are clearly stable minima when $\lambda > 0$, $\kappa > 0$, $\rho < 0$ and $\tau < 0$. The extra zero eigenvalue comes from breaking an accidental $U(1)$ phase symmetry. This gives rise to a pseudo-goldstone boson that can gain a mass through quantum corrections.

Value	Multiplicity
0	4
$4m^2$	1
$\frac{2m^2\kappa}{3(2\lambda+\kappa+\rho+\tau)}$	2
$\frac{4m^2(\kappa+\rho+\tau)}{2\lambda+\kappa+\rho+\tau}$	1
$\frac{-3m^2(2\rho+3\tau)}{5(2\lambda+\kappa+\rho+\tau)}$	1
$\frac{-2m^2(2\rho+3\tau)}{5(2\lambda+\kappa+\rho+\tau)}$	2
$\frac{-m^2(6\rho+7\tau)}{5(2\lambda+\kappa+\rho+\tau)}$	1
$\frac{-2m^2(8\rho+9\tau)}{15(2\lambda+\kappa+\rho+\tau)}$	2

Table 3.4: Scalar mass eigenstates for the SSB pattern $SU(2) \to Q_6$ using a complex **7** of $SU(2)$.

3.4.2.2 T'

The potential and the vacuum alignment of the breaking of of SU(2) to T′ with a real **7** are the same as for SO(3)→ A_4. Therefore the breaking scale and the mass states will be exactly the same, as the two models can only be differentiated by the non-scalar part of the Lagrangian.

For a the breaking with a complex **7** we minimize the potential in Eq.(3.5) but this time using the alignment Eq.(3.31) to obtain the VEV

$$\mathcal{V} = \sqrt{\frac{3m^2}{(12\lambda + 6\kappa + 4\rho + 3\tau)}}\,[0, -1, 0, 0, 0, 1, 0, 0, 0, 0, 0, 0, 0, 0, 0] \tag{3.49}$$

which leads to the constraint that $12\lambda + 6\kappa + 4\rho + 3\tau > 0$. The eigenvalues of the Hessian are shown in Table 3.5.

From the requirement of positive eigenvalues we deduce the constraints

$$\tau > 0$$

Value	Multiplicity
0	4
$4m^2$	1
$\frac{12m^2\tau}{5(12\lambda+6\kappa+4\rho+3\tau)}$	3
$\frac{16m^2(2\rho+3\tau)}{5(12\lambda+6\kappa+4\rho+3\tau)}$	3
$\frac{4m^2(8\kappa+8\rho+9\tau)}{3(12\lambda+6\kappa+4\rho+3\tau)}$	3

Table 3.5: Scalar mass eigenstates for the SSB pattern $SU(2) \to T'$ using a complex **7** of $SU(2)$.

$$\rho > -\tfrac{3}{2}\tau$$

$$\tfrac{3}{8}\tau > \kappa > -8\rho - \tfrac{9}{8}\tau$$

As in the Q_6 example, the extra zero eigenvalue is a result of breaking the accidental $U(1)$ phase symmetry in the potential.

3.4.2.3 O'

The breaking scale and scalar mass spectrum of $SU(2)$ to O' with a real **9** is exactly the same as that for $SO(3)$ to S_4, where differences between two models would come from the non-scalar part of the Lagrangian.

For a complex **9** we minimize the potential in Eq.(3.6) using the alignment Eq.(3.33) and obtain a VEV

$$\begin{aligned}\mathcal{V} = &\sqrt{\frac{25m^2}{4(60\lambda+30\kappa+20\rho+15\tau+14\sigma)}} \\ &\times[1,1,0,0,0,0,0,0,\frac{14}{\sqrt{70}},0,0,0,0,0,0,0,0,0,0,0]\end{aligned} \tag{3.50}$$

Thus $60\lambda + 30\kappa + 20\rho + 15\tau + 14\sigma$ must be > 0. The eigenvalues of the Hessian (see Table 3.6) are all real and positive semidefinite for positive scalar quartic couplings, while

more detailed constraints on the scalar quartics can clearly be extracted from the individual mass eigenvalues. There are 3 zeros corresponding to the 3 broken $SU(2)$ generators, as well as an extra zero from breaking the $U(1)$ phase symmetry.

Value	Multiplicity
0	4
$4m^2$	1
$\frac{-24m^2\sigma}{7(60\lambda+30\kappa+20\rho+15\tau+14\sigma)}$	2
$\frac{5m^2(10\rho+15\tau+16\sigma)}{7(60\lambda+30\kappa+20\rho+15\tau+14\sigma)}$	3
$\frac{20m^2(10\rho+15\tau+16\sigma)}{7(60\lambda+30\kappa+20\rho+15\tau+14\sigma)}$	2
$\frac{2m^2(25\kappa+25\rho+25\tau+24\sigma)}{60\lambda+30\kappa+20\rho+15\tau+14\sigma}$	3
$\frac{3m^2(25\tau+32\sigma)}{7(60\lambda+30\kappa+20\rho+15\tau+14\sigma)}$	3

Table 3.6: Scalar mass eigenstates for the SSB pattern $SU(2) \to O'$ using a complex **9** of $SU(2)$.

We have the additional constraints

$$\sigma < 0$$

$$10\rho + 15\tau + 16\sigma > 0$$

$$25\kappa + 25\rho + 25\tau + 24\sigma > 0$$

and

$$25\tau + 32\sigma > 0.$$

3.4.2.4 I'

The breaking of $SU(2)$ to I' and $SO(3)$ to A_5 with a real **13**, are completely analogous to the breakings of $SU(2)$ and $SO(3)$ to T' and A_4 respectively with a real **7**.

For a complex **13** we minimize the potential of Eq.(3.7) using the alignment Eq.(3.35) and obtain a VEV

$$\begin{aligned}\mathcal{V} &= 7\sqrt{\frac{6m^2}{5(420\lambda+210\kappa+140\rho+105\tau+84\nu+70\sigma+65\chi)}} \\ &\times[0,0,1,-1,0,0,0,0,0,0,0,0,\sqrt{\frac{11}{7}},0,0,0,0,0,0,0,0,0,0,0,0,0]\end{aligned} \tag{3.51}$$

Thus $420\lambda+210\kappa+140\rho+105\tau+84\nu+70\sigma+65\chi$ must be >0. The eigenvalues of the Hessian (see Table 3.7) are all real and positive semidefinite for positive scalar quartic couplings. (More detailed constraints on the scalar quartics can clearly be extracted from the individual mass eigenvalues.) There are 3 zeros corresponding to the 3 broken $SU(2)$

Value	Multiplicity
0	4
$4m^2$	1
$\frac{28m^2(14\nu+35\sigma+45\chi)}{33(420\lambda+210\kappa+140\rho+105\tau+84\nu+70\sigma+65\chi)}$	4
$\frac{5m^2(49\sigma+72\chi)}{33(420\lambda+210\kappa+140\rho+105\tau+84\nu+70\sigma+65\chi)}$	5
$\frac{14m^2(210\rho+315\tau+392\nu+455\sigma+480\chi)}{33(420\lambda+210\kappa+140\rho+105\tau+84\nu+70\sigma+65\chi)}$	5
$\frac{m^2(980\kappa+980\rho+882\tau+784\nu+735\sigma+720\chi)}{3(420\lambda+210\kappa+140\rho+105\tau+84\nu+70\sigma+65\chi)}$	3
$\frac{4m^2(441\tau+882\nu+1225\sigma+1350\chi)}{33(420\lambda+210\kappa+140\rho+105\tau+84\nu+70\sigma+65\chi)}$	4

Table 3.7: Scalar mass eigenstates for the SSB pattern $SU(2)\to I'$ using a complex **13** of $SU(2)$.

generators, as well as an extra zero from breaking the $U(1)$ phase symmetry.

3.4.3 SU(3) cases

3.4.3.1 A_4

For the nonminimal breaking $SU(3) \to A_4$ we minimize the potential Eq.(3.9) and use the alignment Eq.(3.37) to get the VEV [18]

$$\mathcal{V} = \sqrt{\frac{m^2}{2(3\lambda+\eta+\kappa+\rho+\tau)}}\,[0,0,0,0,0,0,0,0,0,0,0,0,0,1,1,1,0,0,0,0,0,0,0,0,0,0,0,0,0,0,0,0,0] \tag{3.52}$$

Thus $3\lambda+\eta+\kappa+\rho+\tau$ must be > 0. The eigenvalues of the Hessian are are shown in Table 3.8.

Value	Multiplicity
0	9
$4m^2$	1
$\frac{m^2(-2\eta+\kappa-2\rho+4\tau)}{3\lambda+\eta+\kappa+\rho+\tau}$	2
$\frac{-3m^2\eta}{3\lambda+\eta+\kappa+\rho+\tau}$	6
$\frac{m^2}{4(3\lambda+\eta+\kappa+\rho+\tau)}(5\kappa+2\rho+4\tau+\sqrt{(4\tau+2\rho-3\kappa)^2+16(\rho+\kappa+2\eta)^2})$	3
$\frac{m^2}{4(3\lambda+\eta+\kappa+\rho+\tau)}(5\kappa+2\rho+4\tau-\sqrt{(4\tau+2\rho-3\kappa)^2+16(\rho+\kappa+2\eta)^2})$	3
$\frac{m^2}{2(3\lambda+\eta+\kappa+\rho+\tau)}(3\kappa-5\eta-2\rho+4\tau+\frac{1}{3}\sqrt{(9\eta-7\kappa+10\rho-4\tau)^2+8(\rho+2\kappa-4\tau)^2})$	3
$\frac{m^2}{2(3\lambda+\eta+\kappa+\rho+\tau)}(3\kappa-5\eta-2\rho+4\tau-\frac{1}{3}\sqrt{(9\eta-7\kappa+10\rho-4\tau)^2+8(\rho+2\kappa-4\tau)^2})$	3

Table 3.8: Scalar mass eigenstates for the SSB pattern $SU(3) \to A_4$ using a **15** of $SU(3)$.

We expect eight zeros corresponding to the broken generators of $SU(3)$, but again an extra zero eigenvalue arises from breaking the accidental $U(1)$ phase symmetry. As for constraints, we can readily see that

$$\eta < 0,$$

$$5\kappa+2\rho+4\tau > \sqrt{(4\tau+2\rho-3\kappa)^2+16(\rho+\kappa+2\eta)^2},$$

and

$$3\kappa - 5\eta - 2\rho + 4\tau > \tfrac{1}{3}\sqrt{(9\eta - 7\kappa + 10\rho - 4\tau)^2 + 8(\rho + 2\kappa - 4\tau)^2}$$

are required. An example of where all these constraints can be satisfied is

$$2\rho = 3\kappa,\ \rho + \kappa = -2|\eta|, \text{ and } 5\kappa + 3\rho > 0, \text{ where } \kappa, \rho, \text{ and } \tau > 0.$$

3.4.3.2 T_7

For this breaking we again minimize Eq.(3.9), now using the alignment Eq.(3.38) to obtain the VEV [18]

$$\mathcal{V} = \sqrt{\frac{m^2}{2(3\lambda + \kappa + \rho + \tau)}}\,[0,0,0,0,0,0,0,0,0,0,0,0,1,1,1,0,0,0,0,0,0,0,0,0,0,0,0,0,0,0] \tag{3.53}$$

Thus $3\lambda + \kappa + \rho + \tau$ must be > 0. The eigenvalues of the Hessian are shown in Table 3.9, where α, β, γ are the three roots of the polynomial $10368\eta^2(\rho - \kappa - \tau) + 3888\eta\rho^2 -$

Value	Multiplicity
0	9
$4m^2$	1
$\frac{2(2\kappa-\rho+2\tau)m^2}{\kappa+3\lambda+\rho+\tau}$	2
$\frac{m^2}{12(3\lambda+\kappa+\rho+\tau)} \times \alpha$	6
$\frac{m^2}{12(3\lambda+\kappa+\rho+\tau)} \times \beta$	6
$\frac{m^2}{12(3\lambda+\kappa+\rho+\tau)} \times \gamma$	6

Table 3.9: Scalar mass eigenstates for the SSB pattern $SU(3) \to T_7$ using a **15** of $SU(3)$.

$15552\eta\kappa\tau + (648\eta^2 + 972\eta\kappa - 648\eta\rho - 180\rho^2 + 1296\eta\tau + 720\kappa\tau)x + (6\rho - 54\eta - 21\kappa - 36\tau)x^2 + x^3$. We have the constraints

$$2\kappa - \rho + 2\tau > 0$$

and

$$\alpha,\ \beta,\ \gamma > 0.$$

The extra zero is once again due to breaking an accidental $U(1)$ symmetry. We cannot remedy this by including cubic terms this time, because we need the couplings on those terms to vanish in order to have a stable minimum. Numerical studies show that there is a range of scalar quartic coupling constant values where the minimum is stable. An example of such numerical analysis will be discussed below.

3.4.3.3 $\Delta(27)$

Minimizing the potential of Eq.(3.10) with the alignment Eq.(3.40) we obtain a VEV

$$\mathcal{V} = \sqrt{\frac{m^2}{2(3\lambda+\kappa)}}\,[1,1,1,0,0,0,0,0,0,0,0,0,0,0,0,0,0,0,0,0,0] \tag{3.54}$$

giving the constraint $3\lambda + \kappa > 0$. The eigenvalues of the Hessian are in Table 3.10, from

Value	Multiplicity
0	11
$4m^2$	1
$\frac{4\kappa m^2}{3\lambda+\kappa}$	2
$\frac{\kappa m^2}{3(3\lambda+\kappa)}$	6

Table 3.10: Scalar mass eigenstates for the SSB pattern $SU(3) \to \Delta(27)$ using a **10** of $SU(3)$.

which we see that $\kappa > 0$ is required. Again we have an extra zero from an accidental $U(1)$, and in this case the cubic terms vanish upon summation. The two extra zeros are the result of an additional $\Delta(27)$ singlet within the **10**. (For a detailled explanation see [18].)

3.4.3.4 $PSL(2,7)$

Minimizing the potential of Eq.(3.12) with the alignment Eq.(3.42) we obtain a VEV

$$\mathcal{V} = \sqrt{\frac{m^2}{6\lambda + 2\kappa + \rho}}\,[0,0,0,0,1,1,0,0,1,0,0,0,0,0,0,0,0,0,0,0,0,0,0,0,0,0,0,0,0,0,0] \tag{3.55}$$

Thus $6\lambda + 2\kappa + \rho > 0$. The eigenvalues of the Hessian are found in Table 3.11 from

Value	Multiplicity
0	9
$4m^2$	1
$\frac{(7\kappa+8\rho)m^2}{2(6\lambda+2\kappa+\rho)}$	8
$\frac{2(3-\sqrt{2})\rho m^2}{3(6\lambda+2\kappa+\rho)}$	6
$\frac{2(3+\sqrt{2})\rho m^2}{3(6\lambda+2\kappa+\rho)}$	6

Table 3.11: Scalar mass eigenstates for the SSB pattern $SU(3) \to PSL(2,7)$ using a $\mathbf{15'}$ of $SU(3)$.

which we get the constraints

$$\rho > 0 \qquad \text{and} \qquad 7\kappa + 8\rho > 0.$$

We once again have an extra zero, but this time it is possible to include cubic terms to break the $U(1)$ phase. The two cubic terms we can include are

$$\epsilon_{imq}\epsilon_{jnr}\epsilon_{lpt}T^{ijkl}T^{mnop}T^{qrst}$$
$$\text{and} \tag{3.56}$$
$$\epsilon^{imq}\epsilon^{jnr}\epsilon^{lpt}T_{ijkl}T_{mnop}T_{qrst}$$

which are Hermitian conjugates and are included in the potential with the same real cou-

pling constant, ζ. The VEV scale for the potential including the cubic is now

$$\frac{-3\zeta \pm \sqrt{9\zeta^2 + 4m^2(6\lambda + 2\kappa + \rho)}}{2(6\lambda + 2\kappa + \rho)} \tag{3.57}$$

Notice that there may be two possible solutions. The constraint that must hold in both cases is $9\zeta^2 + 4m^2(2\kappa + 6\lambda + \rho) \geq 0$.

Calculating the eigenvalues of the Hessian produces solutions involving the roots of very large polynomial which is much too large to display, but it is notable that it does produce 8 zeros rather than 9. Furthermore, following the usual procedure, but this time numerically setting all quartic coupling constants to unity, the quadratic coupling to -1 and the cubic to 0.001 (these values are selected to ensure a stable minimum) produces a VEV scale of approximately 0.3335 and eigenvalues whose multiplicities match the branching rules

Value	Multiplicity
0	8
4.002	1
.006003	1
0.323647	6
0.125244	6
0.838169	8

Table 3.12: Numerical results where cubic terms are included for the scalar mass eigenstates of the SSB pattern $SU(3) \rightarrow PSL(2,7)$ using a $\mathbf{15'}$ of $SU(3)$.

SU(3)$\rightarrow$ $PSL(2,7)$, as shown in Table 3.12. The degeneracy of the pseudo-Goldstone mass with that of the true Goldstones is lifted as expected, as can be seen in Table 3.12. Finally note that although we have set all the coupling constants except for the cubic to integer values, we can easily rescale them to smaller values to be sure we are in the perturbative regime of the theory without disturbing the stability of the result. Specifically, while

the scalar quartic couplings in the numerical example are not in the perturbative range, we can rescale all the quartics by a factor s and ζ by a factor $\sqrt{s}$. This leaves the eigenvalues unchanged and puts us into the perturbative regime.

Moving on to the **28**, we minimize the potential in Eq.(3.13) with the alignment Eq.(3.44) to obtain a VEV

$$\mathcal{V} = \sqrt{\frac{9m^2}{2(42\lambda+14\kappa+7\rho+6\tau)}}[0,0,0,1,0,0,1,1,0,0,0,0,0,0,0,0,0,0,0,0,0,$$
$$0,0,0,0,0,0,-\sqrt{\frac{5}{3}},...] \tag{3.58}$$

Thus $42\lambda + 14\kappa + 7\rho + 6\tau > 0$. The eigenvalues of the Hessian are given in Table 3.13 Further constraints are

Value	Multiplicity
0	16
$4m^2$	1
$\frac{4(7\rho+9\tau)m^2}{5(42\lambda+14\kappa+7\rho+6\tau)}$	7
$\frac{(21\kappa+20\rho+18\tau)m^2}{42\lambda+14\kappa+7\rho+6\tau}$	8
$\frac{1}{200(42\lambda+14\kappa+7\rho+6\tau)^2} \times A$	6
$\frac{1}{200(42\lambda+14\kappa+7\rho+6\tau)^2} \times B$	6
$\frac{1}{200(42\lambda+14\kappa+7\rho+6\tau)^2} \times C$	6
$\frac{1}{200(42\lambda+14\kappa+7\rho+6\tau)^2} \times D$	6

Table 3.13: Scalar mass eigenstates for the SSB pattern $SU(3) \to PSL(2,7)$ using a **28** of $SU(3)$.

$$7\rho + 9\tau > 0$$

$$21\kappa + 20\rho + 18\tau > 0$$

$$A,\ B,\ C,\ D > 0$$

where A, B, C, and D are the roots of a very large quartic polynomial. Numerical work shows that all four roots can be positive, simultaneously leading to all positive eigenvalues in Table 3.13 and a stable minimum when the other constraints are also satisfied. We see that there are eight zeros from the broken generators of SU(3), and one zero from breaking the broken U(1) phase. But unique to this breaking we have seven extra zeros, which implies that there are seven more broken generators from an accidental symmetry of the Lagrangian that we have so far been unable to identify, leading to a total of 8 pseudo-Goldstone bosons.

3.4.4 Symmetry Breaking Summary

Let us briefly summarize our results. We have shown that we can break from G to Γ for the gauge and discrete groups listed in the introduction. The minima can be stable since none of the eigenvalues of the scalars are negative for allowed regions of parameter space. Zero eigenvalues correspond to Goldstone bosons in each case and to additional pseudo-Goldstone bosons in several cases. Specifically for the cases we have studied of $SO(3)$ breaking to a discrete symmetry the results are summarized in Table 3.14. The G subscript indicates the Goldstones. In each case the masses of the particles in different discrete group irreps are all different, so the initial degeneracy of the scalar masses is lifted to the extent allowed by the discrete group. For the cases of $SU(2)$ breaking to discrete symmetries,

SSB pattern	decomposition
$SO(3) \to A_4$	$\mathbf{7} \to \mathbf{1} + \mathbf{3_G} + \mathbf{3}$
$SO(3) \to S_4$	$\mathbf{9} \to \mathbf{1} + \mathbf{2} + \mathbf{3_G} + \mathbf{3}$
$SO(3) \to A_5$	$\mathbf{13} \to \mathbf{1} + \mathbf{3_G} + \mathbf{4} + \mathbf{5}$

Table 3.14: Scalar mass eigenstates for the SSB patterns $SO(3) \to A_4$, S_4 and A_5 using real irreps of $SO(3)$.

the results are summarized in Table 3.15. Again all the discrete group irreps correspond to different masses except for the zero eigenvalue states where we have indicated the true Goldstones and the pseudo-Goldstones (by subscripts pGB) due to breaking of the phase symmetry on the potentials. The subscript c indicates that the irreps are complexified and the decompositions are written in terms of real components. The results begin to become more complicated for the $SU(3)$ cases we have investigated, and this can be seen in Table 3.16. Now some irreps masses have become degenerate and we have indicated these cases by collecting those discrete group irreps with parentheses and labeling the collection with a $deg.$ subscript. All the cases have a pseudo-Goldstone associated with breaking of phase invariance. The breaking to T_7 with a $\mathbf{10}$ leads to two additional pseudo-Goldstones as discussed in [18] and the breaking to $PSL(2,7)$ with a $\mathbf{28}$ has seven additional pseudo-Goldstones. Since the $\mathbf{28}$ was derived from $\mathbf{3^6}$ one could conjecture that the potential has a $Spin(6) \sim SU(4)$ accidental symmetry that contains the gauged $SU(3)$, and that the VEV breaks all 15 $SU(4)$ plus the phase to give a total of 16 massless states. Finally, recall that for the breaking to $PSL(2,7)$ with a $\mathbf{15'}$ we have shown that phase symmetry can be avoided if we add cubic terms, hence there is no pseudo-Goldstone after SSB in that case, see Table 3.12.

SSB pattern	decomposition
$SU(2) \to Q_6$	$\mathbf{7_c} \to \mathbf{1} + \mathbf{1'} + (\mathbf{1'} + \mathbf{2'})_{\mathbf{G}} + \mathbf{2'} + \mathbf{1}_{\mathbf{pGB}} + \mathbf{1'} + \mathbf{1'} + \mathbf{2'} + \mathbf{2'}$
$SU(2) \to T'$	$\mathbf{7_c} \to \mathbf{1} + \mathbf{3}_{\mathbf{G}} + \mathbf{3} + \mathbf{1}_{\mathbf{pGB}} + \mathbf{3} + \mathbf{3}$
$SU(2) \to O'$	$\mathbf{9_c} \to \mathbf{1} + \mathbf{2} + \mathbf{3}_{\mathbf{G}} + \mathbf{3} + \mathbf{1}_{\mathbf{pGB}} + \mathbf{2} + \mathbf{3} + \mathbf{3}$
$SU(2) \to I'$	$\mathbf{13_c} \to \mathbf{1} + \mathbf{3}_{\mathbf{G}} + \mathbf{4} + \mathbf{5} + \mathbf{1}_{\mathbf{pGB}} + \mathbf{3} + \mathbf{4} + \mathbf{5}$

Table 3.15: Scalar mass eigenstates for the SSB patterns $SU(2) \to Q_6, T', O'$ and I' using complexified irreps of $SO(3)$.

SSB pattern	decomposition
$SU(3) \to A_4$	$\mathbf{15} \to \mathbf{1} + (\mathbf{1'} + \mathbf{1''} + \mathbf{3} + \mathbf{3})_{\mathrm{G}} + (\mathbf{3} + \mathbf{3})_{\mathrm{deg.}} + \mathbf{1}_{\mathrm{pGB}} + (\mathbf{1'} + \mathbf{1''})_{\mathrm{deg.}} + \mathbf{3} + \mathbf{3} + \mathbf{3} + \mathbf{3}$
$SU(3) \to T_7$	$\mathbf{15} \longrightarrow \mathbf{1} + (\mathbf{1'} + \mathbf{1''} + \mathbf{3'} + \mathbf{3''})_{\mathrm{G}} + (\mathbf{3'} + \mathbf{3''})_{\mathrm{deg.}}$
	$+\mathbf{1}_{\mathrm{pGB}} + (\mathbf{1'} + \mathbf{1''})_{\mathrm{deg.}} + (\mathbf{3'} + \mathbf{3''})_{\mathrm{deg.}} + (\mathbf{3'} + \mathbf{3''})_{\mathrm{deg.}}$
$SU(3) \to \Delta(27)$	$\mathbf{10} \to \mathbf{1} + \mathbf{1}_{\mathrm{pGB}} + (\mathbf{\Sigma^9_{n=2}})_{\mathrm{G}} + \mathbf{3} + (\mathbf{1} + \mathbf{1})_{\mathrm{pGB}} + (\mathbf{1_2} + \mathbf{1_3})_{\mathrm{deg.}} + (\mathbf{\Sigma^9_{n=4}})_{\mathrm{deg.}}$
$SU(3) \to PSL(2,7)$	$\mathbf{15'} \to \mathbf{1} + \mathbf{6} + \mathbf{8}_{\mathrm{G}} + \mathbf{1}_{\mathrm{pGB}} + \mathbf{6} + \mathbf{8}$
$SU(3) \to PSL(2,7)$	$\mathbf{28} \to \mathbf{1} + \mathbf{6} + \mathbf{6} + \mathbf{7} + \mathbf{8}_{\mathrm{G}} + \mathbf{1}_{\mathrm{pGB}} + \mathbf{6} + \mathbf{6} + \mathbf{7}_{\mathrm{pGB}} + \mathbf{8}$

Table 3.16: Scalar mass eigenstates for the SSB patterns $SU(3) \to A_4$, T_7, $\Delta(27)$ and $PSL(2,7)$ using various complex irreps of $SU(3)$.

3.5 Discussion and Conclusions

The standard model includes 28 unspecified parameters, some of which describe fermion masses and mixing angles. Consequently, we do not know why the quark and lepton masses and mixings are what they are. To fix these parameters, a standard approach has been to extend the SM by a discrete symmetry, but this approach is not without its difficulties as discussed above. What would seem more natural would be to increase the gauge group to $SU(3) \times SU(2) \times U(1) \times G$ and extend the scalar sector. Then this model can be of the same general type as the SM, i.e., an anomaly-free gauge theory with fermions that gets spontaneously broken by VEVs of scalar fields. If the SSB of G results in a discrete subgroup Γ then we arrive at a $SU(3) \times SU(2) \times U(1) \times \Gamma$ via a route that avoids the problems just mentioned, without choosing an *ad hoc* discrete group for extending the SM.

Here, based on the techniques of Luhn[18] and Merle and R. Zwicky[19], we have demonstrated that we can carry out the $G \to \Gamma$ SSB in many cases of interest, specifically breaking to $A_4, S_4, A_5, Q_6, T', O', I', T_7, \Delta(27)$ and $PSL(2,7)$. Other cases can be handled by the same techniques. Many other discrete groups have been occasionally used to extend the SM, e.g., $D_4, D_5, D_7, D_{14}, \Delta(54), \Delta(96)$, and $\Sigma(81)$ have all appeared in the literature [55–57]. For a discussion of breaking $SO(3)$ to dihedral groups see [53]. Further information about the classification of the discrete subgroups of $SU(3)$ can be found in

[19, 58–60]. In addition products of discrete groups are often employed, where the products often contain Z_n factors. To gauge these cases we can start with a product gauge group and break to the desired discrete group, $G_1 \times G_2 \times ... \rightarrow \Gamma_1 \times \Gamma_2 \times ....$ As long as there are no cross terms in the scalar potential, then we can proceed as above. In some cases the cross terms can destabilize the minima, so they must either be eliminated, or dealt with by other means. If the fundamental charge of a $U(1)$ gauge group is q, then by breaking a $U(1)$ with scalar particle of charge nq one arrives at Z_n. Results given here could be applied to extend recent work on gauging two Higgs doublet models [61]. Using our results to extend models currently in the literature can solve some existing problems, and the inclusion of new scalars in the spectrum may be of interest since some may be detectable either directly or indirectly depending on the details of the model. Such phenomenological investigations need to proceed on a model by model basis, and we plan to look at some specific examples in future work.

Chapter 4

Flavor Mixing in the Standard Model

As stated above, one of the motivating factors for the study of discrete symmetries are their utility in describing flavor mixing. In this section we will derive forms for the Cabbibo-Kobayashi-Maskawa (CKM) and Pontecorvo-Maki-Nakagawa-Sakata (PMNS) matrices, which parameterize flavor mixing in the quark and lepton sectors, respectively. We start by listing all fermions (with the addition of right-handed neutrinos) in their representations under standard model gauge groups, (see Table 4.1 below).

4.1 Quark Mixing

As stated in Section 2, all fermions listed in Table 4.1 will have masses generated via Yukawa terms, and we will soon see that the Yukawa couplings determine the form of the mixing matrices. We begin with the quark sector[1]. Strictly speaking, since we have three left handed doublets and six right handed singlets, there are 18 separate Yukawa terms. We can write these more compactly by using the vectors $Q = ((u,d)_L, (c,s)_L, (t,b)_L))$, $u_r = (u_R, c_R, t_R)$, and $d_r = (d_R, s_R, b_R)$ defined above equation 2.3 so that the quark sector Yukawa terms are:

$$\mathcal{L}_{QuarkY} = -Y^d_{ij}\,\overline{Q}^i\,\Phi\,d^j_R - Y^u_{ij}\,\overline{Q}^i\,\tilde{\Phi}\,u^j_R + \text{h.c.} \tag{4.1}$$

Where indices i and j are summed over the three quark generations and $\tilde{\Phi} \equiv i\tau_2\Phi^*$ is defined in order to preserve the gauge invariance of the up-type Yukawa terms. We see that we have eighteen free parameters contained in two 3x3 Yukawa matrices Y^d and Y^u. After symmetry breaking, Φ obtains a VEV and the SU(2) doublets Q split into $u_L = (u_L, c_L, t_L)$

[1]The following derivation is adapted from Chapter 29 of [79]

Table 4.1: Fermionic content of Standard Model plus right-handed neutrinos

Particles	SU(3)	SU(2)	U(1) Charge
$((\nu_e, e), (\nu_\mu, \mu), (\nu_\tau, \tau))_L$	1	2	-1
e^c_R	1	1	2
μ^c_R	1	1	2
τ^c_R	1	1	2
$(N_1, N_2, N_3)_R$	1	1	0
$(u, d)_L$	3	2	$\frac{1}{3}$
$(c, s)_L$	3	2	$\frac{1}{3}$
$(t, b)_L$	3	2	$\frac{1}{3}$
u^c_R	3	1	$-\frac{4}{3}$
d^c_R	3	1	$\frac{2}{3}$
c^c_R	3	1	$-\frac{4}{3}$
s^c_R	3	1	$\frac{2}{3}$
t^c_R	3	1	$-\frac{4}{3}$
b^c_R	3	1	$\frac{2}{3}$

and $d_L = (d_L, s_l, b_L)$. Equation (4.1) becomes:

$$\mathcal{L}_{QuarkY} = -\frac{v}{\sqrt{2}}\, Y^d_{ij}\, \overline{d}^i_L\, d^j_R - \frac{v}{\sqrt{2}}\, Y^u_{ij}\, \overline{u}^i_L\, u^j_R + \text{h.c.} = -\frac{v}{\sqrt{2}}\, [\overline{d}_L\, Y^d\, d_R + \overline{u}_L\, Y^u\, u_R] + \text{h.c.} \tag{4.2}$$

Where we have rewritten our Lagrangian in matrix form. We still have 18 separate mass terms. To recover the six physical masses we must change basis by diagonalizing the Yukawa matrices Y^u and Y^d. First note that we can diagonalize the hermitian squares of these matrices with unitary transformations V_u and V_d:

$$V^\dagger_d\, Y_d\, Y^\dagger_d\, V_d = M^2_d \qquad V^\dagger_u\, Y_u\, Y^\dagger_u\, V_u = M^2_u \tag{4.3}$$

Where $M_{u,d}$ are diagonal matrices with terms corresponding to the up and down quark masses. From the above relation we can write an expression for the Yukawa matrices in terms of $M_{u,d}$, $V_{u,d}$ and one more pair of unitary transformations $K_{u,d}$:

$$Y_d = V_d M_d K^\dagger_d, \qquad Y_u = V_u M_u K^\dagger_u \tag{4.4}$$

Substituting this relation into Equation (4.2):

$$\mathcal{L}_{QuarkY} = -\frac{v}{\sqrt{2}}[\overline{d}_L V_d M_d K_d^\dagger d_R + \overline{u}_L V_u M_u K_u^\dagger u_R] + \text{h.c.} \tag{4.5}$$

Now we see that changing to the mass basis requires redefining our quark fields by:

$$\begin{aligned} d_R &\equiv K_d^\dagger d_R \\ u_R &\equiv K_u^\dagger u_R \\ d_L &\equiv V_d d_L \\ u_L &\equiv V_u u_L \end{aligned} \tag{4.6}$$

So that finally our Lagrangian in the mass basis is:

$$\mathcal{L}_{Mass\ basis} = -\frac{v}{\sqrt{2}}[\overline{d}_L M_d d_R + \overline{u}_L M_u u_R] + \text{h.c.} \tag{4.7}$$

Our redefinition of the quark fields will change other terms in the quark Lagrangian (2.3), specifically it will alter terms that couple the $W^\pm$ bosons to the left handed quarks. After symmetry breaking, but before the basis change these terms are:

$$\frac{e}{\sqrt{2}\text{sin}\Theta_W}[\overline{u}_L \not{W}^+ d_L + \overline{d}_L \not{W}^- u_L] \tag{4.8}$$

In the flavor basis there should be no mixing between quark generations and we see that indeed there is no mixing involved in either of these terms, i.e. the up only couples to the down, the charm only couples to the strange, etc. But after making the transformations (4.6) we find that Equation (4.8) becomes:

$$\frac{e}{\sqrt{2}\text{sin}\Theta_W}[\overline{u}_L^i \not{W}^+ V_u^\dagger V_d d_L^i + \overline{d}_L^i \not{W}^- V_d^\dagger V_u u_L^i] \tag{4.9}$$

We now see that there is a mixing between up and down quark generations induced by

the matrix $V_{CKM} = (V_u^\dagger V_d)_{ij}$. Physically, the square of each element of this matrix gives the probability of the ith up-type quark coupling to the jth down type quark. Explicitly:

$$V_{CKM} = \begin{pmatrix} V_{ud} & V_{us} & V_{ub} \\ V_{cd} & V_{cs} & V_{cb} \\ V_{td} & V_{ts} & V_{tb} \end{pmatrix} \tag{4.10}$$

The magnitudes of the CKM matrix elements depend solely on the 18 Yukawa couplings mentioned above, (although unitarity and other constraints reduce the number of independent parameters in the matrix to four). Because these couplings are free parameters, so too are the elements of the CKM matrix, their values are not predicted by the Standard Model and can only be measured experimentally. The latest measured values are [72]:

$$\begin{pmatrix} 0.97446 \pm 0.0001 & 0.22452 \pm 0.00044 & 0.00365 \pm 0.00012 \\ 0.22438 \pm 0.00044 & 0.97359 \pm 0.00011 & 0.04214 \pm 0.00076 \\ 0.00896 \pm 0.00024 & 0.04133 \pm 0.00074 & 0.999105 \pm 0.000032 \end{pmatrix} \tag{4.11}$$

We see that there is very little mixing in the quark sector. We will show below that the neutrino sector is a different story.

4.2 Neutrino Mixing

We now return to the lepton sector, we introduce the vectors for the left handed leptons $L = ((\nu_e, e), (\nu_\mu, \mu), (\nu_\tau, \tau))$, right handed charged leptons $l_R = (e_R, \mu_R, \tau_R)$ and right handed neutrinos $N_R = (N_1, N_2, N_3)$. We note that in the standard model neutrinos were massless and thus right handed components were not necessary. But because we now know neutrinos do in fact have mass we include the right handed components as a mechanism for

mass generation. The Yukawa part of the lepton Lagrangian is then:

$$\mathcal{L}_{leptonY} = -Y^l_{ij}\ \overline{L}^i\ \Phi\ l^j_R - Y^\nu_{ij}\ \overline{L}^i\ \Phi\ N^j_R + \text{h.c.} \tag{4.12}$$

If these were the only mass terms, the analysis would proceed more or less identically to the last section, with the caveat that the Yukawa couplings would need to be tuned to incredibly small values to reflect the near vanishing masses of the neutrinos. A more "natural" reason for the smallness of neutrino mass comes from what is known as the "see-saw mechanism", which we will detail here[2]. If the right handed neutrinos are taken to be "sterile" i.e., singlets under $SU(2)_L \times U_Y(1)$, the Majorana mass term:

$$-iM_{Rij}(N^i_R)^c N^j_R \tag{4.13}$$

(Where $(N_R)^c = N^T_R \tau_2$) is gauge invariant and thus remains part of the Lagrangian. The left-right neutrino mass term in Eq.(4.12), and the above Majorana mass term combine to give a mass matrix:

$$M_\nu = \begin{pmatrix} \nu_L\nu_L & \nu_L N_R \\ (\nu_L N_R)^T & N_R N_R \end{pmatrix} = \begin{pmatrix} 0 & M_D \\ M^T_D & M_R \end{pmatrix} \tag{4.14}$$

Where each entry in Eq.(4.14) is a 3×3 block matrix and the matrix of Yukawa couplings $Y^\nu \equiv M_D$ is called the Dirac mass matrix. To illustrate how a matrix of this form naturally generates small neutrino masses we examine a model with one sterile neutrino and one standard model type "active neutrino". In this case our neutrino mass Lagrangian is:

$$-Y_\nu \begin{pmatrix} \nu_e \\ e \end{pmatrix}_L \Phi\ N_R - iM_R\ (N_R)^c\ N_R \tag{4.15}$$

After symmetry breaking, Φ obtains a VEV and the neutrino gains a Dirac mass $m =$

[2]The following derivation is adapted from [80]

$Y_\nu \frac{v}{\sqrt{2}}$ which is on the order of the electroweak scale 10^{2-3} GeV (assuming $O(1)$ Y_ν). Because the right handed neutrinos are sterile we expect their mass term M to be on the order of some higher breaking scale, which we can take to be the grand unified or even the Planck scale, i.e. 10^{10-19} GeV. Our mass matrix is then just 2×2:

$$\begin{pmatrix} 0 & m \\ m & M \end{pmatrix} \tag{4.16}$$

Similarly to the quark sector, we must diagonalize this matrix in order to find the physical mass eigenstates. We find eigenvalues:

$$\begin{aligned} m_1 &= \frac{M - \sqrt{M^2 + 4m^2}}{2} \approx \frac{m^2}{M} \approx 10^{-1 \text{ to } -15}\text{GeV} \\ m_2 &= \frac{M + \sqrt{M^2 + 4m^2}}{2} \approx M \approx 10^{10-19}\text{GeV} \end{aligned} \tag{4.17}$$

We see now why this is called the see-saw, the heavier m_1 is, the lighter the observable neutrino state m_2 is.

In our case we have three generations of neutrinos, so that diagonalizing M_ν will yield a 6×6 block diagonal matrix:

$$\begin{pmatrix} M_1 & 0 \\ 0 & M_2 \end{pmatrix} \tag{4.18}$$

Where $M_{1,2}$ are 3×3 matrices. M_1 and M_2 can then each be diagonalized to obtain the light and heavy neutrino mass states respectively. In other words, the unitary transformation that diagonalizes M_1 transforms the light neutrino flavor basis into the light neutrino mass basis, this is precisely the definition of the PMNS matrix. Our task now is to find an explicit form for M_1 so that we can specify the precise form of the PMNS matrix. We start with the

diagonalization condition:

$$\begin{pmatrix} M_1 & 0 \\ 0 & M_2 \end{pmatrix} = U^T \begin{pmatrix} 0 & M_D \\ M_D^T & M_R \end{pmatrix} U \tag{4.19}$$

We take U to be a generic unitary transformation:

$$\begin{pmatrix} C_1 & S_2^\dagger \\ -S_1 & C_2^\dagger \end{pmatrix} \tag{4.20}$$

with the ansatz that the magnitude of the entries of the C matrices are much larger than the entries of the S matrices. From the unitarity constraint and the fact that we can ignore terms quadratic in S,M_D that do not include M_R one can show:

$$\begin{aligned} M_1 &\approx -C_1^T M_D M_R^{-1} M_D^T C_1 \\ M_2 &\approx C_2^* M_R C_2^\dagger \end{aligned} \tag{4.21}$$

We can further simplify these expressions by noting that in the limit of vanishing M_D, we may specify $C_1,\ C_2 \to I$, with I being the identity matrix. Then we have

$$\begin{aligned} M_1 &\approx -M_D M_R^{-1} M_D^T \\ M_2 &\approx M_R \end{aligned} \tag{4.22}$$

Now that we have an explicit form for M_1 we can diagonalize the hermitian squares of the neutrino and charged lepton mass matrices in the same way we did for the quark sector:

$$V_l^\dagger Y_l Y_l^\dagger V_l = M_l^2 \qquad V_\nu^\dagger M_1 M_1^\dagger V_\nu = M_\nu^2 \tag{4.23}$$

This redefinition of lepton fields will alter other terms in the lepton Lagrangian (2.1),

with those terms again involving W bosons. This time the terms coupling left handed charged leptons to left handed neutrinos are altered. After symmetry breaking, but before the basis change these terms are:

$$-\frac{g}{\sqrt{2}}[\overline{e}_L \not{W} \nu_{Le} + \overline{\mu}_L \not{W} \nu_{L\mu} + \overline{\tau}_L \not{W} \nu_{L\tau} + \text{h.c.}] \tag{4.24}$$

Prior to redefinition there is no mixing between lepton generations. After making the appropriate basis transformations our Lagrangian becomes:

$$-\frac{g}{\sqrt{2}} V_{PMNS}^{ij} [\bar{l}_L^i \not{W} \nu_{Lj} + \text{h.c.}] \tag{4.25}$$

Where $V_{PMNS} = V_l^\dagger V_\nu$ and $\nu_{Lj}, \quad j = 1, 2, 3$ are now neutrino mass eigenstates, not neutrino flavor eigenstates. Each charged lepton couples to each neutrino mass eigenstate with probability equal to the square of the corresponding element of the PMNS matrix.

$$V_{PMNS} = \begin{pmatrix} V_{e1} & V_{e2} & V_{e3} \\ V_{\mu 1} & V_{\mu 2} & V_{\mu 3} \\ V_{\tau 1} & V_{\tau 2} & V_{\tau 3} \end{pmatrix} \tag{4.26}$$

Just as in the quark sector, PMNS matrix values are not predicted by the Standard Model and can only be measured experimentally. The present 3σ experimental ranges of the magnitudes of the matrix elements are given below [63, 71, 72]:

$$\begin{pmatrix} 0.799 \leftrightarrow 0.844 & 0.516 \leftrightarrow 0.582 & 0.141 \leftrightarrow 0.156 \\ 0.242 \leftrightarrow 0.494 & 0.467 \leftrightarrow 0.678 & 0.639 \leftrightarrow 0.774 \\ 0.284 \leftrightarrow 0.521 & 0.490 \leftrightarrow 0.695 & 0.615 \leftrightarrow 0.754 \end{pmatrix} \tag{4.27}$$

One sees that in contrast to the quark sector, there is significant mixing between lepton generations. This has led to explorations of specific patterns in the mixing matrices, and

how imposing discrete symmetries on the lepton Lagrangian can reproduce these patterns.

Historically experimental data was compatible with the form of the PMNS matrix known as tribimaximal (TBM) mixing (see [68]) shown below, this form is often used as a starting point for estimations of PMNS matrix elements:

$$U_{TBM} = \begin{pmatrix} \sqrt{\frac{2}{3}} & \sqrt{\frac{1}{3}} & 0 \\ -\sqrt{\frac{1}{6}} & \sqrt{\frac{1}{3}} & -\sqrt{\frac{1}{2}} \\ -\sqrt{\frac{1}{6}} & \sqrt{\frac{1}{3}} & \sqrt{\frac{1}{2}} \end{pmatrix}. \tag{4.28}$$

The relatively simple form of this matrix can be elegantly derived from theories symmetric under various discrete groups (e.g. $A_4,\ S_4,\ A_5$). TBM mixing has been ruled out by more recent experiments, but it is still useful as a first order approximation to the PMNS matrix. In the following section we detail a particular model with the discrete symmetry T'. We initially use the model to derive the TBM matrix but we then augment the theory to obtain experimentally compatible predictions for both the PMNS and CKM matrices.

Chapter 5

A Gauged Model of Quarks and Leptons

5.1 Introduction

Flavor models of elementary particles have had to evolve as new data becomes available. As the data becomes more precise, the models become more sophisticated. The usual model building practice is to extend the standard model (SM) with a discrete symmetry which is used to fit the data. But variations abound, from extending a supersymmetric SM, to discrete group extended grand unified models (For reviews see [8–12]), to top-down fully gauged theories where the gauge group is sufficiently large to accommodate both the GUT and flavor symmetries [62]. Here we take a minimalist approach and look for the smallest fully gauged model that can explain all the data.

One of the simplest and most natural flavor models is the SM extended by the discrete group T' [8, 37–43], where the one and two dimensional irreducible representations (irreps) accommodate the quarks, while the leptons fit naturally into one and three dimensional irreps. For a phenomenological discussion and recent summary of the data, see e.g., [63]. The current challenge is to fit the most recent neutrino data with a T' model. A shortcoming of nearly all discrete flavor models is their lack of compliance with gravity [13], i.e., gravity breaks discrete global symmetries. But since gravity does not interfere with gauge symmetries, gauging a discrete symmetry by embedding it in a gauge group is a way to avoid this problem. But one still has to contend with discrete [14, 20, 64–66] or continuous chiral gauge anomalies. Our minimalist approach then leads us to gauge T' flavor. The smallest continuous group that contains T' is $SU(2)$, so this is what we will attempt below. Various complications arise, but we will be able to deal with them as we go along.

We take the simplified renormalizable T' extension of the standard model of [40] and

augment it in two ways. First, we add scalar singlets, that will acquire VEVs and shift the predictions of tribimaximal (TBM) mixing and of the Cabibbo angle from previous models to be more in line with current experimental values. Second, after adding a few fermions, the T' group is embedded into a gauged $SU(2)$ group we will call $SU(2)_{T'}$. This averts problems with gravity and chiral anomalies that can arise from adding discrete groups to the standard model. It also provides an elegant description of the discrete symmetry as a residue of a gauge group acting at higher scale. Finally we summarize how $SU(2)_{T'}$ can be broken directly to T' with a VEV for a particular scalar multiplet.

The next section contains the lepton sector particle assignments, plus the assignments for the scalar fields that enter the lepton Yukawa Lagrangian at the T' scale. Section 5.3 contains similar information for the quark sector; in Section 5.4 we discuss tribimaximal (TBM) mixing, where a T' triplet Higgs gets a vacuum expectation value (VEV). Since there is currently tension between the data and TBM predictions, we add T' scalar singlets with VEVs to shift TBM predictions in Section 5.5, where we show our new fit is in agreement with all lepton data. Section 5.6 focuses on the quark sector, where the new scalar singlet VEVs now contribute to quark mixing.

It is the above described T' model we gauge to $SU(2)_{T'}$, and describe in Section 5.7, where various additional particles need to be added to avoid all chiral anomalies. Section 5.8 describes the spontaneous symmetry breaking (SSB) from $SU(2)_{T'}$ to T', and Section 5.9 contains our conclusions and plans for further work. Appendix B collects all the T' group theory needed for this analysis.

5.2 Lepton Sector Lagrangian at the T' Scale

We begin by reviewing the lepton sector just above the T' scale. Because none of the leptons will be in even dimensional irreducible representations (irreps), this sector is equivalent to an A_4 model [6, 7]. We have also given the model a Z_2 symmetry in order to disallow certain terms in the Lagrangian. This Z_2 will also be gauged.

The standard model leptons are assigned to the following irreps [40] of $T' \times Z_2$ (and of $A_4 \times Z_2$):

$$\left.\begin{array}{l} \left(\begin{array}{c}\nu_\tau\\ \tau^-\end{array}\right)_L \\ \left(\begin{array}{c}\nu_\mu\\ \mu^-\end{array}\right)_L \\ \left(\begin{array}{c}\nu_e\\ e^-\end{array}\right)_L \end{array}\right\} L_L(\mathbf{3},0) \qquad \left.\begin{array}{ll} \tau_R^- \ (\mathbf{1_1},1) & N_R^{(1)} \\ \mu_R^- \ (\mathbf{1_3},1) & N_R^{(2)} \\ e_R^- \ (\mathbf{1_2},1) & N_R^{(3)} \end{array}\right\} N_R(\mathbf{3},0) \tag{5.1}$$

where N_R is a T' triplet of right handed neutrinos. In addition, we will need the following scalars to construct T' singlet Yukawa terms:

$$\begin{array}{c} H_3(\mathbf{3},0) = (H_3^1, H_3^2, H_3^3) \\ H_3'(\mathbf{3},1) = (H_{3'}^1, H_{3'}^2, H_{3'}^3) \\ H_{1_1}(\mathbf{1_1},0) \\ H_{1_2}(\mathbf{1_2},0) \\ H_{1_3}(\mathbf{1_3},0) \end{array} \tag{5.2}$$

Where the subscripts correspond to the T' irrep where the scalars live.

Aside: Note that here and and below we use a different notation from [40] which used a multiplicative form for the Z_2 charges, i.e., ± 1. Since we will be concerned with discrete and continuous chiral gauge anomalies, we use additive Z_2 charges, i.e., integers mod 2, to be consistent with most of the literature. When we later embed Z_2 in a $U(1)$ we will use integer charges.

With the above content, the most general lepton sector Yukawa Lagrangian is:

$$\mathcal{L}_l = Y_\tau L_L \tau_R H_{3'} + Y_\mu L_L \mu_R H_{3'} + Y_e L_L e_R H_{3'} + L_L N_R (Y_x H_{1_2} + Y_y H_{1_3} + Y_z H_{1_1} + Y_{TB} H_3) + m_N N_R N_R \tag{5.3}$$

The proper choice of VEVs for H_3 and $H_{3'}$ lead to values for the charged masses and the TBM mixing matrix. Giving VEVs to the singlets will break T' to Q, the group of unit quaternions, and shift the TBM matrix closer to experimentally compatible values.

5.3 Quark Sector Lagrangian at the T' Scale

The main advantage of a T' flavor model is that it is the discrete group of smallest order with a sufficiently diverse set of irreps that can be used to model both the quark and lepton sectors. Specifically, it has even-dimensional irreps that can also be used to economically describe the quark sector, as we will now summarize [40]. The standard model quarks are assigned to the following irreps:

$$\begin{array}{llll} \left(\begin{array}{c} t \\ b \end{array}\right)_L \; \mathcal{Q}_L & (\mathbf{1_1}, 0) & t_R & (\mathbf{1_1}, 1) \\ & & b_R & (\mathbf{1_2}, 1) \\ \left.\begin{array}{l} \left(\begin{array}{c} c \\ s \end{array}\right)_L \\ \left(\begin{array}{c} u \\ d \end{array}\right)_L \end{array}\right\} Q_L & (\mathbf{2_1}, 0) & \left.\begin{array}{l} c_R \\ u_R \end{array}\right\} \mathcal{C}_R & (\mathbf{2_3}, 1) \\ & & \left.\begin{array}{l} s_R \\ d_R \end{array}\right\} \mathcal{S}_R & (\mathbf{2_2}, 0). \end{array} \tag{5.4}$$

In addition to the scalars listed above, we add three morT' singlets:

$$\begin{array}{l} H_{1'_1}(\mathbf{1_1}, 1) \\ H_{1'_2}(\mathbf{1_2}, 1) \\ H_{1'_3}(\mathbf{1_3}, 1) \end{array} \tag{5.5}$$

Hence the most general quark sector Yukawa Lagrangian is then:

$$\mathcal{L}_q = Y_t \mathcal{Q}_L t_R H_{1'_1} + Y_b \mathcal{Q}_L b_R H_{1'_3} + Q_L \mathcal{C}_R (Y_{\mathcal{C}} H_{3'} + Y_{\mathcal{C}'} H_{1'_2}) + Q_L \mathcal{S}_R (Y_{\mathcal{S}} H_3 + Y_{\mathcal{S}'} H_{1_3}) \tag{5.6}$$

We see that a constraint on our model is that the VEVs of $H_3, H_{3'},$ and H_{1_3} must have values that are simultaneously compatible with the experiment data for both the quark and lepton sector.

5.4 TBM Mixing from T'

Before we derive our experimentally compatible PMNS matrix [67], we show that just below the T' energy scale where only T' triplets have VEVs, the neutrinos exhibit the familiar TBM mixing pattern [68]. Using the Clebsch-Gordan coefficients for T' detailed in Appendix B, we find that the term $m_N N_R N_R$ from equation (5.3) gives a mass matrix for right handed neutrinos:

$$M_N = \begin{pmatrix} m_N & 0 & 0 \\ 0 & 0 & m_N \\ 0 & m_N & 0 \end{pmatrix} \tag{5.7}$$

Similarly, we construct the Dirac mass matrix associated with the term $Y_{TB} L_L N_R H_3$ of the lepton Lagrangian:

$$M_D = \begin{pmatrix} eN_1 & eN_2 & eN_3 \\ \mu N_1 & \mu N_2 & \mu N_3 \\ \tau N_1 & \tau N_2 & \tau N_3 \end{pmatrix} = Y_{TB} \begin{pmatrix} v_2 & -v_1 & 0 \\ -v_3 & 0 & v_1 \\ 0 & v_3 & -v_2 \end{pmatrix} \tag{5.8}$$

Where (v_1, v_2, v_3) is the VEV of the scalar H_3. The Majorana mass matrix is given by:

$$M_\nu = M_D M_N^{-1} M_D^T \tag{5.9}$$

The rows of the Majorana mixing matrix are the normalized eigenvectors of this mass matrix, we find that for a VEV of $< H_3 >= V(1, 1, -2)$, (where V is some constant), we

recover the TB mixing matrix in the form

$$U_{TBM} = \begin{pmatrix} \sqrt{\frac{2}{3}} & \sqrt{\frac{1}{3}} & 0 \\ -\sqrt{\frac{1}{6}} & \sqrt{\frac{1}{3}} & -\sqrt{\frac{1}{2}} \\ -\sqrt{\frac{1}{6}} & \sqrt{\frac{1}{3}} & \sqrt{\frac{1}{2}} \end{pmatrix}. \tag{5.10}$$

Currently TBM is excluded at the 5σ level. For a different perspective see [69].

5.5 Shifted TBM Mixing

OOur next step is to augment this matrix using VEVs for the additional scalars H_{1_1}, H_{1_2} and H_{1_3}. (For an alternative perturbation theory approach see [70].) Including these in the model introduces the terms $L_L N_R(Y_x H_{1_2} + Y_y H_{1_3} + Y_z H_{1_1})$ into the Lagrangian. These terms have a mass matrix:

$$M_{xyz} = \begin{pmatrix} -x & z & y \\ -y & x & z \\ z & -y & -x \end{pmatrix} \tag{5.11}$$

Where x, y, and z represent $Y_x < H_{1_2} >$, $Y_y < H_{1_3} >$, and $Y_z < H_{1_1} >$ respectively. Our Dirac mass matrix is now

$$M_{D'} = M_D + M_{xyz} = Y_{TB} \begin{pmatrix} 1 - x' & -1 + z' & y' \\ 2 - y' & x' & 1 + z' \\ z' & -2 - y' & -1 - x' \end{pmatrix} V \tag{5.12}$$

where $x' = \frac{x}{Y_{TB}V}$, $y' = \frac{y}{Y_{TB}V}$ and $z' = \frac{z}{Y_{TB}V}$. The Majorana mixing matrix, U, is obtained the same way as before. The fit parameters x', y' and z' can now be varied to shift the entries of U from their TBM mixing values closer to current experimental values. The present 3σ experimental ranges of the magnitudes of the matrix elements are given below

[63, 71, 72]:

$$\begin{pmatrix} 0.799 \leftrightarrow 0.844 & 0.516 \leftrightarrow 0.582 & 0.141 \leftrightarrow 0.156 \\ 0.242 \leftrightarrow 0.494 & 0.467 \leftrightarrow 0.678 & 0.639 \leftrightarrow 0.774 \\ 0.284 \leftrightarrow 0.521 & 0.490 \leftrightarrow 0.695 & 0.615 \leftrightarrow 0.754 \end{pmatrix} \tag{5.13}$$

The next step we can take is to vary the parameters x', y', and z' from -1 to 1 (within a reasonable precision), and find the values for which the least accurate elements' error is minimized. We find that to the nearest hundreth, this minimum is obtained at $(x', y', z') = (0.32, -0.26, -.40)$ with the least accurate element being 1.922 standard deviations away from experimental value. Explicitly, these values correspond to a mixing matrix:

$$\begin{pmatrix} -0.829 & 0.539 & 0.148 \\ 0.289 & 0.640 & -0.712 \\ 0.478 & 0.548 & 0.686 \end{pmatrix} \tag{5.14}$$

which can be compared to the experimental numbers above.

The errors are given below in terms of standard deviations away from experimental value:

$$\begin{pmatrix} 1.029 & 0.910 & 0.228 \\ 1.882 & 1.919 & 0.224 \\ 1.922 & 1.313 & 0.083 \end{pmatrix}. \tag{5.15}$$

In addition to minimizing the error of the least accurate entry we can minimize the average error of the matrix elements.

Looping over all possible values of x', y', and z' (again to the nearest hundredth) minimizes the mean error at $(0.32, -0.27, -.045)$, with a value of 0.870 standard deviations.

Our mixing matrix is now

$$\begin{pmatrix} -0.822 & 0.549 & 0.149 \\ 0.298 & 0.638 & -0.710 \\ 0.485 & 0.539 & 0.688 \end{pmatrix}, \tag{5.16}$$

with errors

$$\begin{pmatrix} 0.090 & 0.0351 & 0.199 \\ 1.671 & 1.869 & 0.151 \\ 2.091 & 1.558 & 0.167 \end{pmatrix}. \tag{5.17}$$

From both these perspectives on error analysis, our T' model extended with a pair of scalar singlets agrees with the current experimental data which provides a significant improvement over the simple TBM model.

We can also examine our fitting with a contour plot. Our error values are the most sensitive to changes in x' so we hold it constant at 0.32 and allow our parameters y' and z' to vary between -1 and 0 as shown in the plots below: (The parameter range $(y', z') > 0$ gives very high error values so it is not shown.)

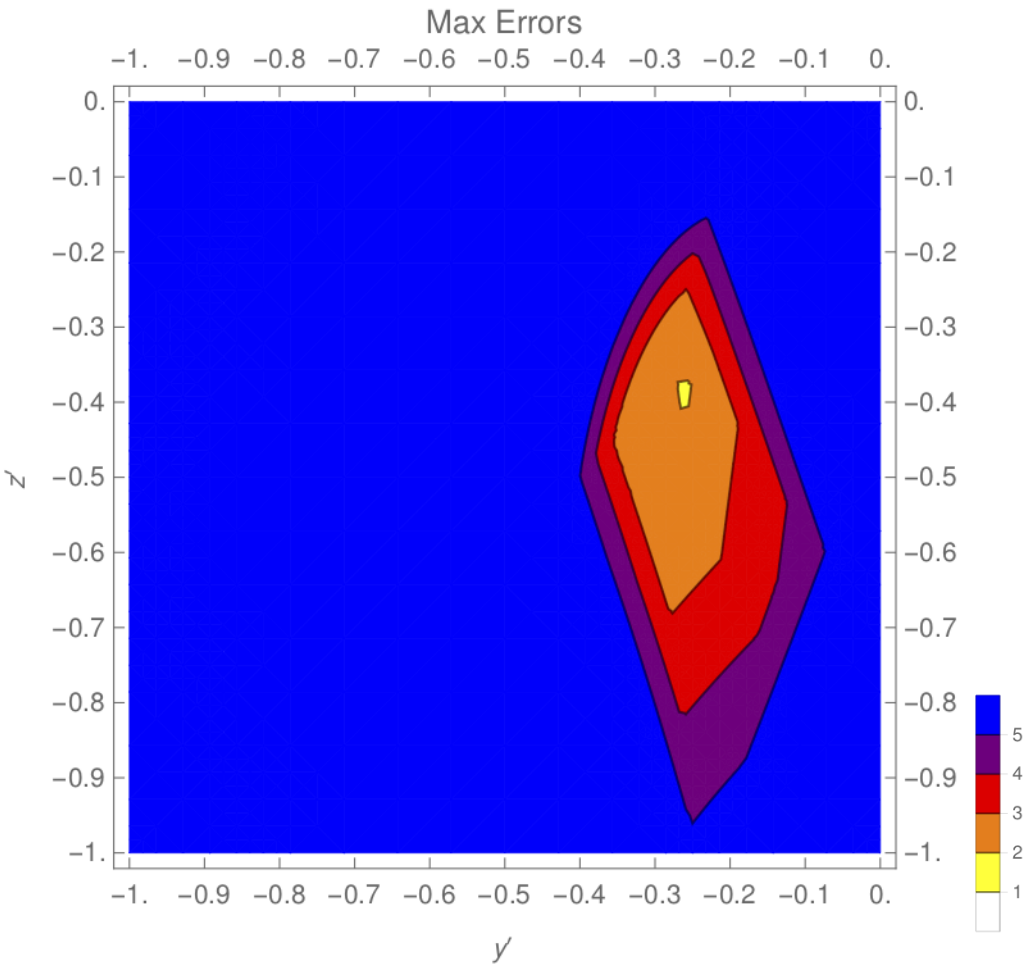

Figure 5.1: Contour plot with x' fixed at 0.32 of maximum mixing matrix error relative to experimental data, where values are in units of standard deviation.

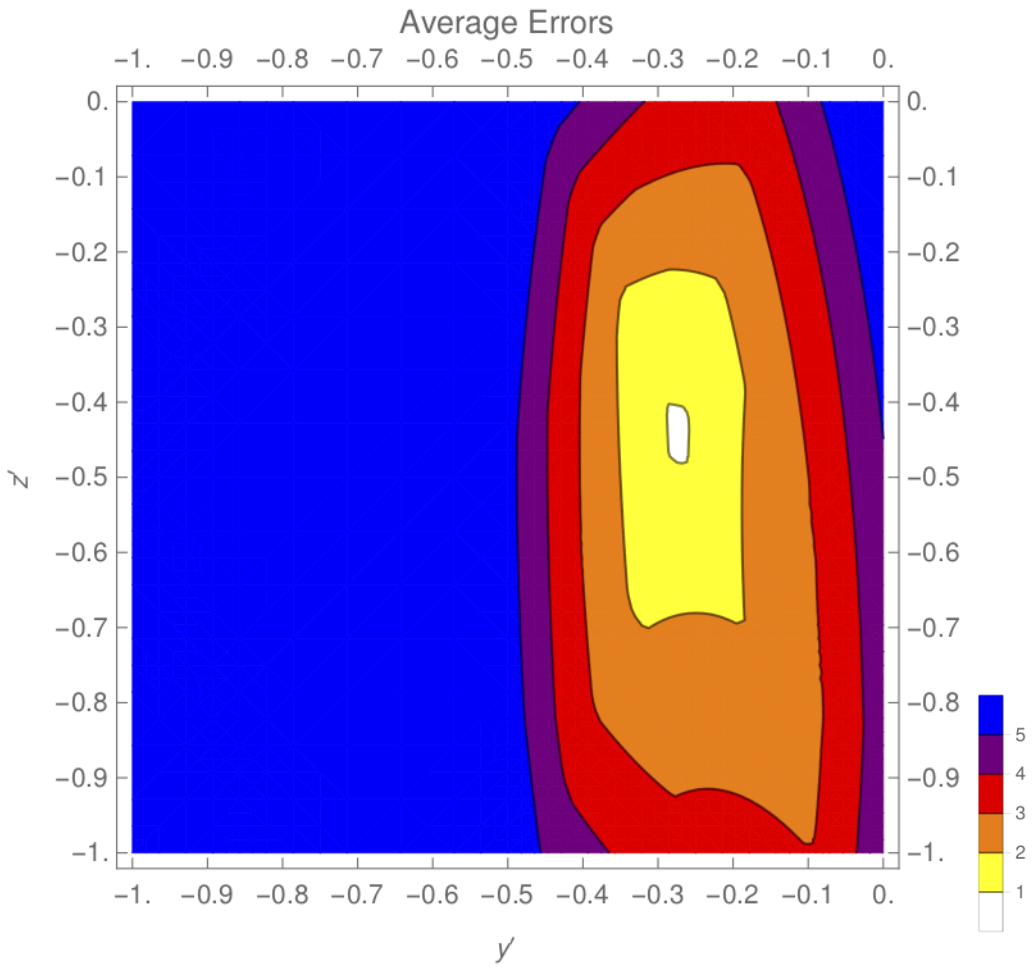

Figure 5.2: Contour plot with x' fixed at 0.32 of average mixing matrix error relative to experimental data, where values are in units of standard deviation.

We see from these plots that there are relatively small ranges, but still without fine tuning beyond an order of magnitude, for our parameters that give us maximum error and average error less that 2σ and 1σ respectively.

5.6 Quark Mixing

As shown in [40], one can derive a reasonable prediction for the Cabbibo angle from the Lagrangian in equation (5.6). We rederive this result here for our basis and then augment the value when an additional scalar has a VEV. We also find the mass matrices for the first two generations of up and down type quarks from the terms $Q_L \mathcal{C}_R(H_{3'} + H_{1'_2})$ and

$Q_L \mathcal{S}_R(H_3 + H_{1_3})$ respectively. From the discussion above we know that H_3 must have a VEV of the form $V(1,1,-2)$. To give masses to the charged leptons $H_{3'}$ gets a VEV:

$$< H_{3'} >= \left(\frac{m_\tau}{Y_\tau}, 0, 0\right) \tag{5.18}$$

.

Note that if the Yukawa couplings on the Dirac mass terms for the charged leptons are of the same order of magnitude this will give approximately degenerate masses. Therefore some tuning or the introduction of an additional $U(1)$ flavor symmetry is necessary to get correct mass values (see [77]). Using these values along with the Clebsch-Gordan coefficients found in the Appendix, we obtain a mass matrix U for the up-type quarks:

$$U = Y_{\mathcal{C}} \begin{pmatrix} 0 & 0 \\ 0 & \frac{-\sqrt{2}m_\tau}{Y_\tau} \end{pmatrix} \tag{5.19}$$

.

This gives a charm quark mass on the order of the tau mass but a zero mass for the up quark. We can correct this by giving a VEV to $H_{1'_2}$, which will give an up-type matrix:

$$U' = Y_{\mathcal{C}} \begin{pmatrix} 0 & \frac{1}{\sqrt{2}}\frac{Y_{\mathcal{C}'} < H_{1'_2} >}{Y_{\mathcal{C}}} \\ -\frac{1}{\sqrt{2}}\frac{Y_{\mathcal{C}'} < H_{1'_2} >}{Y_{\mathcal{C}}} & \frac{-\sqrt{2}m_\tau}{Y_\tau} \end{pmatrix}. \tag{5.20}$$

Setting $\frac{Y_{\mathcal{C}'} < H_{1'_3} >}{\sqrt{2}Y_{\mathcal{C}}} = .05875 \times \frac{m_\tau}{Y_\tau}$ and taking the hermitian square of U' gives:

$$U'U'^{\dagger} = Y_{\mathcal{C}}^2 \begin{pmatrix} 0.00345156(\frac{m_\tau}{Y_\tau})^2 & -0.083085(\frac{m_\tau}{Y_\tau})^2 \\ -0.083085(\frac{m_\tau}{Y_\tau})^2 & 2.00345(\frac{m_\tau}{Y_\tau})^2 \end{pmatrix}. \tag{5.21}$$

with eigenvalues $m_1 = Y_{\mathcal{C}}^2\ 2.0069(\frac{m_\tau}{Y_\tau})^2$ and $m_2 = Y_{\mathcal{C}}^2\ 5.93617 \times 10^{-6}(\frac{m_\tau}{Y_\tau})^2$ which give the squares of the charm and up masses respectively. With these values, the ratio $\frac{m_u}{m_c} =$

0.00171985 closely approximates the measured value of $\frac{m_u}{m_c} = 0.00171875$

For our down-type mass matrix, D we obtain:

$$D = Y_S \begin{pmatrix} \sqrt{2} & 2 + \frac{Y_{S'} < H_{1_3} >}{Y_S V} \\ 2 - \frac{Y_{S'} < H_{1_3} >}{Y_S V} & \sqrt{2} \end{pmatrix} V \tag{5.22}$$

.

We find that setting the factor $\frac{Y_{S'} < H_{1_3} >}{Y_S V} = 2.3815$ will give the best values for the Cabibbo angle and for the down and strange quark masses. Making this substitution, we have:

$$DD^\dagger = Y_S^2 \begin{pmatrix} 21.1975 & 5.65685 \\ -5.65685 & 2.14554 \end{pmatrix} V^2 \tag{5.23}$$

with eigenvalues $m_1 = Y_S^2\ 22.7506 V^2$ and $m_2 = Y_S^2\ .592523 V^2$ which give the squares of the strange and down masses respectively. With these values, the ratio $\frac{m_d}{m_s} = 0.161382$ only roughly approximates the measured value of $\frac{m_d}{m_s} = 0.0489583$.

The mixing matrix for the first two quark generations, (the upper left corner of the CKM matrix) is $W = K_u^\dagger K_d$. Where K_u and K_d are the unitary matrices that diagonalize the Hermitian squares of U and D respectively. We find:

$$K_d = \begin{pmatrix} 0.964319 & 0.264742 \\ -0.264742 & 0.964319 \end{pmatrix} \tag{5.24}$$

$$K_u = \begin{pmatrix} 0.999141 & 0.0414355 \\ -0.0414355 & 0.999141 \end{pmatrix} \tag{5.25}$$

$$W = K_u^\dagger K_d = \begin{pmatrix} 0.974461 & 0.224558 \\ -0.224558 & 0.974461 \end{pmatrix} \tag{5.26}$$

This gives an expression for the Cabibbo angle Θ

$$\tan(2\Theta) = \left(\frac{\sqrt{2}}{3}\right) \;\rightarrow\; \sin(\Theta) = .224558 \tag{5.27}$$

The values for W_{ud} and W_{us}, and thus the prediction for the Cabibbo angle, are almost identical to those found from the latest experimental fit [72]:

$$|W| = \begin{pmatrix} 0.97446 \pm 0.00010 & 0.22452 \pm .00044 \\ 0.22438 \pm 0.00044 & 0.97359^{+0.00010}_{-0.00011} \end{pmatrix}. \tag{5.28}$$

Specifically, our errors are (again in units of σ):

$$\begin{pmatrix} 0.008 & 0.085 \\ 0.404 & 7.917 \end{pmatrix}. \tag{5.29}$$

We see the W_{cd} prediction is also well within 1σ. The prediction for W_{cs} is quite a bit off, but this is to be expected, or at least not surprising, given our neglect of third family mixing effects.

We could adjust our predictions for W_{cs} and $\frac{m_d}{m_s}$ via third family mixing by adding the following terms to the Lagrangian in equation (5.6):

$$\mathcal{L}'_q = Y_{tcu}\mathcal{Q}_L\mathcal{C}_R H_{2_3} + Y_{bsd}\mathcal{Q}_L\mathcal{S}_R H_{2_2} + Y_{cut}Q_L t_R H_{2_1} + Y_{sdb}Q_L b_R H_{2_3}, \tag{5.30}$$

but this introduces at least six more free parameters into the theory, significantly complicating the analysis. Hence these terms are left for a future study.

Finally we note that from the relations $\frac{Y_{\mathcal{S}'}<H_{1_3}>}{Y_{\mathcal{S}}V} = 2.3815$ and $\frac{Y_y<H_{1_3}>}{Y_{TB}V} = -.26$ we have the constraint $\frac{Y_y}{Y_{TB}} = -.109175\frac{Y_{\mathcal{S}'}}{Y_{\mathcal{S}}}$.

5.7 T' Embedding in $SU(2)$

As explained in the Introduction, it is often desirable to embed discrete symmetries into continuous gauge groups at higher energy scales. The remainder of this paper will focus on generalizing our T' model to a gauged $SU(2)_{T'}$ flavor theory.

There are three main tasks needed for our gauge group embedding. First, we must identify which $SU(2)_{T'}$ representations our T' particles can fall into. This is easily accomplished by examining the branching rules from Table A.5. New particles will have to be introduced to fill out these $SU(2)_{T'}$ irreps, as a full theory cannot contain incomplete group representations. Second, we must ensure our theory is anomaly free. This involves checking that our representations satisfy certain sum rules on their quantum numbers (see e.g., [73]). Again we will see we must add more particles to the theory in order to cancel all anomalies. Finally, we formulate a scalar Lagrangian where we can find a particular vacuum expectation value that breaks $SU(2)_{T'}$ down stepwise to T' [18, 19, 74], then to Q, etc. and eventually to nothing.

5.7.1 $SU(2)$ Multiplets

Table I shows the results of embedding the T' irreps of equations (5.1) and (5.4) into SU(2)$_{T'}$. Each row shows the particle in their SU(2)$_{T'}$ multiplet, and each column gives the representation of the constituent particles under the specified gauge group.

Table 5.1: Fermionic content of SU(2)$_{T'}$ gauge theory

Particles	SU(3)	SU(2)	U(1) Charge	SU(2)$_{T'}$
$((\nu_\tau,\tau),(\nu_\mu,\mu),(\nu_e,e))_L$	1	2	-1	3
τ_R^c	1	1	2	1
$(A,B,C)_L$	1	1	-2	3
$(\mu,e,A,B,C)_R^c$	1	1	2	5
$(N_1,N_2,N_3)_R$	1	1	0	3
$((c,s),(u,d))_L$	3	2	$\frac{1}{3}$	2
$(t,b)_L$	3	2	$\frac{1}{3}$	1
t_R^c	3	1	$-\frac{4}{3}$	1
$(X,b,\alpha,\beta,\gamma)_R^c$	3	1	$\frac{2}{3}$	5
X_L	3	1	$-\frac{2}{3}$	1
$(\alpha,\beta,\gamma)_L$	3	1	$-\frac{2}{3}$	3
$(c,u,i,j)_R^c$	3	1	$-\frac{4}{3}$	4
$(s,d,k,l)_R^c$	3	1	$\frac{2}{3}$	4
i_L	3	1	$\frac{4}{3}$	1
j_L	3	1	$\frac{4}{3}$	1
k_L	3	1	$-\frac{2}{3}$	1
l_L	3	1	$-\frac{2}{3}$	1

In order to complete the various irreps of $SU(2)_{T'}$ we have to include a number of new particles. Specifically we have added three new leptons: (a,b,c), and eight new quarks: $X,\alpha,\beta,\gamma,i,j,k,l$.

Our next step is to check our theory for anomalies. With the current irreps, the only anomaly that does not cancel is $SU(2)_{T'}\times SU(2)_{T'}\times U(1)_Y$. To cancel this anomaly and avoid disrupting other cancellations, we add the multiplets listed in Table II to the theory.

Note that this is not the only way to do the embedding, but it is the most straightforward and economical embedding we have found.

Table 5.2: Additional particles needed for cancellation of chiral anomalies

Particles	$SU(3)_C$ irrep	$SU(2)_L$ irrep	$U(1)_Y$ charge	$SU(2)_{T'}$ irrep
$(a_1, a_2, a_3, a_4, a_5)$	1	1	-2	5
(n_1, n_2)	1	1	2	2
m_1	1	1	2	1
$m_{1'}$	1	1	2	1
$m_{1''}$	1	1	2	1

With that we have a complete fermion sector for the theory. Although we have had to add many new particles, all of them can be made sufficiently heavy such that they are only relevant at very high energy scales.

Let us recall that the current [72] b' (charge -1/3) quark mass limit is $\geq$ 1,530 GeV CL=95.0% and the t' (charge +2/3)-quark mass limits is $\geq$ 1,160 GeV CL=95.0% with less stringent bounds $\geq$ 110 GeV for leptons. For the most part the BSM particles in Table 1 are designed to form vector-like pair and become massive once $SU(2)_{T'}$ is broken but before the EW symmetry breaking. This keeps the SM particles massless while the BSM particles are massive and unobserved as long as we require the $SU(2)_{T'}$ breaking scale to be a few TeV. E.g., $(A, B, C)_L$ in the third line of the table pair up with $(A, B, C)_R$ from $(\mu, e, A, B, C)_R$ once $SU(2)_{T'}$ is broken. Hence A, B and C can have relatively large masses compared to SM particles. (Note that at this stage μ and e must remain massless at least until $SU(2)_L$ is broken.) α, β and γ behave in a similar way, as do X and i, j, k and l. (The same holds for the new particles introduced in Table 2.)

5.7.2 Z_2 Anomaly Cancellation

In the above formulation we have canceled all anomalies that come about due to the addition of the T' symmetry to the standard model. However, recall that we also included an extra Z_2 symmetry in order to forbid certain unwanted Lagrangian terms. This Z_2 can be embedded in an extra $U(1)_{Z_2}$ symmetry that breaks at an arbitrary scale independent of the $SU(2)_{T'}$ breaking. We detail the charge assignments for an example anomaly-free $SU(3) \times SU(2)_L \times U(1)_Y \times SU(2)_{T'} \times U(1)_{Z_2}$ theory below in Table III. Notice we have added an SM singlet $SU(2)_{T'}$ **4** with Z_2 charge -1 and fourteen fermions that are trivial singlets under everything but $U(1)_Y \times U(1)_{Z_2}$. Five of them, the Es have charge (2,1) and the other five, the Fs have charge ($-$2,0) under this group, the remaining four have $U(1)_Y$ charge ± 10 and $U(1)_{Z_2}$ charge 0, 1 or -1.

There is significant freedom in assigning $U(1)_{Z_2}$ charges to existing particles as they reduce to particles with identical Z_2 charges modulo 2. So even though this example has involved adding many extra particles, a less baroque model may be possible. The discussion of the masses for the additional particles (from the line $(a1, a2, a3, a4, a5)$ onward) in Table 3 needed to cancel the $U(1)_{Z_2}$ anomaly is similar to the discussion of Table 1. We find that once $U(1)_{Z_2}$ is broken the five Es pair with the five Fs and g_1 and g_2 pair with h_1 and h_2. Once both $SU(2)_{T'}$ and $U(1)_{Z_2}$ are broken the five states $(a1, a2, a3, a4, a5)$ pair with $(n1, n2)$, m_1, $m_{1'}$ and $m_{1''}$. At this stage all the SM particles are still massless since the EW symmetry is not yet broken. Hence, the Table 3 additions are not as bad as they may seem at first sight.

Table 5.3: Example charge assignments for $U(1)_{Z_2}$ anomaly cancellation [64, 65]

Particles	$SU(3)_C$ irrep	$SU(2)_L$ irrep	$U(1)_Y$ charge	$SU(2)_{T'}$ irrep	U(1)$_{Z_2}$ charge
$((\nu_\tau,\tau),(\nu_\mu,\mu),(\nu_e,e))_L$	1	2	-1	3	0
τ_R^c	1	1	2	1	1
$(A,B,C)_L$	1	1	-2	3	0
$(\mu,e,A,B,C)_R^c$	1	1	2	5	-1
$(N_1,N_2,N_3)_R$	1	1	0	3	0
$((c,s),(u,d))_L$	3	2	$\frac{1}{3}$	2	0
$(t,b)_L$	3	2	$\frac{1}{3}$	1	0
t_R^c	3	1	$-\frac{4}{3}$	1	1
$(X,b,\alpha,\beta,\gamma)_R^c$	3	1	$\frac{2}{3}$	5	1
X_L	3	1	$-\frac{2}{3}$	1	-1
$(\alpha,\beta,\gamma)_L$	3	1	$-\frac{2}{3}$	3	0
$(c,u,i,j)_R^c$	3	1	$-\frac{4}{3}$	4	-1
$(s,d,k,l)_R^c$	3	1	$\frac{2}{3}$	4	0
i_L	3	1	$\frac{4}{3}$	1	-1
j_L	3	1	$\frac{4}{3}$	1	0
k_L	3	1	$-\frac{2}{3}$	1	0
l_L	3	1	$-\frac{2}{3}$	1	0
(a_1,a_2,a_3,a_4,a_5)	1	1	-2	5	0
(n_1,n_2)	1	1	2	2	0
m_1	1	1	2	1	1
$m_{1'}$	1	1	2	1	1
$m_{1''}$	1	1	2	1	1
(b_1,b_2,b_3,b_4)	1	1	0	4	-1
$5\times E$	1	1	2	1	1
$5\times F$	1	1	-2	1	0
g_1	1	1	-10	1	1
g_2	1	1	-10	1	-1
h_1	1	1	10	1	0
h_2	1	1	10	1	0

5.8 Spontaneous Symmetry Breaking

Our final step is to provide the spontaneous breaking of SU(2)$_{T'} \to T'$. We have already performed this analysis in Chapter 3, so will only summarize the results here. To have this spontaneous symmetry breaking we must include a scalar multiplet of $SU(2)_{T'}$ that contains a trivial singlet of T'. Looking at the branching rules of table A.5, we see the smallest avalable irrep for this purpose is the **7**. The **7** can be real or complex, but for simplicity we choose a real multiplet with scalar potential 3

$$V_7 = -m^2\, T_{abc}T_{abc} + \lambda\,(T_{abc}T_{abc})^2 + \kappa\; T_{abd}T_{abe}T_{fge}T_{fgd}, \tag{5.31}$$

where T is a traceless, symmetric, $3 \times 3 \times 3$ tensor, λ and κ are the scalar quartic coupling constants, and the indices $a, b, ...$ run from 1 to 3.

Spontaneous breaking to T' occurs when the potential is minimized and the scalar is given a Vacuum Expectation Value (VEV) in a particular direction. For the real **7** this VEV is [74]:

$$\mathcal{V} = \sqrt{\frac{3m^2}{2(3\lambda+\kappa)}}\,[0,0,0,0,0,0,1]. \tag{5.32}$$

After breaking SU(2)$_{T'}$ the **7** real scalars reduce to their T' irreps with mass eigenvalues given by

Value	Multiplicity
0	3
$4m^2$	1
$\frac{8m^2\kappa}{5(3\lambda+\kappa)}$	3

which contains the three requisite Goldstone bosons that get eaten by the $SU(2)_{T'}$ gauge

bosons. To ensure a stable minimum the coupling constants must satisfy the constraints $3\lambda + \kappa > 0$ and $\kappa > 0$. Clearly there is a substantial region of parameter space where this pattern of SSB is the stable minimum of the potential in eq.(5.31).

This **7** is obviously not the only scalar in the theory as more scalars are needed to construct Yukawa terms at the SU(2)$_{T'}$ scale. However, we omit the full scalar Lagrangian in this paper because we will not be exploring its complete phenomenology at present. We are assuming that the coupling of the **7** to the other scalars is sufficiently weak that the breaking to T' is not destabilized. The analysis of a specific example of this type of VEV stability can be found in [74].

5.9 Discussion and Conclusions

We have extended the basic T' flavor model to fit the current best available quark and lepton mass and mixing angle data. More specifically, we have constructed an extended but fairly simple, renormalizable T' model that predicts neutrino mixing parameters within 2σ of experiment, as well as a Cabibbo angle well within 1σ. This has required the addition of T' scalar singlets with VEVs. Once our new T' model was fixed, we then extended it further by embedding it in $SU(2)_{T'}$ such that the entire model was fully gauged. This avoided all problems with gauge and gravity mixed anomalies at the expense of adding a number of new fermions to the lepton and quark sectors. The additional fermions were not necessarily the minimal set, as there are many possible choices, so what we have provided is a proof of principle that fully gauged flavor models can be found to fit all current flavored data. It still remains quite challenging to find a full gauge unification of flavor, but it is perhaps not unreasonable to hope that one could eventually find a top-down GUT flavor model that reduces to a product gauge model of the type we have discussed here.

Besides the T' model discussed here, gauged A_4 models [23, 75, 76] have also appeared, but there remains a long list of discrete groups $S_4, A_5, Q_6, O', I', T_7, \Delta(27)$ and $PSL(2,7)$ that are easy to obtain from breaking $SU(2)$ or $SU(3)$. So it appears possible to gauge

some if not all of the models based on these groups [44–52].

We have argued that all the extra beyond the standard model particles can be made heavy enough to avoid bounds from the LHC. While our model lacks elegance, it is a viable model and it does teach us quite a lot. (i) First, it provides a proof in principle that a good candidate for a discrete group extension of the SM that gives reasonable values for the quark and lepton masses and mixing angles, namely $SU(3)_C \times SU(2)_L \times U(1)_Y \times SU(2)_{T'} \times U(1)_{Z_2}$, can be gauged and survive experimental constraints. (ii) A major lesson is that extra $U(1)$s complicate the model considerably and their elimination appears necessary if a simpler model is to be found. We plan to pursue this line in future work. (iii) The present model has interesting implications for cosmological defects and provides another interesting topic for the future. Domain walls that result from breaking discrete symmetries can be destabalized if the discrete symmetry is embedded in a local gauge group leading to a model more likely to be viable.

Finally we need to comment on the LHC constraints on extra Higgs masses. Searches for a Higgs Boson with Standard Model couplings with mass $m \geq 122$ GeV find nothing in the range 128 – 1000 GeV at CL = 95%, while searches for charged Higgses $H^{\pm}$ provide weaker bounds and give mass $m \geq 80$ GeV, CL = 95%. (These current generally accepted mass bounds are quoted from the Review of Particle Properties Tanabashi:2018.) There are numerous scalars in our model and in fact they are the most likely aspect of the model to lead to testable predictions given a full phenomenological analysis. This would require the study of the complete scalar potential which is well beyond what we had set out to accomplish in this paper. (Note that the full scalar potential contains over a dozen terms, including many cross terms between the various irreps, so it would require a considerable amount of work to do a complete analysis.) However, we would still like to comment on what we would expect from such an analysis. First, the real 7 scalar breaks $SU(2)_{T'}$ to T' at a high scale–above 100 TeV. Three component of the 7 are eaten by the Higgs mechanism and the other 4 should be near the breaking scale, well above current bounds.

Similar comments hold for the scalar that breaks $U(1)_{Z_2}$ to Z_2. The electroweak doublets on the other hand, should naturally be near the EW scale. Besides the Higgs at 125 GeV and the three components eaten by the $W^{\pm}$ and the Z, what remains are charged scalars which need to be above M_W which should take a small amount fine tuning and a number of neutral scalars. To keep the neutrals at or above the current LHC bounds will most likely take some fine tuning. The less tuning the closer they will be to the bounds. Hence the neutrals need to be at least a factor of 4 heavier than their natural scale if we set it to be the EW VEV scale 246 GeV. So the tuning needed is rather mild, but we could expect scalar to show up soon if the model is correct.

There is still more to explore within our present model. Examples include the phenomenology of the additional fermions required for anomaly cancellation and a study of cosmological defects. The phenomenology of the scalar sector would clearly benefit from further study. Beyond this specific model, it would be preferable to avoid Z_n factors by either reassigning irreps of SM states, or by using different initial non-abelian discrete groups. This would simplify the anomaly cancellation and hence minimize the introduction of extra fermionic states. We plan to search for such models in the future.

Chapter 6

CONCLUSION

Thus completes our study of methods in flavor model building. We began in Chapter 2 with an introduction to spontaneous symmetry breaking, detailing electroweak symmetry breaking via the Higgs mechanism. Chapter 3 outlined a systematic approach to symmetry breaking for use in gauged flavor models. Chapter 4 moved to a derivation of flavor mixing in the quark and neutrino sectors, and showed how small neutrino masses can arise via the see-saw mechanism. Finally, in Chapter 5 we constructed a gauged flavor model of quarks and leptons. We showed how one can use a discrete symmetry to derive fermion mixing patterns consistent with experimental predictions.

While making these predictions for the CKM and PMNS matrices required a fairly simple model, in promoting the model to $SU(2)$ it became quite messy, requiring the inclusion of many new particles. Therefore a next step may be to develop a discrete flavor model in which chiral anomaly cancellation requires fewer particles while still maintaining accurate predictions at the electroweak scale. This may involve tweaking the present model by changing particle irreps, or developing a model with a different discrete symmetry. Another problem not fully addressed is fine tuning of the Yukawa couplings. We were able to attribute much of the standard model mass hierarchy to symmetry breaking but there still remained some mass differences, e.g. among the charged leptons, that require significant tuning. Again a deeper search of discrete models will be required to find a more predictive theory.

In summary, the study of flavor physics is an often fruitful approach to the development of theories beyond the Standard Model. Discrete symmetries can help explain the values of Standard Model free parameters, while embedding the symmetry in a gauge group connects to physics above the electroweak scale. These insights bring us closer to a complete theory

of flavor which would be a significant step towards a theory of physics at the unification scale.

Appendix A

Branching Rules

In this Appendix we present the branching rules for the embeddings of discrete groups into Lie groups used in Chapter 3. The vertical axes label the dimensions of the Lie Group reps, and the horizontal the dimensions of the discrete group representations.

Table A.1: $SO(3) \to A_4$

Dimension	$\mathbf{1_1}$	$\mathbf{1_2}$	$\mathbf{1_3}$	$\mathbf{3}$
2	0	0	0	0
3	0	0	0	1
4	0	0	0	0
5	0	1	1	1
6	0	0	0	0
7	1	0	0	2
8	0	0	0	0
9	1	1	1	2
10	0	0	0	0
11	0	1	1	3

Table A.2: $SO(3) \to S_4$

Dimension	$\mathbf{1_1}$	$\mathbf{1_2}$	$\mathbf{2}$	$\mathbf{3_1}$	$\mathbf{3_2}$
2	0	0	0	0	0
3	0	0	0	1	0
4	0	0	0	0	0
5	0	0	1	0	1
6	0	0	0	0	0
7	0	1	0	1	1
8	0	0	0	0	0
9	1	0	1	1	1
10	0	0	0	0	0
11	0	0	1	2	1

Table A.3: $SO(3) \to A_5$

Dimension	**1**	**3**	**3**	**4**	**5**
2	0	0	0	0	0
3	0	0	1	0	0
4	0	0	0	0	0
5	0	0	0	0	1
6	0	0	0	0	0
7	0	1	0	1	0
8	0	0	0	0	0
9	0	0	0	1	1
***10**	0	0	0	0	0
11	0	1	1	0	1
12	0	0	0	0	0
13	1	0	1	1	1

Table A.4: $SU(2) \to Q_6$

Dimension	$\mathbf{1_1}$	$\mathbf{1_2}$	$\mathbf{1_3}$	$\mathbf{1_4}$	$\mathbf{2_1}$	$\mathbf{2_2}$
2	0	0	0	0	1	0
3	0	1	0	0	0	1
4	0	0	1	1	1	0
5	1	0	0	0	0	2
6	0	0	1	1	2	0
7	1	2	0	0	0	2
8	0	0	1	1	3	0
9	2	1	0	0	0	3
10	0	0	2	2	3	0
11	1	2	0	0	0	4

Table A.5: $SU(2) \to T'$

Dimension	$\mathbf{1_1}$	$\mathbf{1_2}$	$\mathbf{1_3}$	$\mathbf{2_1}$	$\mathbf{2_2}$	$\mathbf{2_3}$	**3**
2	0	0	0	1	0	0	0
3	0	0	0	0	0	0	1
4	0	0	0	0	1	1	0
5	0	1	1	0	0	0	1
6	0	0	0	1	1	1	0
7	1	0	0	0	0	0	2
8	0	0	0	2	1	1	0
9	1	1	1	0	0	0	2
10	0	0	0	1	2	2	0
11	0	1	1	0	0	0	3

Table A.6: $SU(2) \to O'$

Dimension	$\mathbf{1_1}$	$\mathbf{1_2}$	$\mathbf{2_1}$	$\mathbf{2_2}$	$\mathbf{2_3}$	$\mathbf{3_1}$	$\mathbf{3_2}$	**4**
2	0	0	0	1	0	0	0	0
3	0	0	0	0	0	0	1	0
4	0	0	0	0	0	0	0	1
5	0	0	1	0	0	1	0	0
6	0	0	0	0	1	0	0	1
7	0	1	0	0	0	1	1	0
8	0	0	0	1	1	0	0	1
9	1	0	1	0	0	1	1	0
10	0	0	0	1	0	0	0	2
11	0	0	1	0	0	1	2	0

Table A.7: $SU(2) \to I'$

Dimension	$\mathbf{1_1}$	$\mathbf{2_2}$	$\mathbf{2_3}$	$\mathbf{3_1}$	$\mathbf{3_2}$	$\mathbf{4_1}$	$\mathbf{4_2}$	**5**	**6**
2	0	1	0	0	0	0	0	0	0
3	0	0	0	0	1	0	0	0	0
4	0	0	0	0	0	0	1	0	0
5	0	0	0	0	0	0	0	1	0
6	0	0	0	0	0	0	0	0	1
7	0	0	0	1	0	1	0	0	0
8	0	0	1	0	0	0	0	0	1
9	0	0	0	0	0	1	0	1	0
10	0	1	0	0	0	0	1	0	1
11	0	0	0	1	1	0	0	1	0
12	0	1	0	0	0	0	1	0	1
13	1	0	0	0	1	1	0	1	0

Table A.8: $SU(3) \to A_4$

Dimension	$\mathbf{1_1}$	$\mathbf{1_2}$	$\mathbf{1_3}$	**3**
3	0	0	0	1
6	1	1	1	1
8	0	1	1	2
10	1	0	0	3
15	1	1	1	4
15′	2	2	2	3
21	1	1	1	6
24	2	2	2	6
27	3	3	3	6

Table A.9: $SU(3) \to T_7$

Dimension	$\mathbf{1_1}$	$\mathbf{1_2}$	$\mathbf{1_3}$	$\mathbf{3_1}$	$\mathbf{3_2}$
3	0	0	0	1	0
6	0	0	0	1	1
8	0	1	1	1	1
10	1	0	0	1	2
15	1	1	1	2	2
15′	1	1	1	2	2
21	1	1	1	3	3
24	1	1	1	4	3
27	1	1	1	4	4

Table A.10: $SU(3) \to \Delta(27)$

Dimension	$\mathbf{1_1}$	$\mathbf{1_2}$	$\mathbf{1_3}$	$\mathbf{1_4}$	$\mathbf{1_5}$	$\mathbf{1_6}$	$\mathbf{1_7}$	$\mathbf{1_8}$	$\mathbf{1_9}$	$\mathbf{3_1}$	$\mathbf{3_2}$
3	0	0	0	0	0	0	0	0	0	1	0
6	0	0	0	0	0	0	0	0	0	0	2
8	0	1	1	1	1	1	1	1	1	0	0
10	2	1	1	1	1	1	1	1	1	0	0
15	0	0	0	0	0	0	0	0	0	5	0
15′	0	0	0	0	0	0	0	0	0	5	0
21	0	0	0	0	0	0	0	0	0	0	7
24	0	0	0	0	0	0	0	0	0	0	8
27	3	3	3	3	3	3	3	3	3	0	0

Table A.11: $SU(3) \to PSL(2,7)$

Dimension	$\mathbf{1}$	$\mathbf{3_2}$	$\mathbf{3_2}$	$\mathbf{6}$	$\mathbf{7}$	$\mathbf{8}$
3	0	1	0	0	0	0
6	0	0	0	1	0	0
8	0	0	0	0	0	1
10	0	0	1	0	1	0
15	0	0	0	0	1	1
15′	1	0	0	1	0	1
21	0	1	1	0	1	1
24	0	1	0	1	1	1
27	0	0	0	2	1	1
28	1	0	0	2	1	1

Appendix B

Useful Information About the Binary Tetrahedral Group T'

B.1 T' Character Table

Dimension	$\mathbf{C_1}$	$\mathbf{C_2}$	$4\mathbf{C_3}$	$6\mathbf{C_4}$	$4\mathbf{C_5}$	$4\mathbf{C_6}$	$4\mathbf{C_7}$
$\mathbf{1_1}$	1	1	1	1	1	1	1
$\mathbf{1_2}$	1	1	ω^2	ω^4	1	ω^2	ω^4
$\mathbf{1_3}$	1	1	ω^4	ω^2	1	ω^4	ω^2
$\mathbf{2_1}$	2	-2	-1	-1	0	1	1
$\mathbf{2_2}$	2	-2	ω^5	ω	0	ω^2	ω^4
$\mathbf{2_3}$	2	-2	ω	ω^5	0	ω^4	ω^2
$\mathbf{3}$	3	3	0	0	-1	0	0

Where $\omega = e^{\frac{2\pi i}{6}}$.

B.2 Kronecker Products of T' Irreps

Dimension	$\mathbf{1_1}$	$\mathbf{1_2}$	$\mathbf{1_3}$	$\mathbf{2_1}$	$\mathbf{2_2}$	$\mathbf{2_3}$	$\mathbf{3}$
$\mathbf{1_1}$	$\mathbf{1_1}$	$\mathbf{1_2}$	$\mathbf{1_3}$	$\mathbf{2_1}$	$\mathbf{2_2}$	$\mathbf{2_3}$	$\mathbf{3}$
$\mathbf{1_2}$	$\mathbf{1_2}$	$\mathbf{1_3}$	$\mathbf{1_1}$	$\mathbf{2_2}$	$\mathbf{2_3}$	$\mathbf{2_1}$	$\mathbf{3}$
$\mathbf{1_3}$	$\mathbf{1_3}$	$\mathbf{1_1}$	$\mathbf{1_2}$	$\mathbf{2_3}$	$\mathbf{2_1}$	$\mathbf{2_2}$	$\mathbf{3}$
$\mathbf{2_1}$	$\mathbf{2_1}$	$\mathbf{2_2}$	$\mathbf{2_3}$	$\mathbf{1_1 + 3}$	$\mathbf{1_2 + 3}$	$\mathbf{1_3 + 3}$	$\mathbf{2_1 + 2_2 + 2_3}$
$\mathbf{2_2}$	$\mathbf{2_2}$	$\mathbf{2_3}$	$\mathbf{2_1}$	$\mathbf{1_2 + 3}$	$\mathbf{1_3 + 3}$	$\mathbf{1_1 + 3}$	$\mathbf{2_1 + 2_2 + 2_3}$
$\mathbf{2_3}$	$\mathbf{2_3}$	$\mathbf{2_1}$	$\mathbf{2_2}$	$\mathbf{1_3 + 3}$	$\mathbf{1_1 + 3}$	$\mathbf{1_2 + 3}$	$\mathbf{2_1 + 2_2 + 2_3}$
$\mathbf{3}$	$\mathbf{3}$	$\mathbf{3}$	$\mathbf{3}$	$\mathbf{2_1 + 2_2 + 2_3}$	$\mathbf{2_1 + 2_2 + 2_3}$	$\mathbf{2_1 + 2_2 + 2_3}$	$\mathbf{1_1 + 1_2 + 1_3 + 3 + 3}$

B.3 T' Clebsch-Gordan Coefficients

For our basis we take the tensor products in section 5 of [9] with $p = i$, $p_1 = -1$, and $p_2 = 1$.

$$\begin{pmatrix} x_1 \\ x_2 \end{pmatrix}_{\mathbf{2}(\mathbf{2'})} \otimes \begin{pmatrix} y_1 \\ y_2 \end{pmatrix}_{\mathbf{2}(\mathbf{2''})} = \left(\frac{x_1y_2 - x_2y_1}{\sqrt{2}}\right)_{\mathbf{1}} \oplus \begin{pmatrix} \frac{-1}{\sqrt{2}}(x_1y_2 + x_2y_1) \\ -x_1y_1 \\ x_2y_2 \end{pmatrix}_{\mathbf{3}}, \quad \text{(B.1)}$$

$$\begin{pmatrix} x_1 \\ x_2 \end{pmatrix}_{\mathbf{2'}(\mathbf{2})} \otimes \begin{pmatrix} y_1 \\ y_2 \end{pmatrix}_{\mathbf{2'}(\mathbf{2''})} = \left(\frac{x_1y_2 - x_2y_1}{\sqrt{2}}\right)_{\mathbf{1''}} \oplus \begin{pmatrix} x_1y_1 \\ x_2y_2 \\ \frac{1}{\sqrt{2}}(x_1y_2 + x_2y_1) \end{pmatrix}_{\mathbf{3}}, \quad \text{(B.2)}$$

$$\begin{pmatrix} x_1 \\ x_2 \end{pmatrix}_{\mathbf{2''}(\mathbf{2})} \otimes \begin{pmatrix} y_1 \\ y_2 \end{pmatrix}_{\mathbf{2''}(\mathbf{2'})} = \left(\frac{x_1y_2 - x_2y_1}{\sqrt{2}}\right)_{\mathbf{1'}} \oplus \begin{pmatrix} x_2y_2 \\ \frac{-1}{\sqrt{2}}(x_1y_2 + x_2y_1) \\ x_1y_1 \end{pmatrix}_{\mathbf{3}}, \quad \text{(B.3)}$$

$$\begin{aligned} \begin{pmatrix} x_1 \\ x_2 \\ x_3 \end{pmatrix}_{\mathbf{3}} \otimes \begin{pmatrix} y_1 \\ y_2 \\ y_3 \end{pmatrix}_{\mathbf{3}} &= [x_1y_1 + x_2y_3 + x_3y_2]_{\mathbf{1}} \\ &\oplus [x_3y_3 - (x_1y_2 + x_2y_1)]_{\mathbf{1'}} \oplus [(x_2y_2 - (x_1y_3 + x_3y_1)]_{\mathbf{1''}} \\ &\oplus \begin{pmatrix} 2x_1y_1 - x_2y_3 - x_3y_2) \\ -2x_3y_3 - x_1y_2 - x_2y_1 \\ -2x_2y_2 - x_1y_3 - x_3y_1 \end{pmatrix}_{\mathbf{3}} \end{aligned}$$

$$\oplus \quad \begin{pmatrix} x_2y_3 - x_3y_2 \\ x_1y_2 - x_2y_1 \\ x_3y_1 - x_1y_3 \end{pmatrix}_{\mathbf{3}} , \tag{B.4}$$

$$\begin{aligned} \begin{pmatrix} x_1 \\ x_2 \end{pmatrix}_{\mathbf{2},\mathbf{2'},\mathbf{2''}} \otimes \begin{pmatrix} y_1 \\ y_2 \\ y_3 \end{pmatrix}_{\mathbf{3}} &= \begin{pmatrix} -\sqrt{2}x_2y_2 + x_1y_1 \\ -\sqrt{2}x_1y_3 - x_2y_1 \end{pmatrix}_{\mathbf{2},\mathbf{2'},\mathbf{2''}} \\ &\oplus \begin{pmatrix} \sqrt{2}x_2y_3 + x_1y_2 \\ -\sqrt{2}x_1y_1 - x_2y_2 \end{pmatrix}_{\mathbf{2'},\mathbf{2''},\mathbf{2}} \\ &\oplus \begin{pmatrix} -\sqrt{2}x_2y_1 + x_1y_3 \\ \sqrt{2}x_1y_2 - x_2y_3 \end{pmatrix}_{\mathbf{2''},\mathbf{2},\mathbf{2'}} , \end{aligned} \tag{B.5}$$

$$(x)_{\mathbf{1'}(\mathbf{1''})} \otimes \begin{pmatrix} y_1 \\ y_2 \end{pmatrix}_{\mathbf{2},\mathbf{2'},\mathbf{2''}} = \begin{pmatrix} xy_1 \\ xy_2 \end{pmatrix}_{\mathbf{2'}(\mathbf{2''}),\mathbf{2''}(\mathbf{2}),\mathbf{2}(\mathbf{2'})} , \tag{B.6}$$

$$(x)_{\mathbf{1'}} \otimes \begin{pmatrix} y_1 \\ y_2 \\ y_3 \end{pmatrix}_{\mathbf{3}} = \begin{pmatrix} xy_3 \\ xy_1 \\ -xy_2 \end{pmatrix}_{\mathbf{3}} , \quad (x)_{\mathbf{1''}} \otimes \begin{pmatrix} y_1 \\ y_2 \\ y_3 \end{pmatrix}_{\mathbf{3}} = \begin{pmatrix} xy_2 \\ -xy_3 \\ xy_1 \end{pmatrix}_{\mathbf{3}} . \tag{B.7}$$

Appendix C

Example Mathematica Notebooks

C.1 Symmetry Breaking Notebook

Below is a walk through of the Mathematica notebook used to examine the symmetry breaking pattern $SO(3) \to A_4$ in Chapter 3. Outputs have been suppressed except in cases where they are useful for explanation.

We begin by defining the seven dimensional basis representing the $\mathbf{7}$ of Higgs particles above the breaking scale:

$\mathbf{Basis} = \mathbf{Table}[a[i], \{i, 7\}]$

Next we define a generic 27 dimensional $3 \times 3 \times 3$ array.

$F = \mathbf{Array}[f, \{3, 3, 3\}]$

We now express this array in terms of the seven dimensional basis defined above. We constrain the array to be symmetric and traceless and thus only have seven degrees of freedom it is then $SO(3)$ invariant by construction.

$F[[1, 1, 1]] = \left(3 \left/ \left(2 * 15^{1/2}\right)\right.\right) * \mathbf{Basis}[[5]] - (1/2)\mathbf{Basis}[[1]]$

$F[[2, 2, 2]] = (1/2)\mathbf{Basis}[[2]] + \left(3 \left/ \left(2 * 15^{1/2}\right)\right.\right) \mathbf{Basis}[[6]]$

$F[[3, 3, 3]] = \left(-2 \left/ \left(10^{1/2}\right)\right.\right) \mathbf{Basis}[[7]]$

$F[[1, 3, 3]] = F[[3, 1, 3]] = F[[3, 3, 1]] = \left(\frac{-2}{\sqrt{15}} * \mathbf{Basis}[[5]]\right) * 3^{-1/2}$

$$F[[2,3,3]] = F[[3,2,3]] = F[[3,3,2]] = \left(\frac{-2}{\sqrt{15}} * \text{Basis}[[6]]\right) * 3^{-1/2}$$

$$F[[3,2,2]] = F[[2,3,2]] = F[[2,2,3]] = \left(\sqrt{\frac{1}{6}}\text{Basis}[[3]] + \sqrt{\frac{1}{10}}\text{Basis}[[7]]\right) * 3^{-1/2}$$

$$F[[1,2,2]] = F[[2,1,2]] = F[[2,2,1]] = \left(\frac{1}{2\sqrt{15}}\text{Basis}[[5]] + (1/2)\text{Basis}[[1]]\right) * 3^{-1/2}$$

$$F[[2,1,1]] = F[[1,2,1]] = F[[1,1,2]] = \left(-(1/2)\text{Basis}[[2]] + \frac{1}{2\sqrt{15}}\text{Basis}[[6]]\right) * 3^{-1/2}$$

$$F[[3,1,1]] = F[[1,3,1]] = F[[1,1,3]] = \left(-\sqrt{\frac{1}{6}}\text{Basis}[[3]] + \sqrt{\frac{1}{10}}\text{Basis}[[7]]\right) * 3^{-1/2}$$

$$F[[1,2,3]] = F[[1,3,2]] = F[[2,1,3]] = F[[2,3,1]] = F[[3,1,2]] = F[[3,2,1]]$$
$$= \left(-\sqrt{\frac{1}{6}}\text{Basis}[[4]]\right) * 6^{-1/2}$$

We define the potential as all independent quadratic, cubic, and quartic terms involving this array. As noted in equation (3.2), the cubic terms vanish upon summation:

$V_7 = -m^2 * \text{Sum}[F[[i,j,k]] * F[[i,j,k]], \{i,1,3\}, \{j,1,3\}, \{k,1,3\}] +$
$\lambda * \text{Sum}[F[[i,j,k]] * F[[i,j,k]], \{i,1,3\}, \{j,1,3\}, \{k,1,3\}] *$
$\text{Sum}[F[[l,m,n]] * F[[l,m,n]], \{l,1,3\}, \{m,1,3\}, \{n,1,3\}] +$
$\kappa * \text{Sum}[\text{Sum}[F[[i,j,m]] * F[[i,j,n]], \{i,1,3\}, \{j,1,3\}] *$
$\text{Sum}[F[[k,l,n]] * F[[k,l,m]], \{k,1,3\}, \{l,1,3\}], \{m,1,3\}, \{n,1,3\}]$

Next we import matrix representations of A_4 from GAP[21] using the package, Discrete (NEED CITATION HERE) and select the three dimensional representation:

```
AppendTo[$Path, NotebookDirectory[]];

Get["GroupList1"]

A4 = DiscreteModelBuildingToolsPrivateGroup$12134["RepMatrices"]
```

A4Triplet = A4[[4]]

$\{\{\{1,0,0\},\{0,1,0\},\{0,0,1\}\},\{\{0,1,0\},\{0,0,1\},\{1,0,0\}\},\{\{-1,0,0\},\{0,1,0\},\{0,0,-1\}\},$
$\{\{-1,0,0\},\{0,-1,0\},\{0,0,1\}\},\{\{0,0,1\},\{1,0,0\},\{0,1,0\}\},\{\{0,1,0\},\{0,0,-1\},\{-1,0,0\}\},$
$\{\{0,-1,0\},\{0,0,1\},\{-1,0,0\}\},\{\{1,0,0\},\{0,-1,0\},\{0,0,-1\}\},\{\{0,0,-1\},\{-1,0,0\},\{0,1,0\}\},$
$\{\{0,0,1\},\{-1,0,0\},\{0,-1,0\}\},\{\{0,-1,0\},\{0,0,-1\},\{1,0,0\}\},\{\{0,0,-1\},\{1,0,0\},\{0,-1,0\}\}\}$

We now use the triplet representation in the Reynolds operator: The first step is to apply all group transformations to a generic vector (x, y, z):

reynolds = Table[A4Triplet[[*i*]].{*x*, *y*, *z*}, {*i*, 12}]

$\{\{x,y,z\},\{y,z,x\},\{-x,y,-z\},\{-x,-y,z\},\{z,x,y\},\{y,-z,-x\},$
$\{-y,z,-x\},\{x,-y,-z\},\{-z,-x,y\},\{z,-x,-y\},\{-y,-z,x\},\{-z,x,-y\}\}$

Now we sum the output of a trial function (We have chosen $x^1y^1z^1$) over the above list.

Sum [reynolds[[*i*, {1}]]^1 * reynolds[[*i*, {2}]]^1 * reynolds[[*i*, {3}]]^1, {*i*, 12}]/ 12//Expand

$\{xyz\}$

We see that the Reynolds operator has returned xyz as the invariant polynomial. Next we define a vector of first derivatives of the potential:

OneD = *D* [*V*$_7$, {{*a*[1], *a*[2], *a*[3], *a*[4], *a*[5], *a*[6], *a*[7]}}]

To restrict the minimum, we impose the A_4 invariant vacuum alignment found from the Reynolds operator (note that in section 3.3.1.1) the nonzero basis state was a[7] but we have defined it here as a[4] due to how we set up the invariant tensor above):

VEV = OneD/.{*a*[1] → 0, *a*[2] → 0, *a*[3] → 0, *a*[4] → *a*[4], *a*[5] → 0, *a*[6] → 0, *a*[7] → 0}

$\left\{0,0,0,-\frac{1}{3}m^2a[4]+\frac{1}{27}\kappa a[4]^3+\frac{1}{9}\lambda a[4]^3,0,0,0\right\}$

Setting all components of the vector equal to zero and solving for a[4] gives us an expression for the breaking scale (the physical value is the positive solution):

Solve[VEV[[4]] == 0, a[4]]

$\left\{\{a[4] \to 0\}, \left\{a[4] \to -\frac{3m}{\sqrt{\kappa+3\lambda}}\right\}, \left\{a[4] \to \frac{3m}{\sqrt{\kappa+3\lambda}}\right\}\right\}$

Finally, we determine the masses of the scalars below the breaking scale. We first define the matrix of second derivatives:

Hess = D [V7, {{a[1], a[2], a[3], a[4], a[5], a[6], a[7]}, 2}]

Then we impose the minimization condition derived above:

VEV2 = Hess/. $\left\{a[1] \to 0, a[2] \to 0, a[3] \to 0, a[4] \to \frac{3m}{\sqrt{\kappa+3\lambda}}, a[5] \to 0, a[6] \to 0, a[7] \to 0\right\}$

Now we take the eigenvalues of the resulting matrix and tally the mass states:

Eigenvalues[VEV2]//Tally

$\left\{\{0, 3\}, \left\{\frac{8m^2\kappa}{15(\kappa+3\lambda)}, 3\right\}, \left\{\frac{2m^2}{3}, 1\right\}\right\}$

We are left with three massless scalars (which are eaten by gauge bosons) and a triplet and singlet of massive Higgs bosons.

C.2 PMNS Notebook

The following notebook derives an experimentally compatible PMNS matrix from the model in Chapter 5. We begin by defining the right-handed neutrino mass matrix:

$$\mathbf{Mn} = \{\{m,0,0\},\{0,0,m\},\{0,m,0\}\}$$

We then define a function h(x,y,z), (with x,y,z from below Equation (5.12)) that outputs the PMNS mixing matrix, i.e. the transformation which diagonalizes the Majorana mass matrix (5.9):

$$h[\mathbf{x\_}, \mathbf{y\_}, \mathbf{z\_}]:=$$

$$\mathbf{Apply}[\mathbf{Normalize},$$

$$\{\{\mathbf{Eigenvectors}[\{\{0+z,-2-x,-1-y\},\{2-x,0+y,1+z\},\{1-y,-1+z,0+x\}\}.\mathbf{Inverse}[\mathbf{Mn}].$$

$$\mathbf{Transpose}[\{\{0+z,-2-x,-1-y\},\{2-x,0+y,1+z\},\{1-y,-1+z,0+x\}\}]][[3]]\},$$

$$\{\mathbf{Eigenvectors}[\{\{0+z,-2-x,-1-y\},\{2-x,0+y,1+z\},\{1-y,-1+z,0+x\}\}.\mathbf{Inverse}[\mathbf{Mn}].$$

$$\mathbf{Transpose}[\{\{0+z,-2-x,-1-y\},\{2-x,0+y,1+z\},\{1-y,-1+z,0+x\}\}]][[2]]\},$$

$$-\{\mathbf{Eigenvectors}[\{\{0+z,-2-x,-1-y\},\{2-x,0+y,1+z\},\{1-y,-1+z,0+x\}\}.\mathbf{Inverse}[\mathbf{Mn}].$$

$$\mathbf{Transpose}[\{\{0+z,-2-x,-1-y\},\{2-x,0+y,1+z\},\{1-y,-1+z,0+x\}\}]][[1]]\}\},\{1\}]$$

We check that with no additional scalar singlets, this function returns the tri-bi-maximal mixing matrix:

$$h[0,0,0]$$

$$\left\{\left\{-\frac{1}{\sqrt{6}},-\frac{1}{\sqrt{6}},\sqrt{\frac{2}{3}}\right\},\left\{\frac{1}{\sqrt{3}},\frac{1}{\sqrt{3}},\frac{1}{\sqrt{3}}\right\},\left\{\frac{1}{\sqrt{2}},-\frac{1}{\sqrt{2}},0\right\}\right\}$$

In order to tune the parameters x,y,z we must define the experimental values and one sigma errors appropriately:

$$\mathbf{stddeverr} = \mathbf{Transpose}[\{\{.237,.205,.139\},\{.252,.211,.135\},\{.045,.066,.015\}\}]/6$$

Exper = Transpose[{{"0.4025", "0.5925", "0.6845"}, {"0.368", "0.5725", "0.7065"}, {"0.8215", "0.549", "0.1485"}}]

Next we define two functions. AvgErrors takes a predicted PMNS matrix as input and outputs the average error of its nine parameters, MaxErrors outputs the error value of the parameter with the highest error. Both outputs are in units of standard deviations from experimental value:

AvgErrors[X_]:=Mean[Mean[(Abs[Abs[X] − Exper])/stddeverr]]

MaxErrors[X_]:=Max[Max[(Abs[Abs[X] − Exper])/stddeverr]]

Next we loop over all values in the parameter space between -1 and 1 with a precision of .01, appending the max and average error values associated with each set of parameters to separate lists. Note that this may take a very long time depending on the type of machine the code is run on:

MaxErrorslist = {};

count = 0;

MaxErrorslist =

Flatten[ParallelTable[MaxErrors[$h[x, y, z]$], $\{x, -1, 1, .01\}, \{y, -1, 1, .01\}, \{z, -1, 1, .01\}$]]

ClearSystemCache[]

AvgErrorslist = {};

count = 0;

AvgErrorslist =

Flatten[ParallelTable[AvgErrors[$h[x, y, z]$], $\{x, -1, 1, .01\}, \{y, -1, 1, .01\}, \{z, -1, 1, .01\}$]]

Additionally we create a list of all possible parameters:

ClearSystemCache[];

Parameterlist $=$ **{}**;

count $=$ **0;**

Parameterlist $=$ **Flatten**[**ParallelTable**[$\{x, y, z\}, \{x, -1, 1, .01\}, \{y, -1, 1, .01\}, \{z, -1, 1, .01\}$], 2]

Next we find the positions which give the minimum error value in each list and then search for them in the parameter list:

Position[**MaxErrorslist, Min**[**MaxErrorslist**]]

$\{\{3016267\}\}$

Position[**AvgErrorslist, Min**[**AvgErrorslist**]]

$\{\{2975861\}\}$

Parameterlist[[**3016267**]]

$\{-0.26, 0.32, -0.4\}$

Parameterlist[[**2975861**]]

$\{-0.27, 0.32, -0.45\}$

We see that the values (x,y,z)=(-0.26,0.32,-0.4) minimize the max error and (x,y,z)=(-0.27,0.32,-0.45) minimize the average error.

Finally we show how to create the contour plots (5.1), (5.2)] that display the maximum and average error values as a function of parameter space:

ContourPlot[**MaxErrors**[$h[x, .32, z]$], $\{x, -1, 0\}, \{z, -1, 0\}$, **FrameLabel** $\rightarrow \{x', z'\}$,

PlotLegends $\rightarrow$ **Automatic, Contours** $\rightarrow \{1, 2, 3, 4, 5\}$,

FrameTicks $\rightarrow \{$**Table**[$i, \{i, -1, 1, .1\}$], **Table**[$j, \{j, -1, 1, .1\}$]$\}$, **PlotLabel** $\rightarrow$ **"Max Errors"**,

ContourShading → {White, Yellow, Orange, Red, Purple, Blue}]

ContourPlot[AvgErrors[h[x, .32, z]], {x, −1, 0}, {z, −1, 0}, FrameLabel → {x′, z′},
PlotLegends → Automatic, Contours → {1, 2, 3, 4, 5},
FrameTicks → {Table[i, {i, −1, 1, .1}], Table[j, {j, −1, 1, .1}]}, PlotLabel → "Average Errors",
ContourShading → {White, Yellow, Orange, Red, Purple, Blue}]

BIBLIOGRAPHY

[1] H. Georgi and S. L. Glashow, Phys. Rev. Lett. **32**, 438 (1974). doi:10.1103/PhysRevLett.32.438

[2] S. Weinberg, Phys. Rev. Lett. **19**, 1264 (1967). doi:10.1103/PhysRevLett.19.1264

[3] S. L. Glashow, Nucl. Phys. **22**, 579 (1961). doi:10.1016/0029-5582(61)90469-2

[4] A. Salam, Conf. Proc. C **680519**, 367 (1968).

[5] S. Pakvasa and H. Sugawara, Phys. Lett. **73B**, 61 (1978). doi:10.1016/0370-2693(78)90172-7

[6] E. Ma and G. Rajasekaran, Phys. Rev. D **64**, 113012 (2001) doi:10.1103/PhysRevD.64.113012 [hep-ph/0106291].

[7] K. S. Babu, E. Ma and J. W. F. Valle, Phys. Lett. B **552**, 207 (2003) doi:10.1016/S0370-2693(02)03153-2 [hep-ph/0206292].

[8] P. H. Frampton and T. W. Kephart, Int. J. Mod. Phys. A **10**, 4689 (1995) [arXiv:hep-ph/9409330].

[9] H. Ishimori, T. Kobayashi, H. Ohki, H. Okada, Y. Shimizu and M. Tanimoto, Prog. Theor. Phys. Suppl. **183**, 1 (2010) [arXiv:1003.3552 [hep-th]].

[10] G. Altarelli and F. Feruglio, Rev. Mod. Phys. **82**, 2701 (2010) doi:10.1103/RevModPhys.82.2701 [arXiv:1002.0211 [hep-ph]].

[11] S. F. King and C. Luhn, Rept. Prog. Phys. **76**, 056201 (2013) doi:10.1088/0034-4885/76/5/056201 [arXiv:1301.1340 [hep-ph]].

[12] S. F. King, A. Merle, S. Morisi, Y. Shimizu and M. Tanimoto, New J. Phys. **16**, 045018 (2014) doi:10.1088/1367-2630/16/4/045018 [arXiv:1402.4271 [hep-ph]].

[13] L. M. Krauss and F. Wilczek, Phys. Rev. Lett. **62**, 1221 (1989). doi:10.1103/PhysRevLett.62.1221

[14] C. Luhn and P. Ramond, JHEP **0807**, 085 (2008) doi:10.1088/1126-6708/2008/07/085 [arXiv:0805.1736 [hep-ph]].

[15] M. B. Hindmarsh and T. W. B. Kibble, Rept. Prog. Phys. **58**, 477 (1995) doi:10.1088/0034-4885/58/5/001 [hep-ph/9411342].

[16] O. Reynolds, Phil. Trans. of the Royal Society A, 186: 123 (1895); B. Sturmfels, *Algorithms in Invariant Theory,* 2^{nd} ed., (2008) Springer, Wien & New York.

[17] T. Molien, Sitz. König Preuss. Akad. Wiss. (1897), N 52, 1152-1156.

[18] C. Luhn, JHEP **1103**, 108 (2011) doi:10.1007/JHEP03(2011)108 [arXiv:1101.2417 [hep-ph]].

[19] A. Merle and R. Zwicky, JHEP **1202**, 128 (2012) doi:10.1007/JHEP02(2012)128 [arXiv:1110.4891 [hep-ph]].

[20] M. Fallbacher, Nucl. Phys. B **898**, 229 (2015) doi:10.1016/j.nuclphysb.2015.07.004 [arXiv:1506.03677 [hep-th]].

[21] GAP - "Groups, Algorithms, Programming - a System for Computational Discrete Algebra," version GAP 4.8.5, 25 Sept. 2016.

[22] P. H. Frampton, T. W. Kephart and R. M. Rohm, Phys. Lett. B **679**, 478 (2009) [arXiv:0904.0420 [hep-ph]].

[23] J. Berger and Y. Grossman, JHEP **1002**, 071 (2010) doi:10.1007/JHEP02(2010)071 [arXiv:0910.4392 [hep-ph]].

[24] E. Ma, Phys. Lett. B **752**, 198 (2016) doi:10.1016/j.physletb.2015.11.049 [arXiv:1510.02501 [hep-ph]].

[25] G. Altarelli, F. Feruglio and C. Hagedorn, JHEP **0803** (2008) 052 doi:10.1088/1126-6708/2008/03/052 [arXiv:0802.0090 [hep-ph]].

[26] S. F. King and C. Luhn, JHEP **1203**, 036 (2012) doi:10.1007/JHEP03(2012)036 [arXiv:1112.1959 [hep-ph]].

[27] P. M. Ferreira, L. Lavoura and P. O. Ludl, Phys. Lett. B **726**, 767 (2013) doi:10.1016/j.physletb.2013.09.058 [arXiv:1306.1500 [hep-ph]].

[28] P. Cvitanovic, Phys. Rev. D **14**, 1536 (1976). doi:10.1103/PhysRevD.14.1536

[29] C. Hagedorn, M. Lindner and R. N. Mohapatra, JHEP **0606**, 042 (2006) doi:10.1088/1126-6708/2006/06/042 [hep-ph/0602244].

[30] C. Hagedorn, S. F. King and C. Luhn, JHEP **1006**, 048 (2010) doi:10.1007/JHEP06(2010)048 [arXiv:1003.4249 [hep-ph]].

[31] L. L. Everett and A. J. Stuart, Phys. Rev. D **79**, 085005 (2009) [arXiv:0812.1057 [hep-ph]];

[32] F. Feruglio and A. Paris, JHEP **1103**, 101 (2011) [arXiv:1101.0393 [hep-ph]];

[33] G. -J. Ding, L. L. Everett and A. J. Stuart, Nucl. Phys. B **857**, 219 (2012) [arXiv:1110.1688 [hep-ph]];

[34] C. -S. Chen, T. W. Kephart and T. -C. Yuan, JHEP **1104**, 015 (2011) [arXiv:1011.3199 [hep-ph]].

[35] P. H. Frampton and T. W. Kephart, Phys. Rev. D **51**, R1 (1995) doi:10.1103/PhysRevD.51.R1 [hep-ph/9409324].

[36] P. H. Frampton and A. Rasin, Phys. Lett. B **478**, 424 (2000) doi:10.1016/S0370-2693(00)00276-8 [hep-ph/9910522].

[37] A. Aranda, C. D. Carone and R. F. Lebed, Phys. Lett. B **474**, 170 (2000) doi:10.1016/S0370-2693(99)01497-5 [hep-ph/9910392].

[38] M. C. Chen and K. T. Mahanthappa, Phys. Lett. B **652**, 34 (2007) doi:10.1016/j.physletb.2007.06.064 [arXiv:0705.0714 [hep-ph]].

[39] P. H. Frampton and T. W. Kephart, JHEP **0709**, 110 (2007) [arXiv:0706.1186 [hep-ph]];

[40] P. H. Frampton, T. W. Kephart and S. Matsuzaki, Phys. Rev. D **78**, 073004 (2008) doi:10.1103/PhysRevD.78.073004 [arXiv:0807.4713 [hep-ph]].

[41] P. H. Frampton, C. M. Ho, T. W. Kephart and S. Matsuzaki, Phys. Rev. D **82**, 113007 (2010) doi:10.1103/PhysRevD.82.113007 [arXiv:1009.0307 [hep-ph]].

[42] A. Natale, Nucl. Phys. B **914**, 201 (2017) doi:10.1016/j.nuclphysb.2016.11.006 [arXiv:1608.06999 [hep-ph]].

[43] C. D. Carone, S. Chaurasia and S. Vasquez, Phys. Rev. D **95**, no. 1, 015025 (2017) doi:10.1103/PhysRevD.95.015025 [arXiv:1611.00784 [hep-ph]].

[44] L. L. Everett and A. J. Stuart, Phys. Lett. B **698**, 131 (2011) doi:10.1016/j.physletb.2011.02.054 [arXiv:1011.4928 [hep-ph]].

[45] C. S. Chen, T. W. Kephart and T. C. Yuan, PTEP **2013**, no. 10, 103B01 (2013) doi:10.1093/ptep/ptt071 [arXiv:1110.6233 [hep-ph]].

[46] C. Luhn, S. Nasri and P. Ramond, Phys. Lett. B **652**, 27 (2007) doi:10.1016/j.physletb.2007.06.059 [arXiv:0706.2341 [hep-ph]].

[47] J. Kile, M. J. Prez, P. Ramond and J. Zhang, Phys. Rev. D **90**, no. 1, 013004 (2014) doi:10.1103/PhysRevD.90.013004 [arXiv:1403.6136 [hep-ph]].

[48] V. V. Vien, Mod. Phys. Lett. A **29**, 28 (2014) doi:10.1142/S0217732314501399 [arXiv:1508.02585 [hep-ph]].

[49] V. V. Vien and H. N. Long, arXiv:1609.03895 [hep-ph].

[50] V. V. Vien, A. E. Crcamo Hernndez and H. N. Long, Nucl. Phys. B **913**, 792 (2016) doi:10.1016/j.nuclphysb.2016.10.010 [arXiv:1601.03300 [hep-ph]].

[51] P. M. Ferreira, W. Grimus, L. Lavoura and P. O. Ludl, JHEP **1209**, 128 (2012) doi:10.1007/JHEP09(2012)128 [arXiv:1206.7072 [hep-ph]].

[52] G. Chen, M. J. Prez and P. Ramond, Phys. Rev. D **92**, no. 7, 076006 (2015) doi:10.1103/PhysRevD.92.076006 [arXiv:1412.6107 [hep-ph]].

[53] M. Koca, R. Koc and H. Tutunculer, Int. J. Mod. Phys. A **18**, 4817 (2003) doi:10.1142/S0217751X03015891 [hep-ph/0410270].

[54] Christoph Luhn, private communication.

[55] C. Hagedorn, M. A. Schmidt and A. Y. Smirnov, Phys. Rev. D **79**, 036002 (2009) doi:10.1103/PhysRevD.79.036002 [arXiv:0811.2955 [hep-ph]].

[56] S. F. King, C. Luhn and A. J. Stuart, Nucl. Phys. B **867**, 203 (2013) doi:10.1016/j.nuclphysb.2012.09.021 [arXiv:1207.5741 [hep-ph]].

[57] V. V. Vien and H. N. Long, J. Korean Phys. Soc. **66**, no. 12, 1809 (2015) doi:10.3938/jkps.66.1809 [arXiv:1408.4333 [hep-ph]].

[58] P. O. Ludl, J. Phys. A **43**, 395204 (2010) Erratum: [J. Phys. A **44**, 139501 (2011)] doi:10.1088/1751-8113/44/13/139501, 10.1088/1751-8113/43/39/395204 [arXiv:1006.1479 [math-ph]].

[59] W. Grimus and P. O. Ludl, J. Phys. A **45**, 233001 (2012) doi:10.1088/1751-8113/45/23/233001 [arXiv:1110.6376 [hep-ph]].

[60] P. O. Ludl, J. Phys. A **44**, 255204 (2011) Erratum: [J. Phys. A **45**, 069502 (2012)] doi:10.1088/1751-8113/45/6/069502, 10.1088/1751-8113/44/25/255204 [arXiv:1101.2308 [math-ph]].

[61] W. C. Huang, Y. L. S. Tsai and T. C. Yuan, JHEP **1604**, 019 (2016) doi:10.1007/JHEP04(2016)019 [arXiv:1512.00229 [hep-ph]].

[62] C. H. Albright, R. P. Feger and T. W. Kephart, Phys. Rev. D **93**, no. 7, 075032 (2016) doi:10.1103/PhysRevD.93.075032 [arXiv:1601.07523 [hep-ph]].

[63] I. Esteban, M. C. Gonzalez-Garcia, M. Maltoni, I. Martinez-Soler and T. Schwetz, JHEP **1701**, 087 (2017) doi:10.1007/JHEP01(2017)087 [arXiv:1611.01514 [hep-ph]].

[64] L. E. Ibanez and G. G. Ross, Nucl. Phys. B **368**, 3 (1992). doi:10.1016/0550-3213(92)90195-H

[65] L. E. Ibanez and G. G. Ross, Phys. Lett. B **260**, 291 (1991). doi:10.1016/0370-2693(91)91614-2

[66] J. Talbert, Phys. Lett. B **786**, 426 (2018) doi:10.1016/j.physletb.2018.10.025 [arXiv:1804.04237 [hep-ph]].

[67] B. Pontecorvo, Soviet Physics JETP. 7: 172. 1958; Z. Maki, M. Nakagawa, S. Sakata, Progress of Theoretical Physics. 28 (5): 870 (1962).

[68] P. F. Harrison, D. H. Perkins and W. G. Scott, Phys. Lett. B **530**, 167 (2002) doi:10.1016/S0370-2693(02)01336-9 [hep-ph/0202074].

[69] M. H. Rahat, P. Ramond and B. Xu, Phys. Rev. D **98**, no. 5, 055030 (2018) doi:10.1103/PhysRevD.98.055030 [arXiv:1805.10684 [hep-ph]].

[70] D. A. Eby, P. H. Frampton and S. Matsuzaki, Phys. Lett. B **671**, 386 (2009) doi:10.1016/j.physletb.2008.11.074 [arXiv:0810.4899 [hep-ph]].

[71] NuFIT 3.2 (2018), www.nu-fit.org.

[72] M. Tanabashi et al. (Particle Data Group), Phys. Rev. D 98, 030001 (2018)

[73] A. Bilal, arXiv:0802.0634 [hep-th].

[74] B. L. Rachlin and T. W. Kephart, JHEP **1708**, 110 (2017) doi:10.1007/JHEP08(2017)110 [arXiv:1702.08073 [hep-ph]].

[75] Y. Grossman and W. H. Ng, Phys. Rev. D **91**, no. 7, 073005 (2015) doi:10.1103/PhysRevD.91.073005 [arXiv:1404.1413 [hep-ph]].

[76] S. F. King and Y. L. Zhou, arXiv:1809.10292 [hep-ph].

[77] G. Altarelli and F. Feruglio, Nucl. Phys. B **741**, 215 (2006) doi:10.1016/j.nuclphysb.2006.02.015 [hep-ph/0512103].

[78] F. Mandl and G. Shaw, Chichester, Uk: Wiley (2010) 478 p.

[79] M. D. Schwartz,

[80] M. Lindner, T. Ohlsson and G. Seidl, Phys. Rev. D **65**, 053014 (2002) doi:10.1103/PhysRevD.65.053014 [hep-ph/0109264].